

(NASA-CR-141393) BISTATIC RADAR SEA STATE
MONITORING SYSTEM DESIGN (Battelle Columbus
Labs., Ohio.) : 104 p HC \$5.25 CSCL 17I

N75-20682

Unclas

G3/35 14731

BISTATIC RADAR SEA STATE MONITORING SYSTEM DESIGN

by: G.T. Ruck, C.K. Krichbaum, and J.O. Everly

Prepared under contract No. NAS6-2006 by:

Battelle

Columbus Laboratories

505 King Avenue

Columbus, Ohio 43201



for:

NATIONAL AERONAUTICS AND SPACE ADMINISTRATION

WALLOPS FLIGHT CENTER

WALLOPS ISLAND, VIRGINIA 23337

March 1975

1. Report No. NASA CR-141393	2. Government Accession No.	3. Recipient's Catalog No.	
4. Title and Subtitle BISTATIC RADAR SEA STATE MONITORING - SYSTEM DESIGN		5. Report Date May 1973	
		6. Performing Organization Code	
7. Author(s) G. T. Ruck, C. K. Krichbaum, and J. O. Everly		8. Performing Organization Report No.	
		10. Work Unit No.	
9. Performing Organization Name and Address Battelle Columbus Laboratories 505 King Avenue Columbus, Ohio 43201		11. Contract or Grant No. NAS6-2006	
		13. Type of Report and Period Covered Contractor Report	
12. Sponsoring Agency Name and Address National Aeronautics & Space Administration Wallops Flight Center Wallops Island, Virginia 23337		14. Sponsoring Agency Code	
		15. Supplementary Notes In accordance with para. 5.d. of NASA Policy Directive, NPD-2220.4, "Use of the International System of Units (SI) in NASA Publications," a waiver has been granted for this report.	
16. Abstract Recent advances in understanding the physical phenomena controlling the interaction of electromagnetic energy with the ocean surface have revealed the possibility of remote measurement of the two-dimensional surface wave height spectrum of the ocean by the use of bistatic radar techniques. The basic feasibility of such a technique operating at frequencies in the HF region (3 to 30 MHz) was examined during a previous study. The results of this previous study indicated potential feasibility and suggested that the concept be experimentally verified by field experiment. The primary effort in this study was devoted to defining the required experimental hardware, and the designing, assembling, and testing of several required experimental hardware components not otherwise available.			
17. Key Words (Suggested by Author(s)) Bistatic Radar FMCW Transmitter Electromagnetic Energy		18. Distribution Statement Unclassified - Unlimited STAR Category 35	
19. Security Classif. (of this report) Unclassified	20. Security Classif. (of this page) Unclassified	21. No. of Pages 104	22. Price*

FOREWORD

PRECEDING PAGE BLANK NOT FILMED

This report covers activities performed by Battelle's Columbus Laboratories (BCL) on behalf of the National Aeronautics and Space Administration, Wallops Station, under Contract No. NAS6-2006, "Services for Oceanography, Geodesy, and Related Areas Task Support". The NASA task monitor was Mr. H. R. Stanley. The Battelle program manager was Mr. A. G. Mourad.

The investigation reported here was one of several tasks under the above mentioned contract and represents the second phase of a program for developing a sea state monitoring system using a bistatic radar technique.

TABLE OF CONTENTS

	<u>Page</u>
FOREWORD	vi
ABSTRACT	vii
I. INTRODUCTION	1
II. SUMMARY OF RESULTS AND RECOMMENDATIONS.	3
Program Summary	3
Results	3
Recommendations	4
III. EXPERIMENTAL SYSTEM REQUIREMENTS	5
Frequency Synthesizer/Driver	12
Analog Magnetic Tape Recorder.	13
Communications Receiver.	13
Frequency Standard	14
Power Supplies	14
Verification Equipment	15
IV. EXPERIMENTAL HARDWARE DESIGN ASSEMBLY AND TEST.	16
Sweep Controller-Programmer Requirements.	16
Sweep Controller-Programmer Module Design	17
Digital Logic.	21
Clock Board Description.	21
Decade Board Description	24
Control Board Description.	27
Simulated-Load Waveforms	30
Sweep-Controller-Programmer Physical Layout.	30

TABLE OF CONTENTS
(Continued)

	<u>Page</u>
Broadband HF Linear Power Amplifier.	33
Transmitting Antenna Design Considerations	36
Radiation Pattern of a Vertical Monopole.	39
Input Impedance Characteristics of a Short Vertical Monopole	41
Efficiency and Bandwidth of an Unloaded Monopole	47
Vertical Monopole with High Frequency Trap	52
Capacitive "Top-Hat" Loading of a Short Vertical Monopole	54
Transmitting Antenna Design.	55
Top-Hat Construction.	56
Specification of High Frequency Trap.	60
Transmitting Antenna Impedance Matching Networks.	64
Electromechanical Bandswitch	66
Receiver Preselector.	71
Receiver Mixer.	74
V. THE AIRCRAFT EXPERIMENT	76
Received Signals for an Aircraft Experiment.	78

LIST OF TABLES

Table 1. TRUTH TABLE FOR DECADE BOARD OPERATION.	28
Table 2. ANTENNA EFFICIENCY AS A FUNCTION OF FREQUENCY	48
Table 3. Q, S.W.R. AND BANDWIDTH OF AN UNLOADED MONOPOLE	50
Table 4. INCREASE IN ELECTRICAL LENGTH VERSUS ANTENNA HEIGHT	58
Table 5. INPUT IMPEDANCE OF LOADED MONOPOLE AS A FUNCTION OF FREQUENCY AND GROUND CONDUCTIVITY.	59

LIST OF FIGURES

	<u>Page</u>
Figure 1. TRANSMITTING EQUIPMENT LAYOUT.	9
Figure 2. RECEIVING EQUIPMENT LAYOUT	10
Figure 3. INDIRECT SYNTHESIS OF FREQUENCY 12345678.90 Hz USING HP 5100B FREQUENCY SYNTHESIZER	18
Figure 4. FREQUENCY SWEEP WAVEFORMS.	19
Figure 5. BLOCK DIAGRAM OF SWEEP PROGRAMMER.	20
Figure 6. WIRING SCHEMATIC OF CLOCK BOARD.	22
Figure 7. VOLTAGE WAVEFORMS AT INPUT AND OUTPUT OF CLOCK DRIVER NETWORK.	23
Figure 8. WIRING SCHEMATIC OF DECADE BOARD	25
Figure 9. EQUIVALENT CIRCUIT OF 75450B DUAL PERIPHERAL DRIVER AND EXTERNAL DISCRETE COMPONENTS.	26
Figure 10. WIRING SCHEMATIC OF CONTROL BOARD.	29
Figure 11. DUMMY LOAD TO TEST RISE TIME OF HP DRIVER CIRCUIT.	31
Figure 12. PULSE WAVEFORMS AT SWITCHING POINTS OF SIMULATED HP 5100 DIODE MATRIX LOAD.	32
Figure 13. CIRCUIT-BOARD LAYOUT FOR DECADE BOARD (TOP SIDE)	34
Figure 14. CIRCUIT-BOARD LAYOUT FOR DECADE BOARD (BOTTOM SIDE).	35
Figure 15. 3 to 30 MHz LINEAR POWER AMPLIFIER	37
Figure 16. CURVE OF AMPLIFIER POWER GAIN VERSUS FREQUENCY FOR 3 WATTS INTO 50- ohm LOAD.	38
Figure 17. CURRENT DISTRIBUTIONS AND RADIATION PATTERNS FOR VERTICAL ANTENNA OVER PERFECTLY CONDUCTING EARTH	40
Figure 18. INPUT IMPEDANCE OF AN UNLOADED MONOPOLE.	43
Figure 19. RESISTIVE PART OF INPUT IMPEDANCE VERSUS FREQUENCY	45
Figure 20. REACTIVE PART OF INPUT IMPEDANCE VERSUS FREQUENCY.	46

LIST OF FIGURES
(Continued)

	<u>Page</u>
Figure 21. EQUIVALENT CIRCUIT OF AN UNLOADED MONOPOLE AS A FUNCTION OF FREQUENCY	47
Figure 22. ANTENNA Q VERSUS FREQUENCY	51
Figure 23. VERTICAL ANTENNA WITH TRAP	53
Figure 24. ADDITIONAL ANTENNA HEIGHT AT 3.15 MHz FOR A 5 FT DIAMETER TOP HAT.	57
Figure 25. MECHANICAL DETAILS OF CAPACITIVE TOP HAT	61
Figure 26. ELECTRICAL AND MECHANICAL DETAILS OF HIGH FREQUENCY TRAP CONSTRUCTION.	63
Figure 27. MATCHING NETWORKS FOR VERTICAL ANTENNA AS A FUNCTION OF ANTENNA HEIGHT.	65
Figure 28. NETWORK ELEMENTS NECESSARY TO CONJUGATELY MATCH TRANSMISSION LINE TO ANTENNA AT FREQUENCIES LESS THAN 10 MHz.	67
Figure 29. NETWORK ELEMENTS FOR CONJUGATELY MATCHING TRANSMISSION LINE TO ANTENNA AT FREQUENCIES ABOVE 10 MHz	68
Figure 30. BANDSWITCH	70
Figure 31A. RECEIVER PRESELECTION CIRCUIT DIAGRAM	72
Figure 31B. TRANSFORMER PARAMETERS FOR RECEIVER PRESELECTION.	73
Figure 32. MIXER CIRCUIT DIAGRAM.	75
Figure 33. SATELLITE RECEIVED SPECTRUM BEFORE CPA FOR ISOTROPIC SURFACE.	79
Figure 34. SATELLITE RECEIVED SPECTRUM AT CPA IN ISOTROPIC SURFACE	80
Figure 35. SATELLITE RECEIVED SPECTRUM AFTER CPA IN ISOTROPIC SURFACE	81
Figure 36. SATELLITE RECEIVED SPECTRUM BEFORE CPA FOR \cos^2 SURFACE	82
Figure 37. SATELLITE RECEIVED SPECTRUM AT CPA IN \cos^2 SURFACE	83

LIST OF FIGURES
(Continued)

	<u>Page</u>
Figure 38. SATELLITE RECEIVED SPECTRUM AFTER CPA FOR \cos^2 SURFACE.	84
Figure 39. AIRCRAFT RECEIVED SPECTRUM AT CPA ISOTROPIC SURFACE	86
Figure 40. AIRCRAFT SPECTRUM AT CPA FOR \cos^2 SURFACE, ALONG WIND FLIGHT PATH.	87
Figure 41. AIRCRAFT RECEIVED SPECTRUM AT CPA FOR \cos^2 SURFACE- 40° FLIGHT PATH	88
Figure 42. AIRCRAFT RECEIVED SPECTRUM AT CPA FOR \cos^2 SURFACE, CROSS WIND FLIGHT PATH	89
Figure 43. AIRCRAFT RECEIVED SPECTRUM BEFORE CPA FOR \cos^2 SURFACE, ALONG WIND FLIGHT PATH	90
Figure 44. AIRCRAFT RECEIVED SPECTRUM AFTER CPA FOR \cos^2 SURFACE, ALONG WIND FLIGHT PATH	91
Figure 45. AIRCRAFT RECEIVED SPECTRUM BEFORE CPA FOR \cos^2 SURFACE, 40° FLIGHT PATH.	92
Figure 46. AIRCRAFT RECEIVED SPECTRUM AFTER CPA FOR \cos^2 SURFACE, 40° FLIGHT PATH.	93
Figure 47. AIRCRAFT RECEIVED SPECTRUM BEFORE CPA FOR \cos^2 SURFACE, CROSS WIND FLIGHT PATH	94
Figure 48. AIRCRAFT RECEIVED SPECTRUM AFTER CPA FOR \cos^2 SURFACE, CROSS WIND FLIGHT PATH	95

ABSTRACT

Recent advances in understanding the physical phenomena controlling the interaction of electromagnetic energy with the ocean surface have revealed the possibility of remote measurement of the two-dimensional surface wave height spectrum of the ocean by the use of bistatic radar techniques. The basic feasibility of such a technique operating at frequencies in the HF region (3 to 30 MHz) was examined during a previous study. The results of this previous study indicated potential feasibility and suggested that the concept be experimentally verified by field experiment.

The primary effort in this study was devoted to defining the required experimental hardware, and the designing, assembling, and testing of several required experimental hardware components not otherwise available.

The experimental system to be used consists of a surface-based FMCW transmitter radiating from 1 to 5 W. The transmitter sequentially radiates on ten frequency bands within the HF region. On each band, 256 sweeps over a 100-kHz range are performed during a 25.6-sec. interval. Each 100-kHz sweep is synthesized by stepping over this range using 10,000 10-Hz steps. The receiving system is to be flown in an aircraft and will synchronously follow the transmitter sweeps and band switches. Coherent Doppler processing of the received signal is made possible by the use of very stable basic frequency sources at both the transmitter and receiver locations. These sources are initially synchronized and maintain synchronization within the experimental requirements during the course of the experiment.

Specific hardware designed and assembled during this investigation includes the transmitter and receiver sweep controller-programmer modules, transmitting antenna, transmitting antenna matching networks, transmitter power amplifiers, receiver preselector, and receiver mixer assembly.

BISTATIC RADAR SEA STATE MONITORING - SYSTEM DESIGN

by

G. T. Ruck, C. K. Krichbaum, J. O. Everly

I. INTRODUCTION

This report covers activities performed by Battelle's Columbus Laboratories (BCL) on behalf of the National Aeronautics and Space Administration, Wallops Station, under Contract No. NAS6-2006.

As one of the Tasks (Task II) under this contract, BCL had the responsibility for investigating the use of bistatic radar systems for the measurement of sea state. This investigation represents the second phase of a program for developing a sea state monitoring system utilizing a bistatic radar technique.

The bistatic radar approach involves the use of radio waves having a length parameter of the same order as the longer ocean waves contributing dominantly to the state of the sea, so as to produce a strong interaction. It has long been known that the Bragg effect, and its intensity depends directly on the heights of the ocean waves responsible for the scatter. By exploiting polarization, motion of the ocean waves, and motion of the receiver, a relative measure of the heights and direction of the dominant ocean waves can be obtained.

The basic bistatic configuration requires a surface-based HF transmitter located on a buoy or ship which is activated by command from an aerial platform or satellite. Radiation from the transmitter illuminates the nearby sea surface and is scattered toward the receiver. Both the direct and the sea-scattered signals are received. They are recorded or relayed to the ground for subsequent processing.

The basic feasibility of this technique was examined during the initial phase of this program, and the results reported in the final report on that phase.

issued in June 1972^{*}. The results of the initial study indicated the potential of the technique and demonstrated the need for an experimental test of the concept. The activities during this second phase investigation were devoted largely to defining the equipment requirements for an aircraft experiment, assembling and testing this equipment, and planning the experiment.

The primary results of this phase of the program are summarized and the Phase III activities are outlined in Section II of this report. In Section III the system requirements for the experimental hardware are discussed. Section IV consists of a detailed discussion of the experimental hardware design and performance characteristics. The last section discusses the aircraft experiment.

* "Bistatic Radar Sea State Monitoring", NASA CR-137469, G. T. Ruck, D. E. Barrick, and T. Kaliszewski, Research Report, Battelle, Columbus-Laboratories, Contract No. NAS6-2006 (June 1972).

II. SUMMARY OF RESULTS AND RECOMMENDATIONS

Program Summary

The objectives of this study have been the determination of specific experimental hardware requirements, the acquisition, assembly, and testing of the required experimental hardware, and the design of a field test experiment utilizing an aerial platform for the validation of the system concept. During this phase, design specifications for the experimental systems were prepared, a number of components of test hardware were designed, tested, and assembled, and a field test experiment using an aircraft receiving platform has been planned.

Results

Analysis of the experimental hardware requirements for an aircraft experiment reveal that Doppler processing to a resolution of 0.05 Hz will be required. This is due to the geometric Doppler imposed on the received signal, due to the aircraft's velocity, being smaller than the Doppler that would result when a satellite is used. This requires that the transmitter and receiver be capable of maintaining a relative coherency of the order of 1 part in 10^9 .

The only system concept meeting all the requirements is a linearly swept FMCW waveform capable of range resolutions of the order of 3 to 6 km and Doppler resolutions of the order of 0.04 Hz. The required waveform can be synthesized using commercially available digitally controlled frequency synthesizers.

The digital sweep controller-programmer units to generate the required control signals for these synthesizers have been designed, assembled, and tested. These units each utilize approximately 100 medium scale integration (MSI) TTL integrated circuits, and in effect constitute special-purpose minicomputers. To implement these units using conventional transistor circuits would have required approximately 1500 to 2000 transistors and associated components per unit.

A broadband transmitter which uses the frequency synthesizers as a driver has also been assembled and tested. In addition, a transmitting antenna assembly

with automatic switching of the required matching networks has been designed and assembled.

For the receiving system an automatic band-switching preselector and mixer assembly has been designed and assembled.

Some hardware design and experimental plan decisions have not been possible due to the unavailability of Government furnished equipment items and lack of knowledge of the specific GFE hardware available for the conduct of the experiment. It is expected that these will be made and the associated hardware completed early in the next phase.

The experiment planning has resulted in determining the required transmission frequencies, transmitting antenna calibration requirements, synchronization requirements for the transmitter and receiver, and suggested flight paths for the conduct of the experiment.

Recommendations

It is recommended that the Phase III effort be undertaken as soon as practicable. During this phase the following specific steps should be carried out:

- (1) complete the experimental hardware assembly and test,
- (2) complete the experiment planning,
- (3) carry out the flight test experiment, and
- (4) reduce and analyze the experimental data.

III. EXPERIMENTAL SYSTEM REQUIREMENTS

For a satellite-borne HF bistatic sea state sensor, the orbital motion of the satellite and the resultant Doppler shift imposed on the scattered signal can be used in conjunction with range resolution to determine the directional dependence of the ocean surface spectrum. Doppler spreads of as much as 40 to 50 Hz can result, and Doppler processing to provide a 1-Hz resolution would allow the surface spectrum directionality to be obtained with about a 10° resolution under these conditions.

For a typical aircraft-borne receiver, however, the Doppler spread would typically be of the order of a few hertz. Thus, to achieve the same surface resolution would require Doppler processing to a resolution of the order of 0.04 to 0.05 Hz. Doppler processing to this order presents several problems and complicates the experimental equipment requirements.

For an aircraft experiment, an alternative to the use of the signal Doppler for determination of the surface spectrum directionality is the use of the average signal polarization, and a proper experimental geometry. For example, for a flight path which is essentially a constant direction flight passing over, or near, the transmitting site, those surface regions which are intersected by a vertical plane through the flight path are the primary contributors to a horizontally polarized receiving antenna oriented along the flight path. A trailing wire would be representative of such an antenna. Thus, by using such a horizontally polarized antenna, combined with flights at a number of azimuths over the transmitter, the surface spectrum directionality can be estimated. For a horizontally polarized receiving antenna, unless a directional transmitting antenna is used, there will be a 180° ambiguity in the directional information obtained. For example, the upwind-downwind spectral component versus the crosswind spectral component can be obtained; however, the upwind component cannot be separated from the downwind component. The use of a directional transmitting antenna at the frequencies of interest is not generally possible due to space limitations on the ship or buoy.

It is desirable, however, to utilize a coherent waveform during the experiment and carry out Doppler processing. This would allow the unambiguous directional spectrum to be obtained, and would validate the concept of using the signal Doppler

for obtaining the directional spectrum. In addition, if the direct signal is available, such factors as variations in the transmitter power output and the transmitting and receiving antenna gains with operating frequency can be removed by referencing the scattered signal level to the direct signal level. If the direct signal is not available, these factors must be initially measured in order that the measured scattered signal levels can subsequently be corrected.

Two approaches could be utilized to achieve the required range and Doppler resolution for the aircraft experiment. These are a pulse-Doppler system and an FMCW chirp system.

The pulse-Doppler system requires an HF transmitter capable of being either stepped or swept over the HF band and which radiates a pulse train with pulse widths of the order of 10 to 20 μ sec. The receiver must have an IF bandwidth of 50 to 100 kHz, and both transmitter and receiver must have a frequency stability of the order of one part in 10^9 . The receiver would also require the necessary range-gating and Doppler processing circuitry. The only off-the-shelf equipment having properties resembling these requirements are various HF ionosondes. The specifications of several ionosondes, including those used with the Alouette, ISIS, and Explorer XX satellites, were examined to determine if they could be suitably modified for use in the aircraft experiment. The parameters and characteristics of these various HF ionosondes are such that the pulse widths are excessive for the experimental application and the frequency stability is not sufficient to allow the required order of Doppler processing. It appears that modification of such equipment to provide the required pulse widths and coherency along with the necessary range gating and Doppler processing circuitry would be expensive and time consuming. Thus, the modification of a conventional ionosonde to provide a pulse-Doppler system for the experiment did not appear tenable.

After examination of the available hardware, it was concluded that no pulse-Doppler system was available that possessed the fine Doppler resolution required for the experiment. Also, it would be prohibitively expensive to build or have built such a transmitter. Consequently, since the design and construction of an FMCW system appeared economically feasible and since such a system has advantages over a pulse-Doppler system for this application, the FMCW approach was chosen.

An FMCW hardware configuration meeting the experimental requirements consists of two digitally controlled HF frequency synthesizers. One is used to drive an amplifier capable of providing a power output of the order of 5 W and constitutes the transmitting equipment. The other is used as the local oscillator for the receiving equipment. An off-the-shelf HF communications receiver supplied by NASA will be used with this configuration. The two synthesizers constitute the most critical and expensive items in this configuration, with the rest of the required components, such as the transmitter power amplifier, receiver, recording equipment, etc, available either as off-the-shelf equipment or assembled at a nominal cost. This configuration also requires the assembly of the digital sweep controllers necessary to control and program the synthesizer switching so as to provide the required frequency sweeps.

The basic FMCW system is relatively simple, in that the transmitter radiates a coherent waveform which is swept over intervals of 50 to 100 kHz at a basic sweep rate of perhaps a megahertz, thus providing 10 sweeps per second. The frequency versus time waveform is essentially a sawtooth in shape. At the receiver, the local oscillator is synchronously swept over the same frequency interval at the same rate, except that the sweep starting points are delayed in frequency by an amount corresponding to the range delay between the transmitter and received. The receiver local oscillator is also offset by an additional fixed amount corresponding to a desired IF frequency. This is nominally somewhere in the HF band, and a conventional communications receiver will be used as the IF amplifier. The scattered signal, after mixing with the receiver local oscillator then has a spectral spread which corresponds to different ranges. At the receiver output, the signal for each sweep is sampled, A/D converted, and recorded on digital tape. The number of sweeps recorded is determined by the desired Doppler resolution. For example, if one recorded 256 sweeps at a rate of 10 sweeps per second, a Doppler resolution of 0.04 Hz would result. Typically, a 100-kHz bandwidth might be swept 10 times per second for 25.6 sec. If 128 received signal samples per sweep are recorded, then sufficient data would exist to generate 64 range cells with a 3-km resolution per cell and 256 Doppler cells with a resolution of 0.04 Hz per cell. These would be generated digitally by the application of the fast Fourier transform row by row and then column by column to the 128 x 256 matrix of data consisting of the 128 samples per sweep and the 256 sweeps. Actually, to save processing time, only the desired

range cells will be generated. Thus, only a few of the columns resulting from the first row-by-row transform will be subsequently transformed.

In terms of hardware requirements, the stability and spectral purity required of the transmitter and receiver local oscillator for the FMCW case are the same as for a pulse-Doppler system. For the FMCW waveform, however, no peak power problems exist and the IF bandwidth required in the receiver is comparable to that normally encountered in HF communications receivers. For example, with the waveform parameters quoted above, an IF bandwidth of only 1.28 kHz is required.

The FMCW approach does require good time synchronization between the transmitter and receiver, however. For example, a 1- μ sec. timing error in the sweep start time corresponds to a 0.3-km range error. This technique is very flexible in that extensive preprocessing data editing can be carried out if desired. For example, various weightings can be applied to reduce frequency sidelobes, the effects of aircraft acceleration on a curved flight path can be compensated, etc. This technique has been used recently for several applications. For example, several HF backscatter oblique ionosondes have very successfully used this approach.

The basic hardware requirements for an FMCW system are two digitally controlled frequency synthesizers with a high spectral purity and a stability of the order of 1×10^{-9} capable of operating in the frequency range from 3 to 30 MHz, and sweep controller-programmers for these synthesizers. A transmitter power amplifier, capable of supplying 1 W or more over the range from 3 to 30 MHz, is also required. The transmitting antenna system consists of a broadband vertical radiator and associated matching networks which are capable of operating satisfactorily over the range from 3 to 30 MHz. A block diagram of the transmitting equipment layout is shown in Figure 1.

The receiving equipment consists of one of the synthesizers and its associated sweep controller-programmer, an automatically band switchable RF preselector-mixer, and a conventional communications receiver. The output of the receiver will be recorded on an analog tape recorder for subsequent A/D conversion and recording or will be A/D converted and recorded directly. A block diagram of the receiving equipment layout is given in Figure 2.

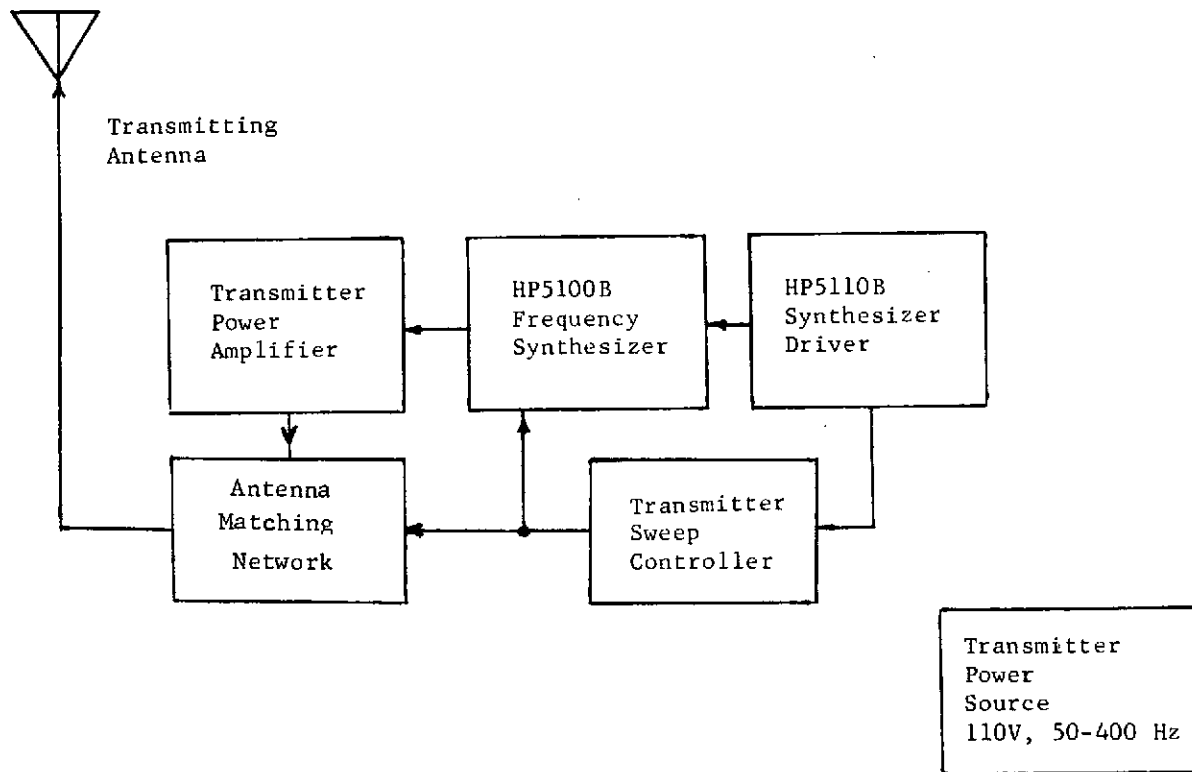


FIGURE 1. TRANSMITTING EQUIPMENT LAYOUT

ORIGINAL PAGE IS
OF POOR QUALITY

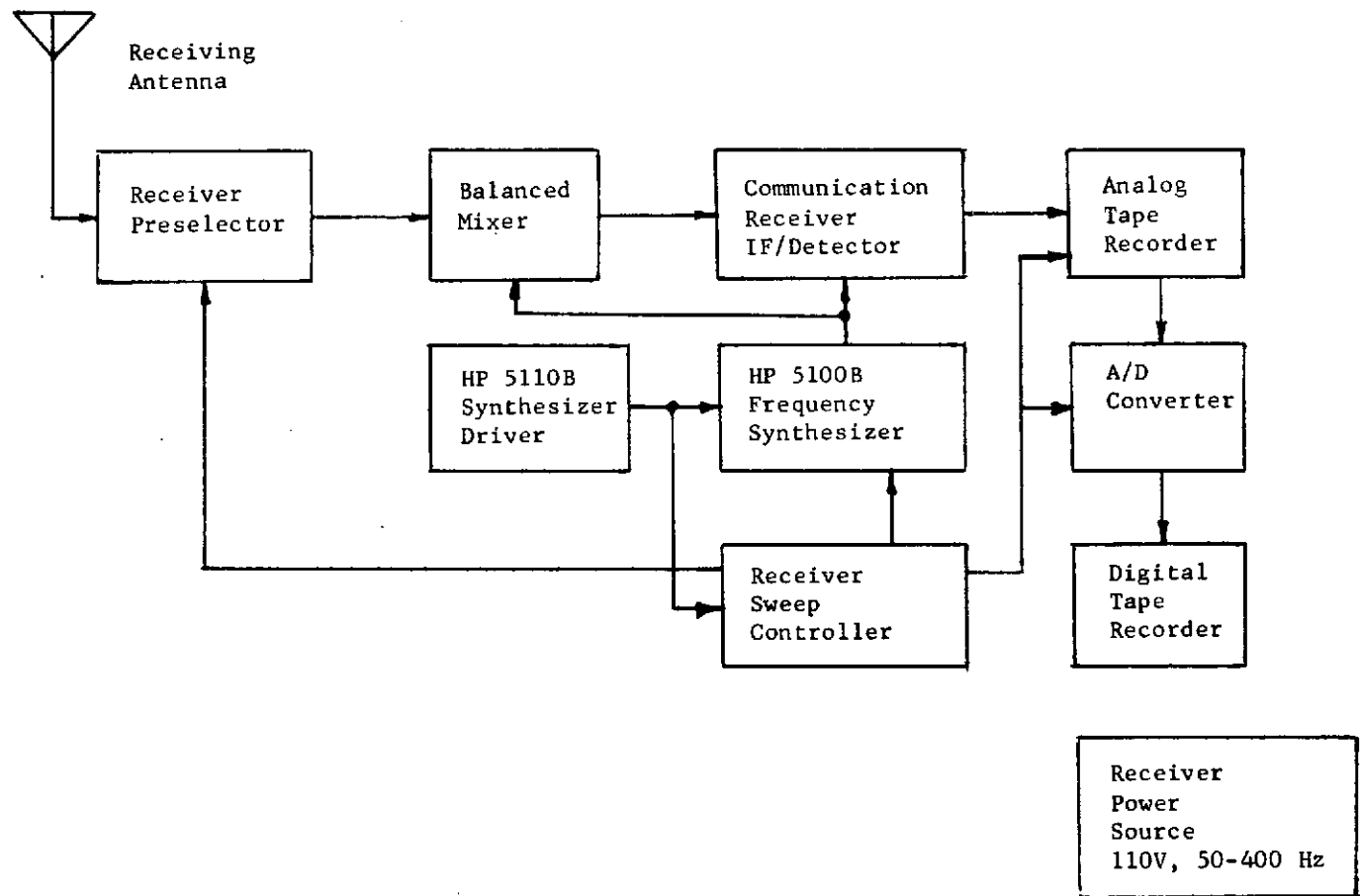
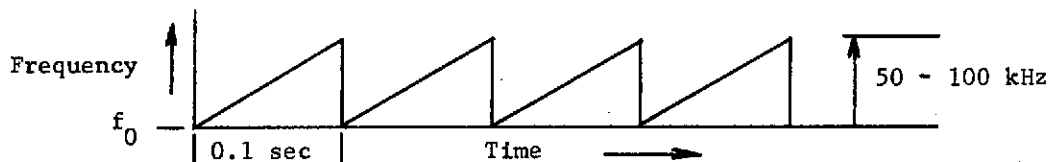


FIGURE 2. RECEIVING EQUIPMENT LAYOUT

The radiated waveform will consist of an FMCW signal which occupies a bandwidth of 50 to 100 kHz. The specific time waveform is shown below.



From 50 to 100 kHz sweeps of 0.1 sec. duration will be repeated 256 times over a total span of 25.6 sec. These basic 256 sweeps will be repeated in sequence at ten frequencies throughout the HF band from 3 to 25 MHz. The total time required to cover the entire band will be of the order of 5 min. The frequency allocation requirements are thus ten 100-kHz bands ranging from 3 MHz to the vicinity of 25 MHz.

It is desirable, if possible, that 100-kHz blocks be allocated which start at intervals of 0.1 MHz. For example, allocated frequencies might be as shown below:

<u>Band</u>	<u>Frequency Interval (MHz)</u>
1	3.1- 3.2
2	4.1- 4.2
3	5.1- 5.2
4	6.1- 6.2
5	7.1- 7.2
6	9.1- 9.2
7	12.1-12.2
8	15.1-15.2
9	19.1-19.2
10	25.1-25.2

The band should be spaced at intervals of approximately 1 MHz from 3 MHz to 7 MHz, and spaced at 2 to 3 MHz intervals from 7 to 15 MHz.

Of the equipment items required for the FMCW system, the following have been assembled at BCL during this investigation.

- Transmitting antenna and matching networks
- Transmitter power amplifier
- Transmitter sweep controller-programmer
- Receiver preselector
- Receiver mixer
- Receiver sweep controller-programmer

The items required to be supplied by NASA are

- 2 Frequency synthesizers
- 2 Synthesizer drivers
- 1 Communication receiver
- 1 Frequency standard
- 1 Analog tape recorder
- Verification equipment
- Necessary power for transmitting and receiving equipment

Specific requirements for the equipment to be supplied by NASA are as follows.

Frequency Synthesizer/Driver

Recommended Model: Hewlett-Packard HP 5100B Synthesizer, HP 5110B Driver.

Critical Specifications:

- Frequency coverage of 3 to 30 MHz in minimum 10-Hz steps
- Frequency switching speed of 10 μ sec. or less
- Frequency stability of ± 3 parts in 10^9 per day

The switching speed specification is essential in order to achieve an FMCW waveform with the required time-delay resolution. The frequency stability specification is necessary to achieve the required Doppler resolution. The HP synthesizer is preferred because BCL personnel are familiar with its circuitry and the modifications required to utilize this equipment. If a different synthesizer is used, additional costs and time delays could be incurred. These items should be acquired by Wallops Station on a permanent basis if possible because of the modification required and their possible subsequent use for GEOS-C ground truth measurements.

In the event that the HP 5100B and 5110B are not available, the earlier models 5100A and 5110A can be used although they will require more modification.

Analog Magnetic Tape Recorder

Critical Specifications:

- Instrumentation recorder
- Minimum of 4 channels
- S/N ratio 20 to 40 dB
- Direct record bandwidth needed

<u>Tape Speed (ips)</u>	<u>3-dB Passband (kHz)</u>
7-1/2	0.5 - 125
3-3/4	0.5 - 63
1-7/8	0.5 - 35

- Supply voltage 115/230 V single phase, 50 to 400 Hz, weight 50 to 75 lb
- Portable

The above specifications are considered to be typical of the characteristics available from most commercial instrumentation recorders. Typical models are Sanborn Model 2004, Borg Warner Model R-106 or R-206, Hewlett-Packard HP 3960.

Communications Receiver

The plan for fabricating an FMCW radar receiver is to use an appropriate communications receiver as an intermediate frequency amplifier. The frequency synthesizer will be used to provide the required local oscillator signal in place of the local oscillator contained in the receiver. Thus, it is desirable that if other than a single conversion receiver is acquired, all the local oscillator signals used in the various frequency conversion stages be coherently derived from a single master-oscillator. With respect to the other receiver characteristics any high-quality communication receiver with an overall IF bandwidth of 2 to 3 kHz will be

satisfactory. It is desirable that the receiver be capable of operating on 110 V, 50 to 400 Hz power, although this is not absolutely necessary.

Again, this receiver must be modified for use on the experiment and will require remodification to return it to its original state.

Frequency Standard

A frequency standard is desired for several reasons. The first is to serve as a reference oscillator in the laboratory to verify the frequency characteristics of the synthesizers and to verify the transmitter waveform characteristics. The second is to serve as a stable reference source to synchronize and calibrate the synthesizers in the transmitter and receiver prior to making radar measurements. If the frequency stability characteristics of the HP 5110B driver oscillators are not adequate, a frequency standard can also be used as a reference oscillator in the transmitter or in the receiver. The specific frequency standard could be a high-precision quartz oscillator, a Rubidium standard, a Cesium standard, or standard signals derived from WWVB.

Power Supplies

110 V, 50 to 400 Hz supplies are required for both ground and airborne equipment.

Ground Based Equipment

<u>Equipment</u>	<u>Power (W)</u>	<u>Weight (lbs)</u>
Power Amplifier	50	10
Frequency Synthesizer	35	75
Driver	35	54
Controller	35	54
Digital Power Supply	<u>35</u>	<u>5</u>
Totals	190	198

Airborne Equipment

<u>Equipment</u>	<u>Power (W)</u>	<u>Weight (lbs)</u>
Preselector	40	10
Frequency Synthesizer	35	75
Driver	35	54
Communications Receiver	75	25
Sweep Controller	35	50
Tape Recorder	80	75
Digital Power Supply	<u>35</u>	<u>10</u>
Totals	335	299

The power generating equipment should be capable of providing approximately 115/230 V 50 to 400 Hz at 0.5 to 1 kW for both the airborne and ground installations.

Verification Equipment

These items such as wave spars or a laser profilometer, etc, are required to independently measure the wave height spectrum in the region of observation. It is anticipated that this equipment will be installed at NASA's Chesapeake light tower site or on board a NASA aircraft.

IV. EXPERIMENTAL HARDWARE DESIGN ASSEMBLY AND TEST

The specific components of the experimental hardware assembled by BCL consisted of those components which were not available commercially. In particular, this included the sweep controller-programmers for both the transmitter and receiver, the transmitter power amplifier, the transmitting antenna and matching networks, and the preselector and mixer assemblies for the receiving system. The key components of the entire experimental system are the sweep controller-programmers which provide for all timing functions including the fine frequency steps for the synthesizers, initiation of each sweep, and all band switching. Those components which require bandswitching, such as the transmitting antenna matching networks and the receiver preselector tuned circuits, are switched automatically under the direct control of the respective sweep controller-programmer with time synchronization between the two units maintained to less than one microsecond.

Sweep Controller-Programmer Requirements

In the FMCW system, a signal whose frequency is a linear function of time is synthesized in the transmitter. An identical synchronized sweep is synthesized in the receiver for demodulation of the received time-delayed ramps of frequency versus time, giving at the receiver output audio tones proportional to time delay. Various modes are then separated by spectral analysis. Thus, range and Doppler gating are accomplished digitally in nonreal time.

The primary building block of both the FMCW transmitter and receiver is the frequency sweep control module and its programming circuitry. There are a number of frequency synthesizer instruments available which can be programmed to produce a linear frequency ramp. They are of two types, (1) those using indirect methods involving phase-locked oscillators, and (2) those using direct methods involving arithmetic operations (multiplication, division, and mixing) of a set of fundamental frequencies simultaneously available from a frequency standard. Investigators who have considered this problem in the past have concluded that with the indirect synthesizers, frequencies cannot be switched sufficiently fast enough to be used as FMCW radar sweep oscillators. Of the commercially available synthesizers of the direct type, the Hewlett-Packard HP 5100/5110 instruments have been used successfully for

this application in the past. Since they have been manufactured for about 7 years, it was concluded that they would likely be among available NASA equipment. Consequently, it was decided to design the transmitter and receiver circuitry around the HP 5100/5110 instruments.

The HP 5110 driver module supplies the 5100 synthesizer module with 22 fixed-frequency, spectrally pure, signals derived from an internal 1-MHz quartz oscillator. These signals are the basis for the digital synthesis of the output frequency. The desired output frequency is generated, digit by digit, by a straightforward mathematical process in which one of ten frequencies is chosen, divided by ten, and added to the next choice. The process is repeated until the selected frequency has been completely generated as illustrated in Figure 3. The output frequency may be selected with push-buttons located on the front panel of the synthesizer or it may be programmed remotely by a digital programmer module which supplies the proper logic levels to each of ten cable lines to each controlled frequency decade.

The top waveform in Figure 4 shows the desired sweep as a function of time. The bottom waveform in Figure 4 shows the design goal to be achieved by using the HP synthesizer. The equivalent time (range) resolution of this waveform is approximately the reciprocal of the transmitted bandwidth, i.e., 10 μ s. The Doppler resolution is approximately the reciprocal of the integration time, i.e., the duration of the sweep waveform at a fixed band between F_1 and F_2 . The sweep duration has been chosen to be 25.6 sec. consisting of 256 sweeps each of duration of 1/10 sec. 256 was chosen since it is the nearest power of 2 which will give the required Doppler resolution of 0.05 Hz. Having a number of samples which is a power of 2 is desirable since fast Fourier transform (FFT) algorithms, which will be used to process the measured data in range and Doppler, are most conveniently applied to data sets having dimensions of a power of 2.

Sweep Controller-Programmer Module Design

As indicated previously, the dwell time of the synthesizer at a constant frequency along the frequency ramp is 10 μ sec. Consequently, the switching time of the programmer/synthesizer combination must be much smaller than 10 μ sec., on the order of 1 μ sec. This is a critical requirement which eliminated all of the indirect synthesizers

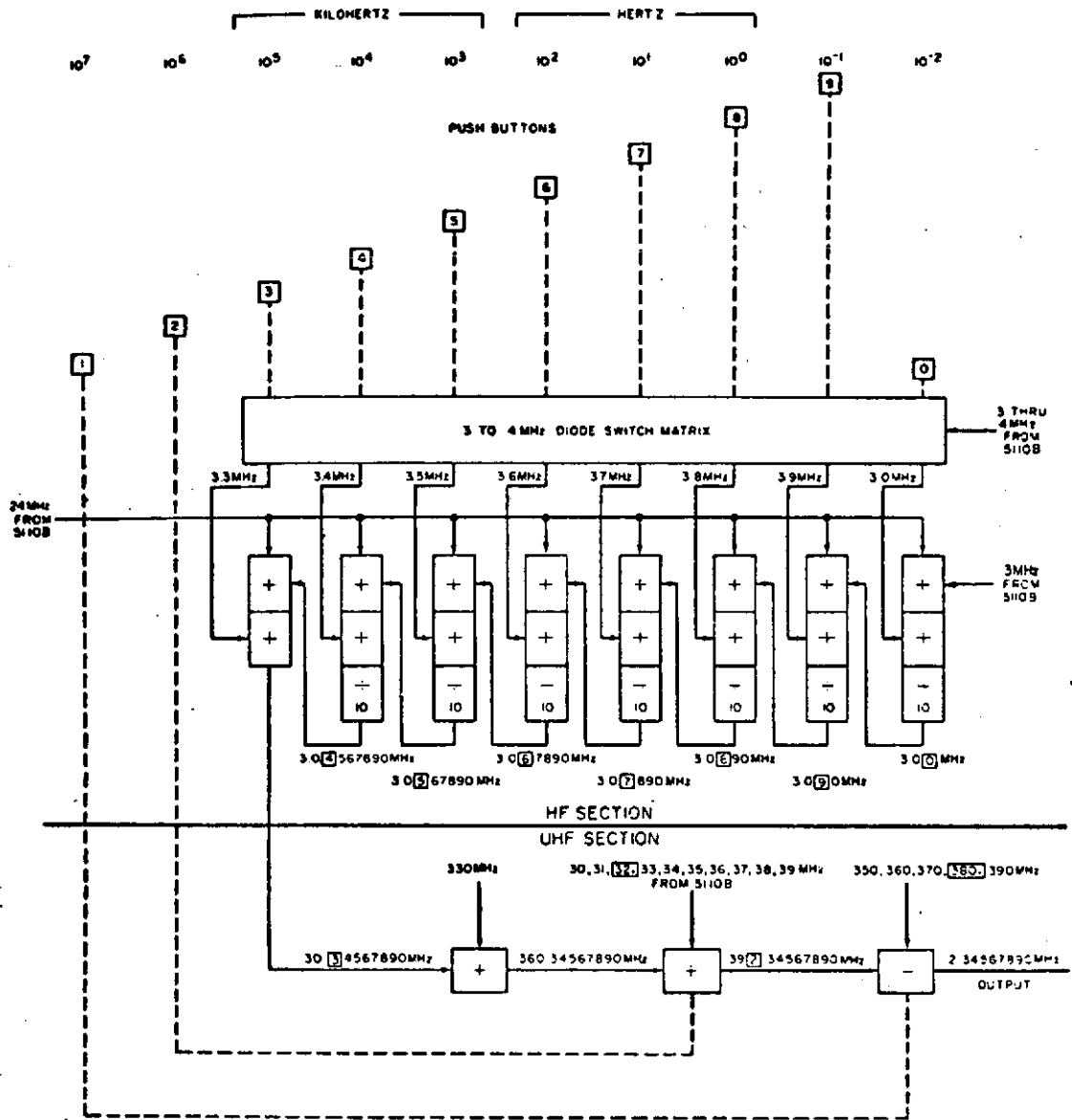


FIGURE 3. INDIRECT SYNTHESIS OF FREQUENCY 12345678.90 Hz USING HP 5100B FREQUENCY SYNTHESIZER

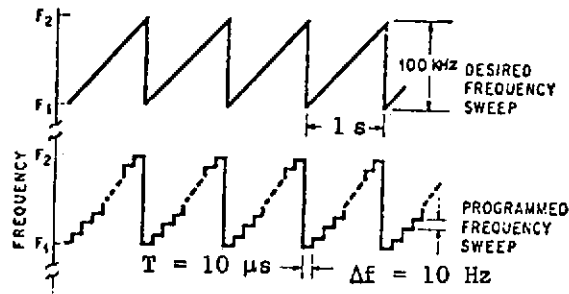


FIGURE 4. FREQUENCY SWEEP WAVEFORMS

and almost all of the direct synthesizers from consideration for use in this system. The switching time of the HP synthesizer as built by the manufacturer varies according to which decade is being switched and increases with decreasing frequency. For the lowest frequency decade which must be programmed (the ten's decade), the switching time is specified by the manufacturer to be at most 20 $\mu\text{sec.}$, which is too large to achieve the desired sweep waveform. However, this time can be reduced by modifying the circuitry within the 3 to 4 MHz diode switching matrix of the synthesizer. Since the actual HP instruments were not available during design of the synthesizer programmer, the switching characteristics of the synthesizer were simulated by fabricating the critical circuitry of the diode switching matrix. Modifications were made to reduce the time constant of the switching network. This modified circuit was used as a dummy load to test the design of the sweep programmer in the laboratory. 10- $\mu\text{sec.}$ pulses with a rise time of less than 1 $\mu\text{sec.}$ were achieved at the switching points of the modified diode switching matrix.

Figure 5 shows a block diagram of the sweep programmer design. Each of seven decade circuit boards provides the output of the programmer directly to the synthesizer via ten lines, one for each possible digit for the decade. The logic levels are generated digitally on each decade board according to signals generated on the control board. The clock board generates certain fundamental digital clock frequencies which are synchronized with a fundamental 1-MHz sinewave oscillator signal available from the 5110 driver. Thus, all digital circuitry is synchronized with the quartz frequency standard in the driver. The load-address register and initial-frequency register are thumbwheel switches mounted on the front of the sweep controller

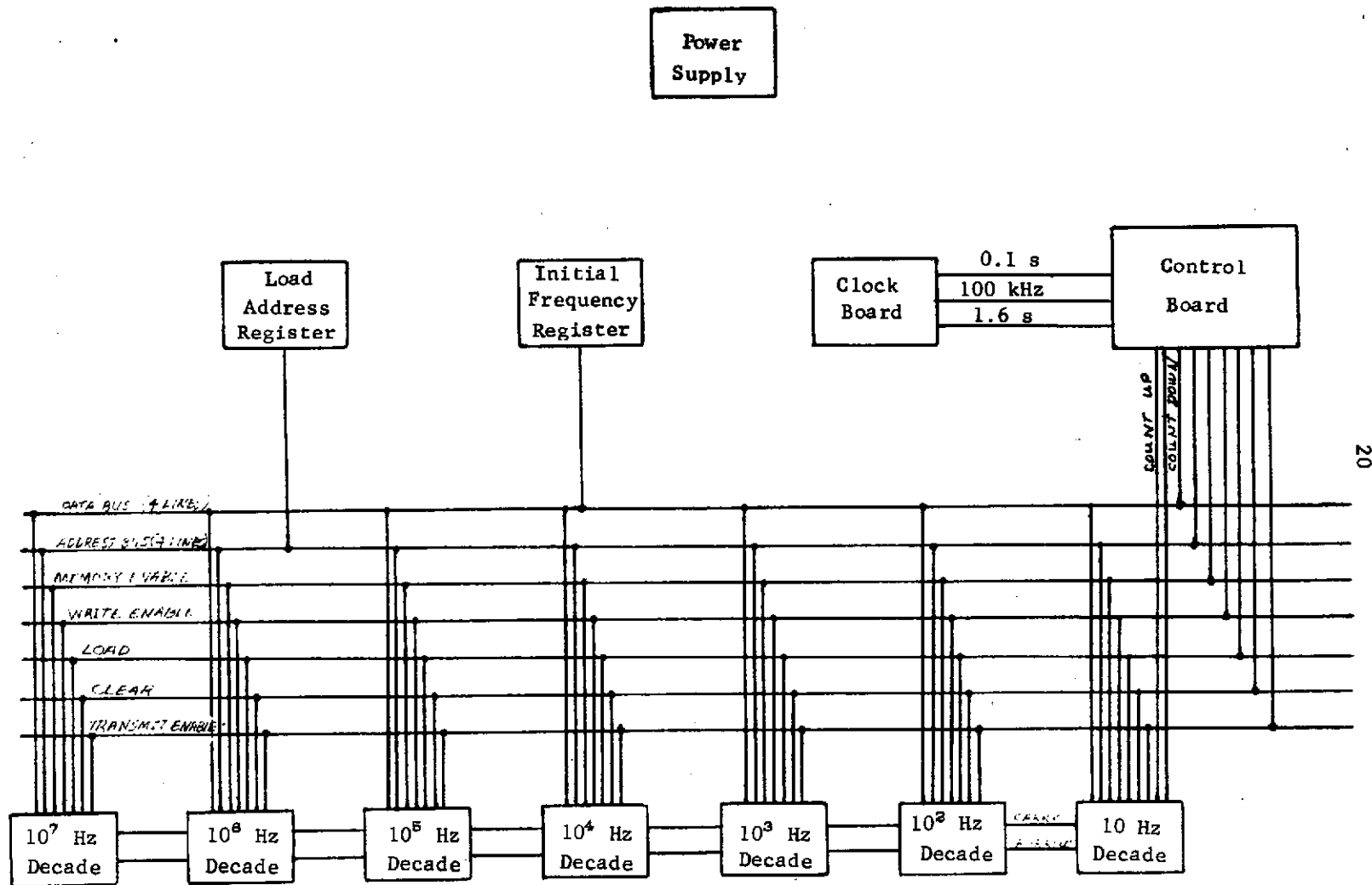


FIGURE 5. BLOCK DIAGRAM OF SWEEP PROGRAMMER

programmers and are used to load initial frequency conditions into storage registers located on each decade board. These initial conditions consist of ten, seven-digit start frequencies. A frequency ramp of 50 or 100 kHz with respect to a preset start frequency is generated in succession for each of ten frequency bands. A basic frequency-band period of 30.4 sec. is used. 25.6 sec. is used to transmit 256 sweeps each of 1/10 sec. duration. The remaining 4.8 sec. are used to change address pointers which select the next start frequency location, and to switch in appropriate matching networks in both the transmitter and receiver front ends. In addition, a pilot or marker pulse of constant frequency at the start frequency is transmitted prior to sweep initiation in each frequency band.

Digital Logic

The basic logic component used in the design of the sweep programmer was TTL logic. This choice was made because (1) TTL is sufficiently fast for this application, (2) the TTL logic family has a larger selection of components than others, (3) TTL components are in abundant supply, and (4) TTL components are cheaper than those of newer logic families. TTL logic levels are about 0.2 V for the low state (logical 0) and about 3.3 V for the high state (logical 1). These levels are not directly compatible with the logic levels required to drive the HP synthesizer, but neither are those of any other MSI or LSI logic family. Consequently, a level-conversion driver stage is required to interface between the TTL logic and the HP synthesizer.

Clock Board Description

Figure 6 contains a wiring schematic for the clock board design. The basic design consists of a sequence of 74192 synchronous decade counters. Each counter is in effect a divide-by-ten element so that starting with a basic 1-MHz clock frequency, each counter carry terminal provides a clock frequency one-tenth that provided at the input count-up terminal. The output waveforms consist of negative pulses with the pulse width always one-tenth the pulse period of the signal. A 74193 divide-by-sixteen binary counter driven by a 10-Hz clock signal provides a

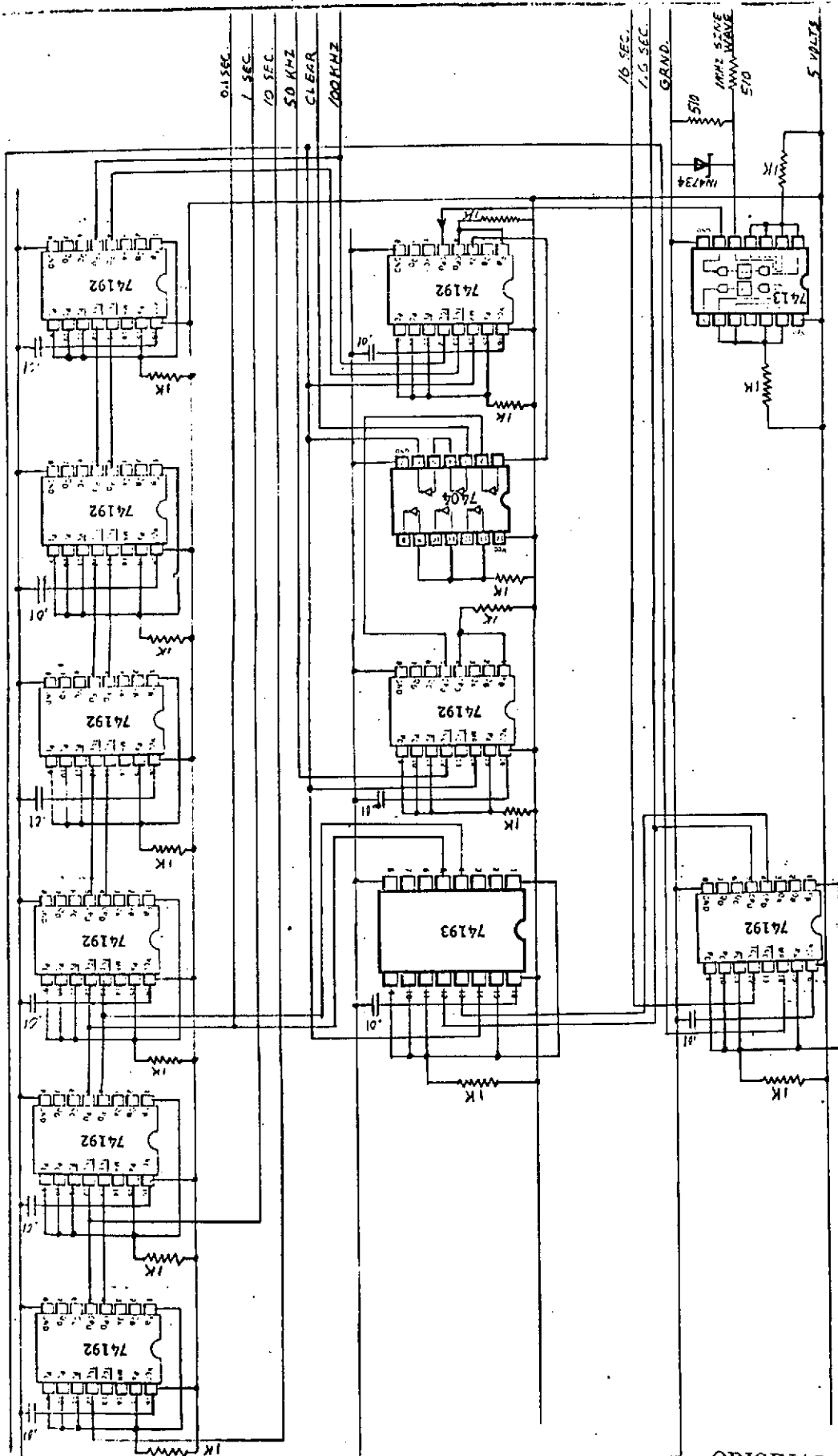


FIGURE 6. WIRING SCHEMATIC OF CLOCK BOARD

ORIGINAL PAGE IS OF POOR QUALITY

1.6 sec. period pulse train for timing the basic 30.4 sec. transmission cycle for each HF frequency band. The 100-kHz or 50-kHz clock frequencies are used to drive the ten's decade on the HP synthesizer to obtain the basic frequency ramp. The first 74192 counter is driven by a waveform derived from a 1-MHz rectified sine wave fed through a 7413 schmidt trigger. The waveforms at input and output of the 7413 are shown in Figure 7.

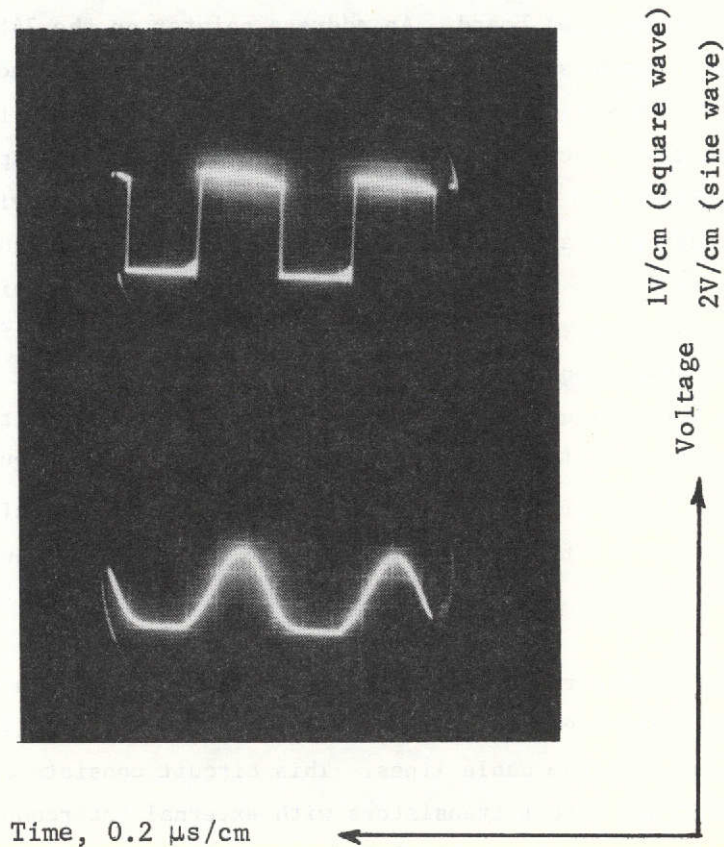


FIGURE 7. VOLTAGE WAVEFORMS AT INPUT AND OUTPUT OF CLOCK DRIVER NETWORK

Decade Board Description

Figure 8 contains a wiring schematic for the decade board design. The basic logic elements include a 7489 read/write memory, a 74192 synchronous BCD decade counter, a 7442 BCD-to-decade decoder, and five 75450A dual peripheral drivers. The 7489 is a 64-bit active-element memory array of 64 flip-flop memory cells organized in a matrix of 16 four-bit words addressable in binary code. It is used to store the set of ten start frequencies, one for each HF band for which measurements are made. The start frequencies are loaded manually before the measurement runs via the initial-frequency and load-address registers on the programmer front panel. At the beginning of each sweep period, the appropriate start frequency digit is loaded into the 74192 counters on all decade boards simultaneously via data input lines upon commands from the control board. An address pointer on the 7489 address lines is maintained on an address bus fed by an address register located on the control board. At this time, a 100-kHz clock signal is fed into the count-up terminal of the 74192 counter on the ten's decade, and the counter begins counting up at this frequency. The carry-out line from the ten's decade board is used to provide a clock input to the hundred's decade board and the remaining 10^3 , 10^4 , 10^5 , 10^6 , 10^7 Hz boards are fed clock signals each from the next lower-frequency board. In this way, the synthesizer is stepped synchronously by ten hertz steps at a 100-kHz rate for one-tenth second, achieving a 100-kHz frequency ramp beginning at a preset start frequency. The actual drive signals are obtained by first decoding the 74192 four-bit BCD-coded output to a one-of-ten-line output via the 7442. Each of the ten 7442 output lines is connected directly to one input of a 75450A dual peripheral driver circuit; the corresponding output of this circuit feeds directly one line of the ten connected to the input lines for this specific decade on the HP 5100.

The 75450A circuit, shown in Figure 9, provides both a level translation from TTL to HP logic levels as well as sufficient drive capability to switch the HP via the remote-program cable lines. This circuit consists of TTL NAND-gate inputs and high-current NPN output transistors with external interconnections. In addition, the substrate of the IC chip is isolated internally from the ground terminal and can be carried at a substantial negative voltage with respect to TTL logical zero. This feature is necessary because the logic level shift involved, when one uses the voltage sources supplied by the synthesizer for this purpose, consists of a voltage change

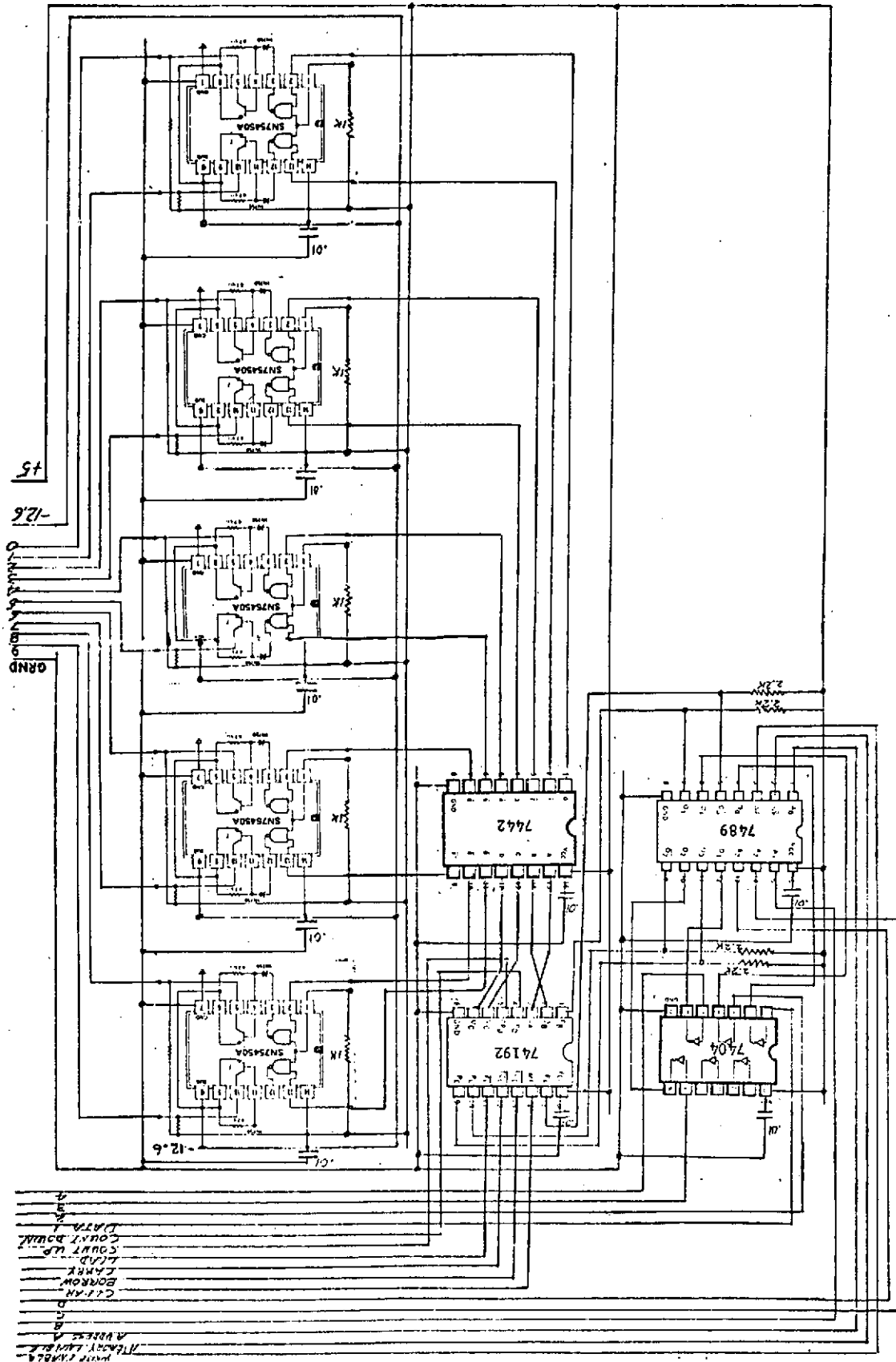


FIGURE 8. WIRING SCHEMATIC OF DECADE BOARD

ORIGINAL PAGE IS
OF POOR QUALITY

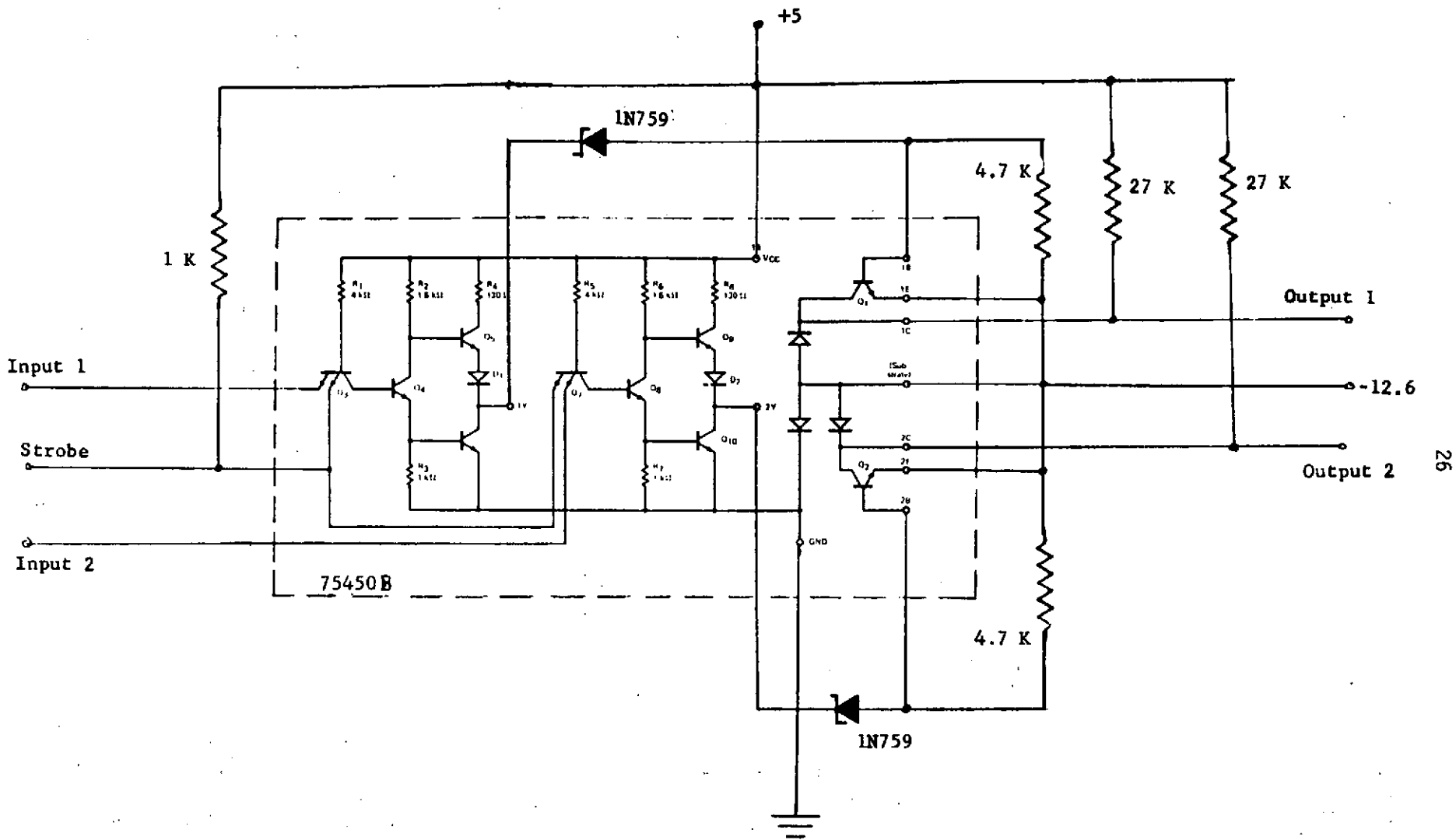


FIGURE 9. EQUIVALENT CIRCUIT OF 75450B DUAL PERIPHERAL DRIVER AND EXTERNAL DISCRETE COMPONENTS

from about +1.5 V to -12.6 V in order to activate a decade line (analogous to depressing a push-button on the front panel). The 75450B output transistors can sink at least 300 mA of current from the load, much more than required for the HP synthesizer.

The details of the 75450B circuit, including elements internal to the IC and external discrete components, are shown in Figure 9. The circuit functions as follows: consider circuit 1. The strobe input to Q_3 is tied high so that the output of the NAND gate (1Y) is high only when input 1 is low. When output 1Y goes high, the reverse-bias voltage across the zener diode (between points 1Y and 1B) is sufficient to put the diode in the zener region, and it conducts in the reverse direction, turning on transistor Q_1 . When Q_1 conducts, its collector-to-emitter voltage drop is sharply reduced, clamping output 1 to the negative voltage supply through the collector-to-emitter junction. When Q_1 is turned off, output 1 is clamped to the +5 volt supply through the 27 K resistor. A truth table describing the logical operation of the 74192/7442/75450 combination is presented in Table 1.

Control Board Description

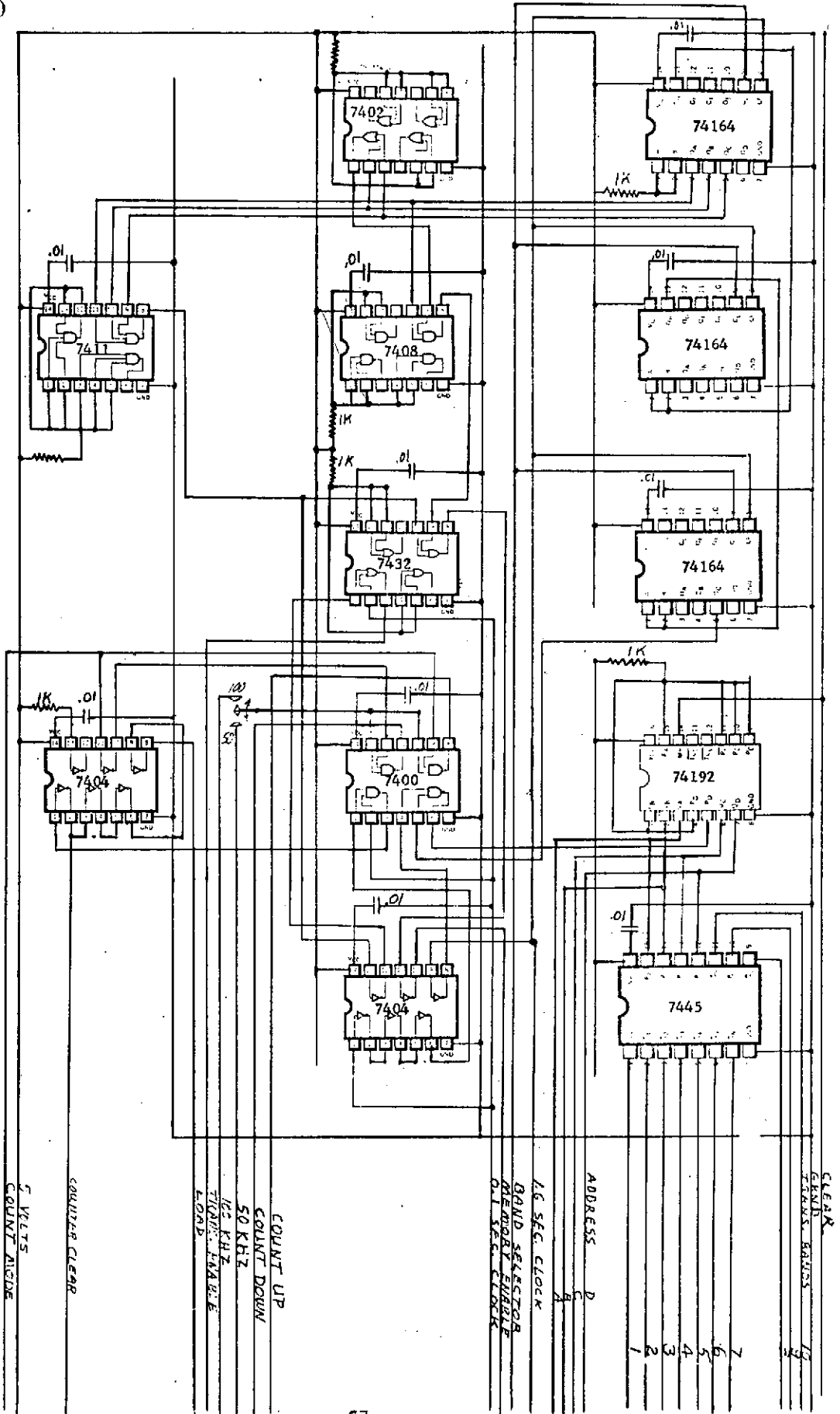
Figure 10 contains a wiring schematic for the control board design. This circuit provides a sequence of timing signals to the decade boards to drive the HP synthesizer so that the output of the synthesizer consists of ten consecutive groups of 256 frequency ramps each. The length of each group is 30.4 sec. as described previously and the ten preset start frequencies are used in sequence to operate in ten different frequency bands. The 30.4-sec. interval consists of three 1.6-sec. periods preceding the 25.6-sec. sweep period. During the first 1.6-sec. period, the synthesizer is turned off to allow time for band switching of front-end matching networks. Then, a 1.6-sec. constant-tone burst at the start frequency is transmitted followed by another 1.6-sec. off period. The basic 30.4-sec. timing is secured by means of three 74164 eight-bit shift registers driven by the 1.6-sec. clock signal from the clock board. Combinatorial circuitry using the first three outputs of the first 74164 shift register provides the basic transmitter off-on-off-on sequence of 1.6, 1.6, 1.6, 25.6 sec. A signal with 30.4-sec. period is obtained from the third stage of the third shift register. This signal is used to terminate the sweep sequence, reset the shift registers back to zero, and to increment the 74192 counter which provides the address register function.

TABLE 1. TRUTH TABLE FOR DECADE BOARD OPERATION

Decimal Count	74192 State					7442 Inputs				7442 Outputs				also		75450 Inputs		also		75450 Outputs	
	D	C	B	A	Carry	D	C	B	A	0	1	2	3	4	5	6	7	8	9		
0	L	L	L	L	H	L	L	L	L	L	H	H	H	H	H	H	H	H	H	H	
1	L	L	L	H	H	L	L	L	H	H	L	H	H	H	H	H	H	H	H	H	
2	L	L	H	L	H	L	L	H	L	H	H	L	H	H	H	H	H	H	H	H	
3	L	L	H	H	H	L	L	H	H	H	H	H	L	H	H	H	H	H	H	H	
4	L	H	L	L	H	L	H	L	L	H	H	H	H	L	H	H	H	H	H	H	
5	L	H	L	H	H	L	H	L	H	H	H	H	H	H	L	H	H	H	H	H	
6	L	H	H	L	H	L	H	H	L	H	H	H	H	H	H	L	H	H	H	H	
7	L	H	H	H	H	L	H	H	H	H	H	H	H	H	H	H	L	H	H	H	
8	H	L	L	L	H	H	L	L	L	H	H	H	H	H	H	H	H	L	H	H	
9	H	L	L	H	L	H	L	L	H	H	H	H	H	H	H	H	H	H	H	L	
0	L	L	L	L	H	L	L	L	L	L	H	H	H	H	H	H	H	H	H	H	

- Notes: (1) L applied to 74192, 7442, 75450 inputs implies low TTL state (~ +0.2 V)
 (2) L applied to 75450 output implies a large negative voltage (-5 to -12 V)
 (3) H applied to 74192, 7442, 75450 inputs implies high TTL state (~ +3.3 V)
 (4) H applied to 75450 output implies a small positive voltage (~ +1 V)

FIGURE 10. WIRING SCHEMATIC OF CONTROL BOARD



At the top of each frequency ramp, a series of three submicrosecond pulses are generated using combinatorial logic and driven by the one-tenth-second clock signal to (1) terminate the clock drive to the decade board, (2) activate the counter clear line, and (3) activate the load line, in that sequence. The purpose of this pulse sequence is to turn off the transmission at the top of the frequency ramp long enough to clear the decade-board registers to zero and to again load the start frequency digits into the decade board registers before commencing the next sweep.

Simulated-Load Waveforms

The performance of the decade-board drivers in switching the HP synthesizer was simulated in the laboratory by fabricating the critical circuitry of the diode switching matrix which is used in the HP synthesizer to switch on and off various reference frequencies when a frequency change is entered, either by remote programming or by means of push buttons. Figure 11 shows the circuit used to simulate the load on the 75450 output drivers. In order to decrease the time-constant of this circuit, the value of the capacitance (0.01 μ F in the synthesizer) was reduced to 30 pF. A rise time measurement was made at the switching point where the three diodes are connected. This point is either at a positive voltage (when the channel is inactive) or at a negative voltage (when the channel is active). The signal channel passes through the two germanium diodes, CR2 and CR3, which are forward-biased when the switching point voltage is negative and are reverse-biased when the switching point voltage is positive. Figure 12 shows the voltage waveforms observed at the switching points of two simulated loads driven by adjacent output lines from 75450 drivers on a decade board. The decade board was driven by the basic 100-kHz clock signal from the clock board. The pulse widths are 10 μ sec. and the pulse periods 100 μ sec. The rise time is clearly less than 1 μ sec. It was not possible to test the programmer design further without having an HP 5100 synthesizer available in the laboratory to check the switching time of the entire system.

Sweep Controller-Programmer Physical Layout

Each of the sweep controller-programmer modules consists of 10 plug-in printed circuit cards. One card contains the basic clock circuits, one card contains the basic control circuitry, seven identical cards contain the decade counter circuitry, and one

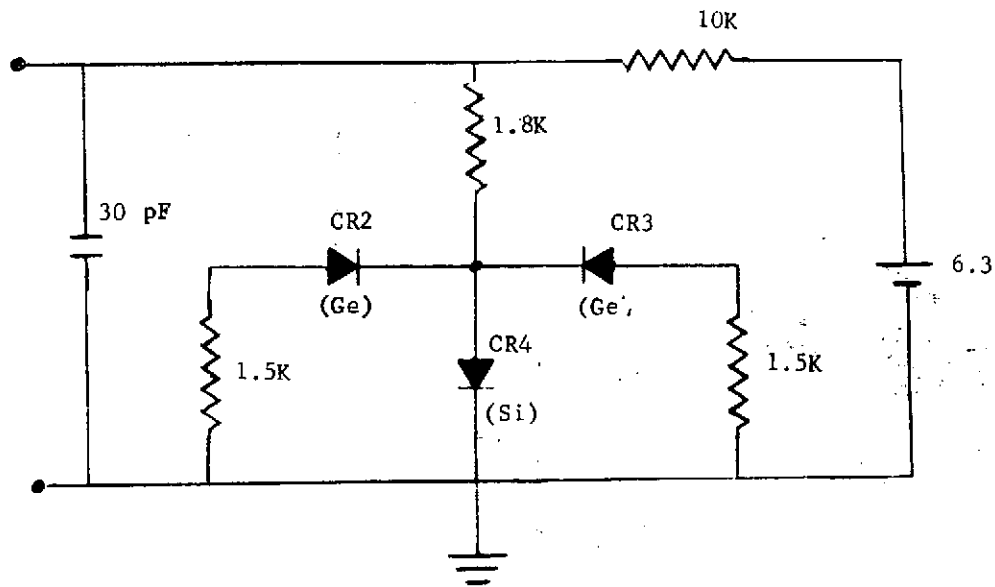


FIGURE 11. DUMMY LOAD TO TEST RISE TIME OF HP DRIVER CIRCUIT

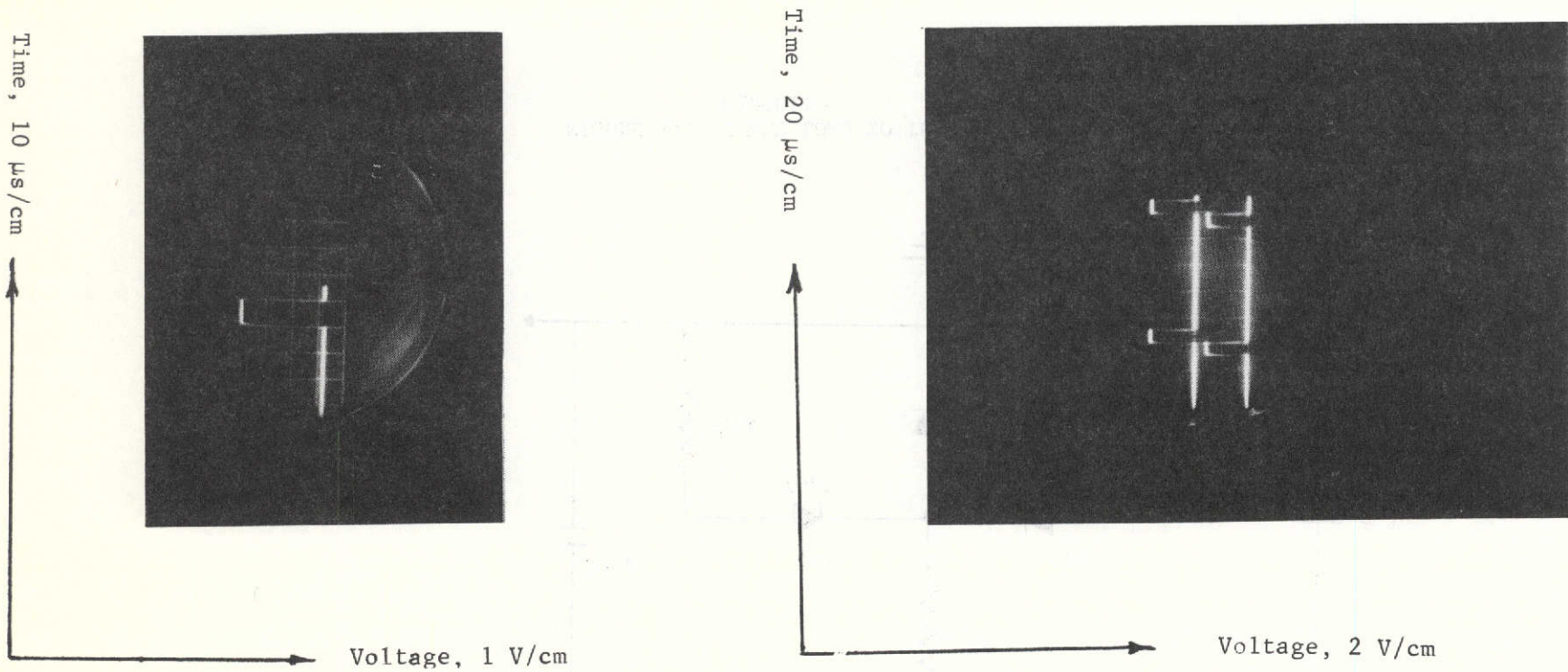


FIGURE 12. PULSE WAVEFORMS AT SWITCHING POINTS OF SIMULATED HP 5100 DIODE MATRIX LOAD

contains miscellaneous logic and control circuits such as 75450 relay drivers which supply switching control pulses to the stepping motor relays for bandswitching. The printed circuit board layout for the seven decade boards is illustrated in Figures 13 and 14. These boards are 5 x 7 in., double-sided G-10 boards with 44-pin connectors.

The front panel of the module contains one seven-decade thumbwheel switch for programming the starting frequency of each band into the internal memory, and a one-decade thumbwheel switch for selecting the specific band being programmed.

A power supply capable of supplying the required +5 V for the TTL integrated circuits from a basic 110 V, 50 to 400 Hz power source is also included with each module.

Broadband HF Linear Power Amplifier

The Hewlett-Packard HP 5100B frequency synthesizer is used as the main source of RF energy in the frequency range from 3 to 30 MHz. Unfortunately, its power output in this frequency range is limited to a maximum of 20 mW when terminated in a 50-ohm load. The experimental hardware requirements mentioned previously indicate that approximately 1 W of average power is required from the transmitter in the HF region. Consequently, a broadband HF power amplifier was constructed to meet this requirement. This amplifier is required to match the 50-ohm output impedance of the frequency synthesizer to a 50-ohm transmission line. Moreover, when impedance matching over bandwidths in excess of an octave are required, reactive elements in the form of L, T, or Pi networks cannot practically maintain proper impedance transformations. The 3 to 30 MHz frequency requirement represents almost 4 octaves in frequency; a requirement decidedly beyond the capabilities of reactive matching networks. Transformers, on the other hand, are useful components for impedance matching. However, at HF frequencies, something other than conventional core material must be used. Also, not to be neglected is the interwinding capacitance which tends to destroy transformer action at high frequencies. Fortunately, a special form of transformer known as a "transmission line transformer" can be used to circumvent these difficulties and have found numerous small-signal applications. These transformers are simply constructed, inexpensive, light weight, and, most important, are capable of very wide bandwidths. They consist of transmission line (twisted pairs) wound on high-permeability cores

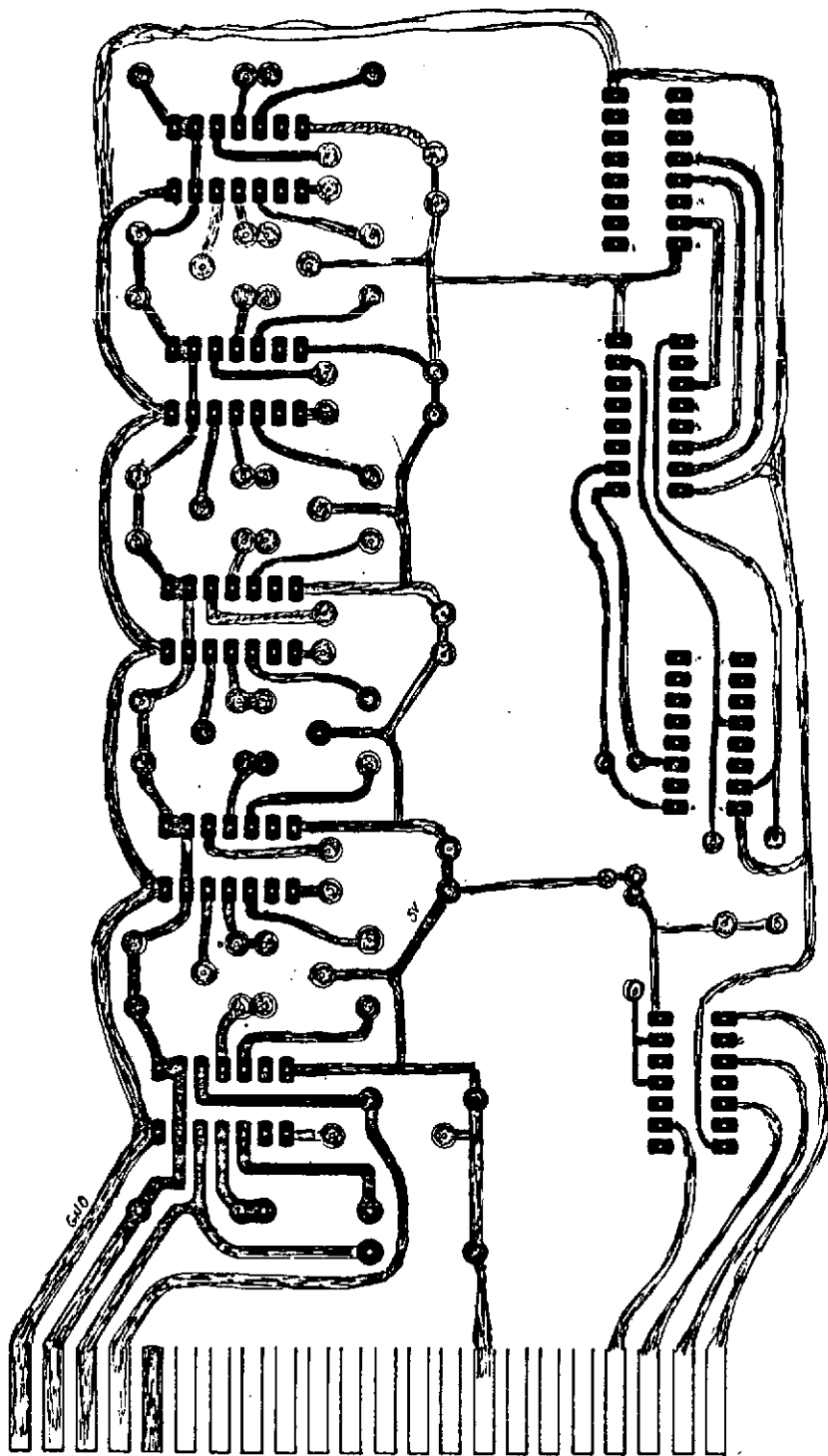


FIGURE 13. CIRCUIT-BOARD LAYOUT FOR DECADE BOARD (TOP SIDE)

ORIGINAL PAGE IS
OF POOR QUALITY

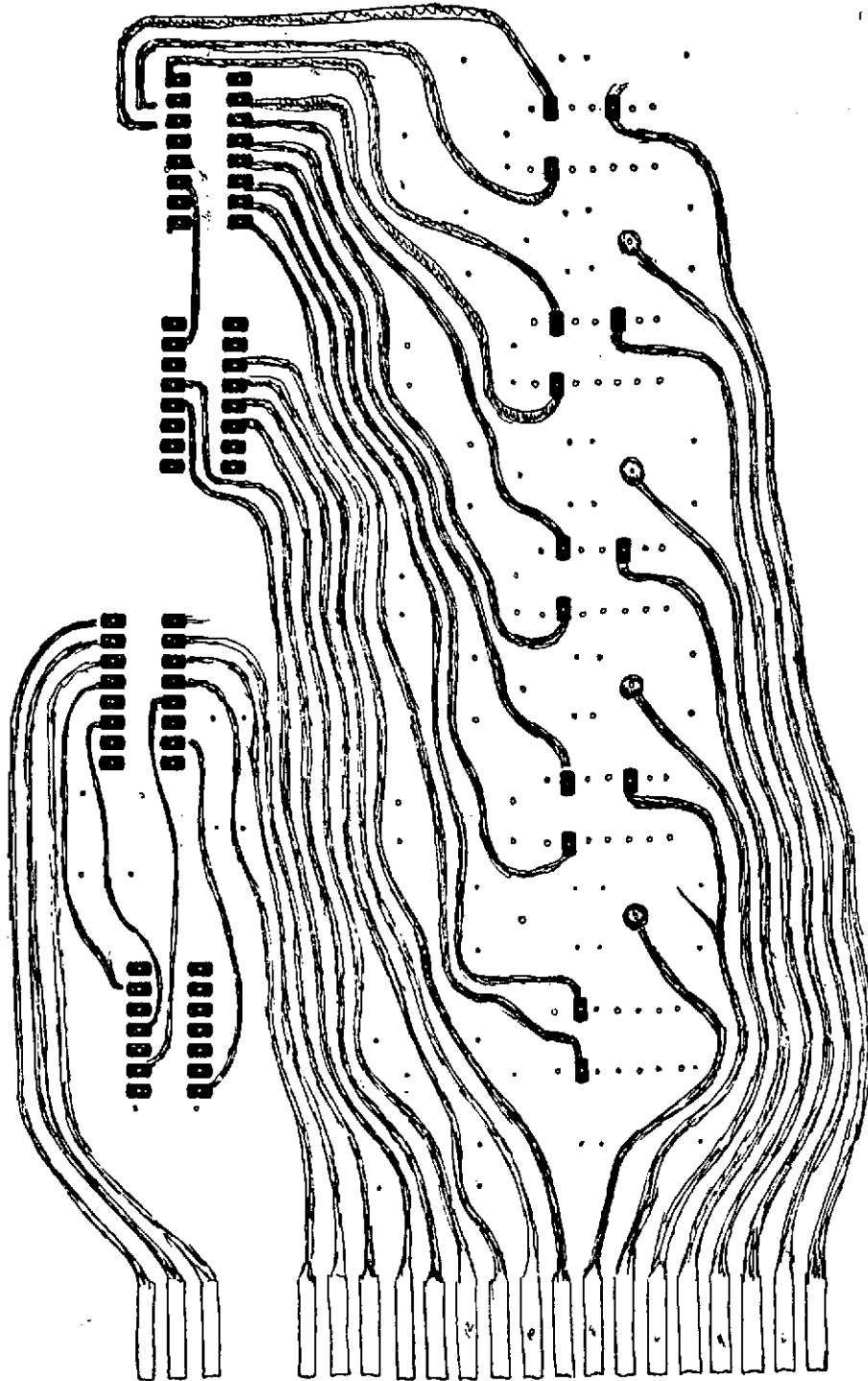


FIGURE 14. CIRCUIT-BOARD LAYOUT FOR DECADE BOARD (BOTTOM SIDE)

which exhibit low loss in the HF region. For this application ferrite toroids serve as typical core material.

Figure 15 shows the circuit layout for the wideband 3 to 30 MHz linear RF power amplifier using transmission line transformers for impedance matching. The amplifier delivers 5 W (PEP) output to a 50-ohm load, and is capable of power gains in excess of 40 dB over the entire frequency range. The input impedance is also 50 ohms and provides for a low loss match to the HP 5100B frequency synthesizer. Each of the amplifier stages are biased for Class-AB operation by silicon diodes used to maintain a nearly constant base-to-emitter voltage on the transistors. Approximately 0.16 V is required to drive the amplifier to full output. Figure 16 shows the measured overall power gain of the amplifier when delivering 3 W to a 50-ohm load. The gain from the first stage is approximately 13 dB. The output stage uses a single 2N5071 transistor which is particularly suited for outstanding reliability in RF operations. This transistor can safely dissipate 65 W at 25^o C case temperature or 40 W at 100^o C case temperature when operating from a 30-V dc supply. At an RF output of 30 W, this transistor is rated to operate without failure or degradation for any load-line voltage standing-wave ratio of 3:1 referenced to a 12.5-ohm load. Hence, this transistor is ideally suited for operations involving antenna load changes. The amplifier is operated from a 28-V dc supply and draws approximately 0.7 ampere current under normal operating conditions.

Transmitting Antenna Design Considerations

This section defines the basic requirements of an HF antenna system to be used for the aircraft experiment and describes the antenna design. The intended environment in which the antenna must operate is not completely known at this time. It is known, however, that the antenna will be erected on a ship. Thus, the antenna has been designed for maximum portability. This fact dictates that the overall height of the antenna be limited to 20 to 30 ft. This constraint on the physical dimensions of the antenna places some fundamental constraints on the antenna's electrical properties such as directivity, efficiency, and bandwidth.

In the sections that follow, the electrical properties of the antenna are discussed in detail. In addition, the design techniques required to improve the antenna's performance are also discussed along with the final design specifications of the matching networks and electromechanical bandswitching arrangements.

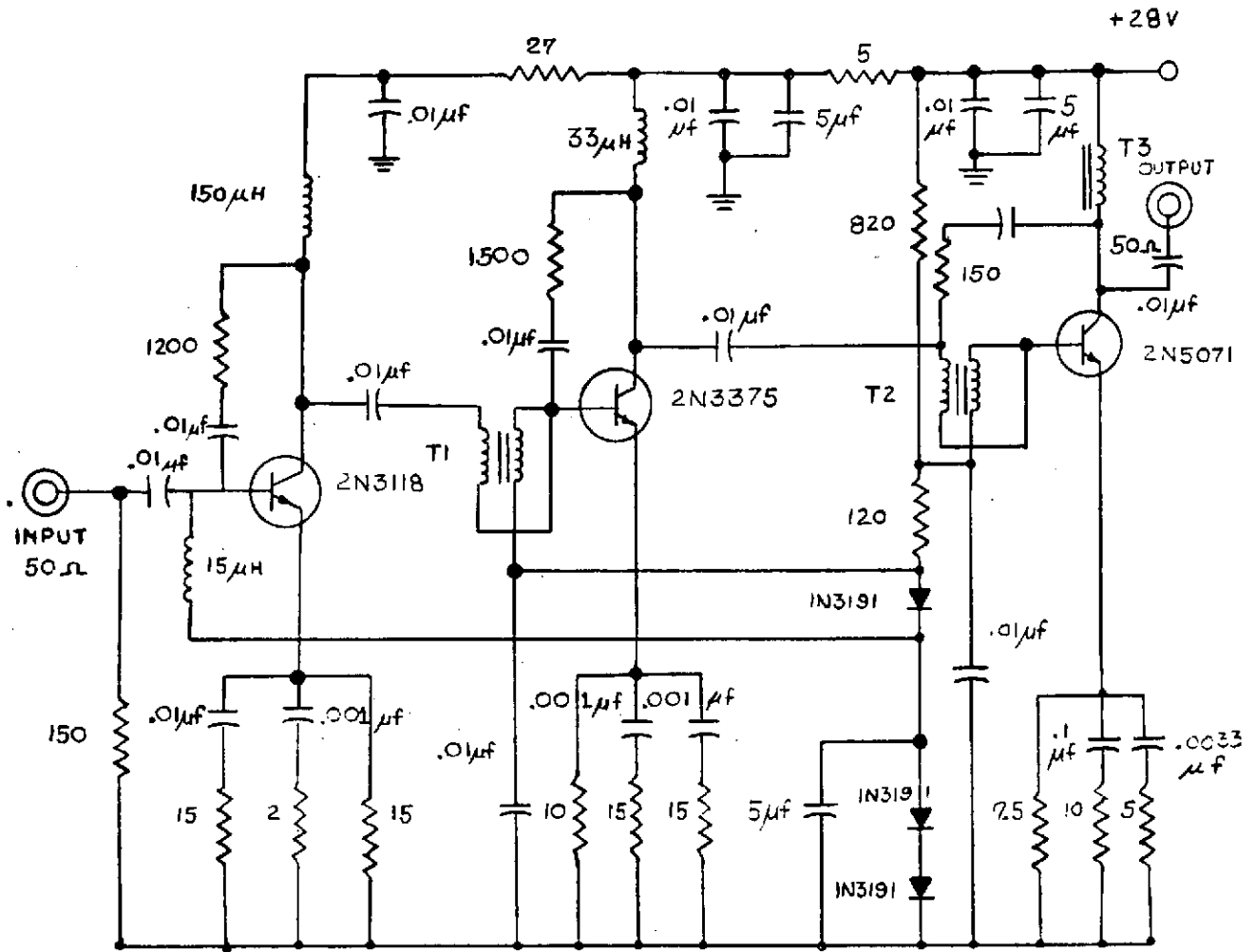


FIGURE 15. 3 to 30 MHz LINEAR POWER AMPLIFIER

ORIGINAL PAGE IS
OF POOR QUALITY

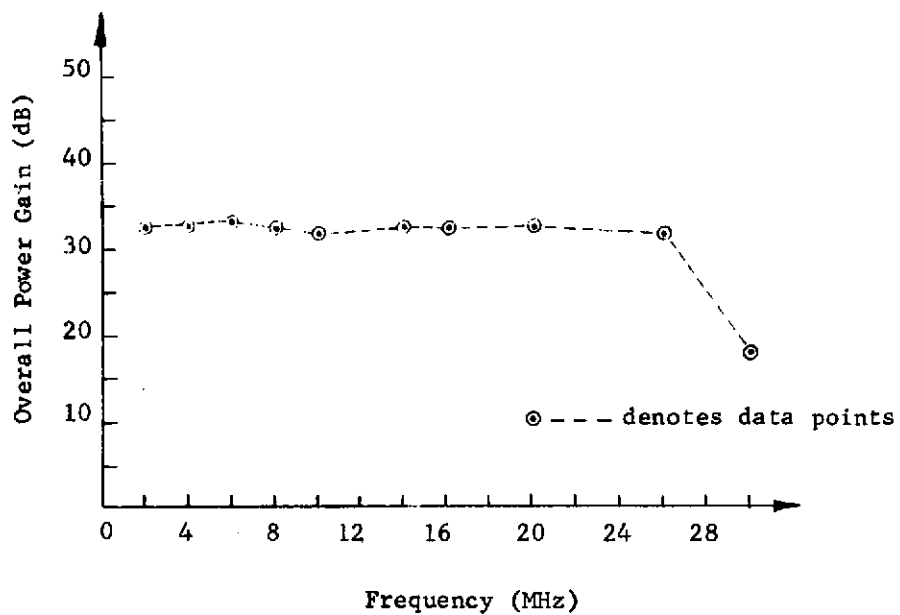


FIGURE 16. CURVE OF AMPLIFIER POWER GAIN VERSUS FREQUENCY FOR 3 WATTS INTO 50- ohm LOAD

ORIGINAL PAGE IS
OF POOR QUALITY

Radiation Pattern of a Vertical Monopole

A simple vertical antenna has a radiation pattern which is omnidirectional in the horizontal plane. The inherent vertical polarization of this antenna makes it ideally suited for ground-wave propagation in the 3 to 30 MHz region. Each element of antenna length produces an electric field intensity at an observation point that is directly proportional to the amplitude of the current in the segment. The integrated fields from all parts of the antenna, together with those reflected from the interface beneath the antenna, produce what is known as the vertical radiation pattern for the antenna in the presence of the half-space. Figure 17 illustrates the general trend in the vertical radiation pattern of a short antenna as its length is increased. Note that the short vertical element mounted over a perfectly conducting half-space has a single maximum in its radiation pattern until its length becomes slightly greater than $1/2$ wavelength. This maximum in the pattern occurs at zero degrees with respect to the horizon. As the electrical length of a short vertical conductor increases, a larger and larger portion of a complete sinusoidal current is distributed along the vertical section. This increase in length causes the main lobe to become more concentrated along the horizon and corresponds to an increase in gain. The vertical pattern changes slowly with height until the length exceeds $1/4$ wavelength. When the electrical length is increased beyond $5/8$ wavelength, the major lobe starts to rise in angle off the horizon, and further increases in electrical length causes minor lobes to appear at lower elevation angles. Lengths greater than $5/8$ wavelength causes the ground lobe to rapidly contract, and the energy is transferred to the high angle lobe. Thus, from the standpoint of horizontal gain, a height of $5/8$ wavelength represents an optimum condition.

The finite conductivity of the actual earth environment also influences the radiation pattern of the antenna as well as its input impedance and radiation efficiency. The effect of the imperfectly conducting earth is to cause the single maximum in the radiation pattern of the short vertical segment to occur at angles somewhat above zero degrees with respect to the horizon. Moreover in this case as the antenna's length is increased the angle at which the maximum radiation occurs decreases until the antenna reaches an electrical length equal to $5/8$ wavelength. Similarly, additional increases in electrical length beyond $5/8$ wavelength cause

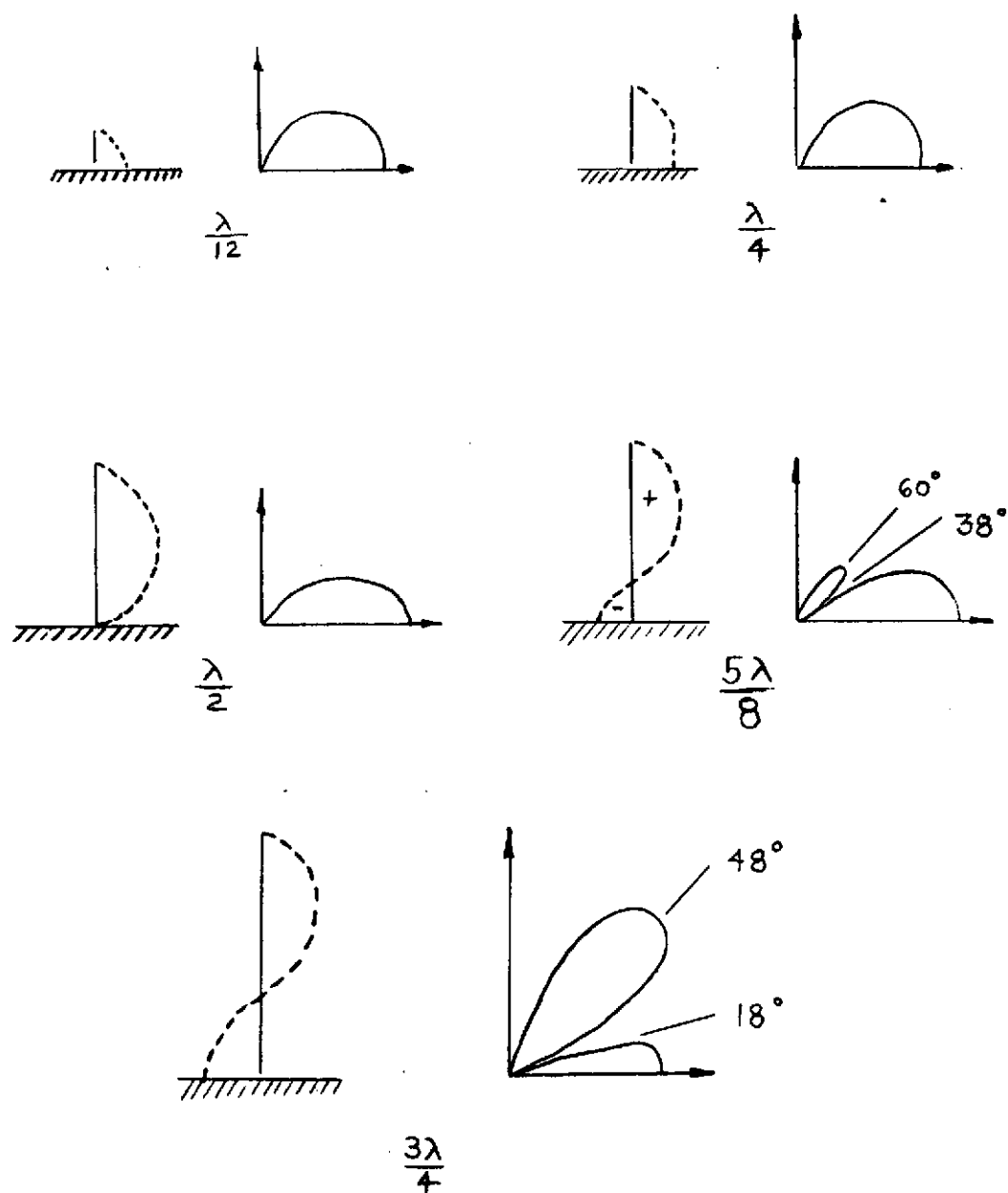


FIGURE 17. CURRENT DISTRIBUTIONS AND RADIATION PATTERNS FOR VERTICAL ANTENNA OVER PERFECTLY CONDUCTING EARTH

minor lobes to appear at the lower elevation angles. Hence, for low-angle radiation the antenna's length should correspond to $5/8$ wavelength at each frequency of interest. In the HF region these heights can easily be obtained for frequencies above 20 MHz. Unfortunately, at lower frequencies the physical size of the antenna is a serious limiting factor.

Input Impedance Characteristics of a Short Vertical Monopole

The input impedance of a cylindrical monopole antenna depends upon the radius of the antenna as well as its length and conductivity. This last fact increases the difficulty in evaluating the antenna's input impedance, because the terms involving conductivity are dependent upon frequency. Fortunately, the dependence of the antenna input impedance upon conductivity is negligible if the conductivity of the tubing is high, as for example, in aluminum or copper. Unfortunately, antennas are not often located in free space. The presence of nearby material bodies such as an imperfectly conducting ground complicates calculation of the input impedance. When nearby boundaries are such that they possess a high degree of conductivity, the concept of images can be employed to give a reasonable simple account of the effects of such boundaries. For a cylindrical monopole antenna located over sea water, the concepts of image theory are of considerable value. In this case the properties of the vertical antenna mounted perpendicular to a perfectly conducting half-space are closely related to those of a dipole antenna of twice the length isolated in free space. The desired input resistance and reactance of the vertical antenna are just one-half those obtained for the dipole.

In order to obtain values for the theoretical input impedance, two techniques were employed. The first makes use of a dipole-antenna-moment-method computer code which utilizes piecewise polynomial basis functions to compute the mutual and self-impedances of antenna segments. These impedances represent those of an equivalent dipole antenna and hence must be divided by a factor of two in order to represent values of the monopole antenna over a perfectly conducting earth. When the image plane has a finite conductivity as in the case of sea water, this first technique fails. For this situation a modified induced EMF method solution was used to determine values of the input impedance.

The variation of the radiation resistance and series reactance of a base-fed vertical antenna over perfectly conducting earth are shown in Figure 18. These values were obtained numerically for an antenna whose physical height is 21 ft with a length-to-diameter ratio of approximately 200. The antenna's resistance or reactance is plotted logarithmically along the ordinate, and the vertical length is plotted in wavelengths along the abscissa. These impedances are representative of the values which would appear at the terminals of a 21-ft antenna over perfectly conducting ground as the frequency is swept through a range from 3 to 30 MHz. One should note that these impedance values depend upon the diameter of the conductor. In this example, the effect of the diameter of the conductor on the input impedance is most noticeable when the antenna length approaches 0.5 wavelength.

Considerable insight into the terminal characteristics of the antenna as a function of height can be obtained by noting the variation in antenna input impedance as shown in Figure 18. Note that for an antenna of fixed physical height, an effective increase in antenna height corresponds to a change in transmitter frequency. This point is emphasized by the two scales along the abscissa in Figure 18. The upper scale corresponds to the wavelength of the 21-ft antenna, and the lower scale corresponds to the transmitter frequency. At 3 MHz the antenna is 0.064 wavelength long, and increases to 0.64 wavelength at 32 MHz. As the effective length of the antenna is increased, the resistance increases approximately in proportion to the square of the length, while the reactance starts out with a large capacitive value and decreases to zero near a length of 0.25 wavelength. The resistance at this point is approximately 36 ohms. For further increases in length, the resistance increases, reaching a maximum value of 890 ohms near 0.5 wavelength at 20.75 MHz. The reactance, on the other hand, becomes inductive beyond the quarter-wave resonance and increases to a maximum of 350 ohms near 0.5 wavelength and then decreases rapidly to zero. As the diameter of the antenna increases, the position at which the peak resistance occurs shifts to the left, and the value of the resistance decreases. In practice, antennas often have peak resistances ranging from 300 ohms for thick antennas to values of about 15,000 ohms for thinner ones. The reactance of the cylindrical antenna behaves in a similar manner as the diameter is increased.

For additional increases in length beyond 0.5 wavelength the resistance goes through minima whenever the length is close to an odd quarter wavelength, i. e., $3/4 \lambda$, $5/4 \lambda$, etc, and a maximum when close to an integral number of half wavelengths.

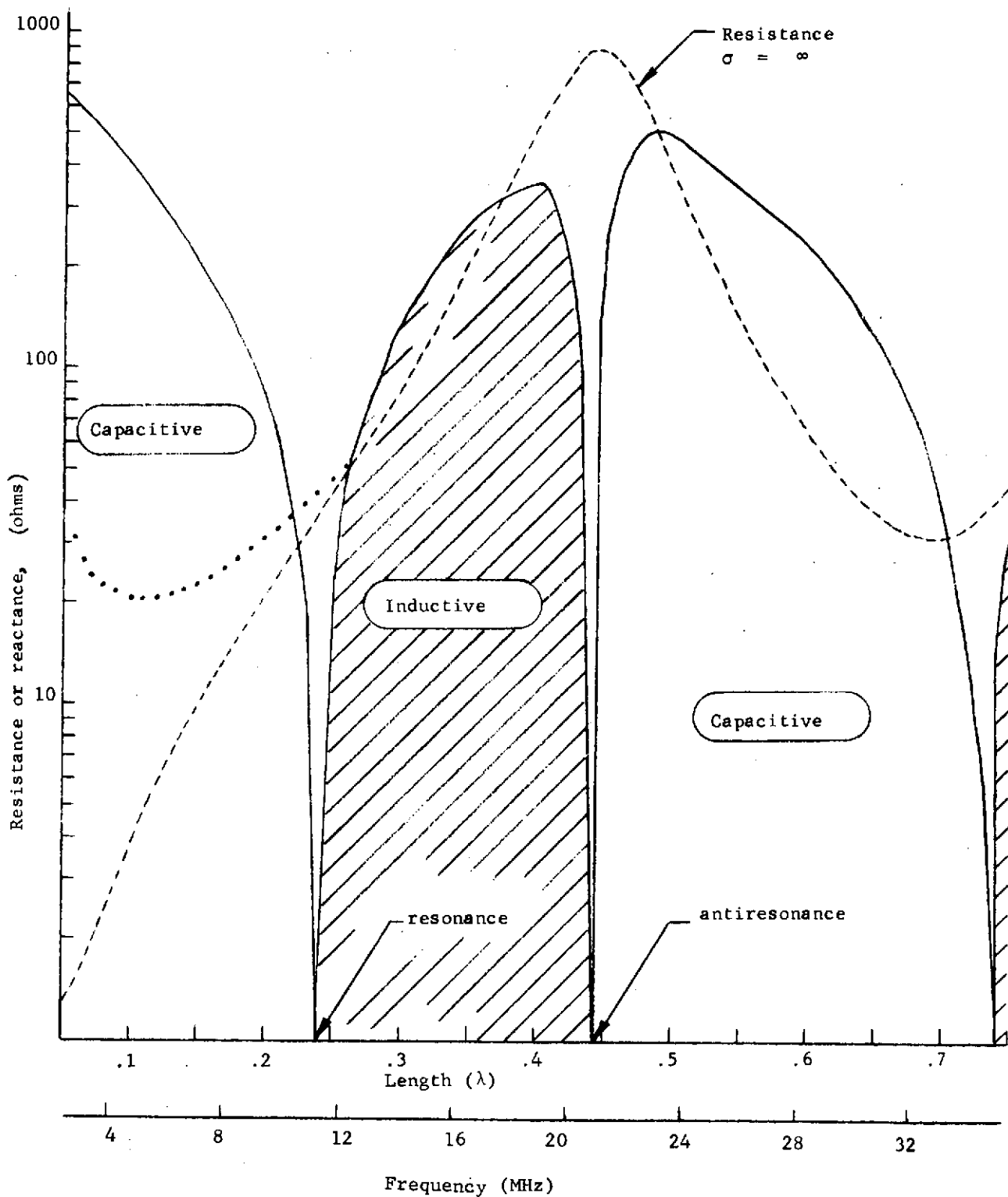


FIGURE 18. INPUT IMPEDANCE OF AN UNLOADED MONOPOLE

ORIGINAL PAGE IS
OF POOR QUALITY

The resistance values for succeeding minima are larger and larger while values for succeeding maxima are smaller. Typical values of resistance at the first minimum, near 0.7λ , range from 20 to 90 ohms. With each half-wavelength variation in length, the reactance curve repeats. The fact that the zero crossings in the reactance curves do not occur at exactly an integral number of half wavelengths is due to end effects.

The dotted curve in Figure 18 represents the change in radiation resistance when the antenna is located over sea water. These values were obtained by using a modified version of the induced EMF method. At the low frequencies the conduction current predominates over displacement current, and changes in the dielectric constant of the medium beneath the antenna do not appreciably affect the input impedance. On the other hand, changes in the conductivity are readily noticeable. Since energy cannot be dissipated as heat in the perfectly conducting case, the difference between the two curves is indicative of heat losses in the imperfectly conducting region in the vicinity of the antenna. Hence, the resistance values obtained by the induced EMF method represent total resistance values including both ground-loss and radiation resistances. Figures 19 and 20 are additional plots of the antenna's resistance and reactance, respectively, as a function of frequency over perfectly conducting earth. Figure 19 clearly emphasizes the low radiation resistance in the frequency range from 3 to 8 MHz. Later it will be shown that the efficiency of the antenna is directly proportional to the radiation resistance, and hence it is precisely in this frequency range where the antenna will be least efficient.

A knowledge of the terminal impedance properties of the antenna as a function of frequency in the HF band allows the antenna to be represented as an equivalent circuit consisting of a series resistance and reactance. For example, in the frequency range between 3 and 12 MHz the antenna is below resonance and the equivalent circuit consists of a series radiation resistance and a capacitor. The equivalent circuit representations of a monopole over a frequency range from 3 to 30 MHz are shown in Figure 21. Note that an additional resistance, R_g , has been included in the circuit to represent ground losses. The equivalent circuit representation of the antenna allows the antenna's efficiency as a function of frequency to be calculated using circuit theory.

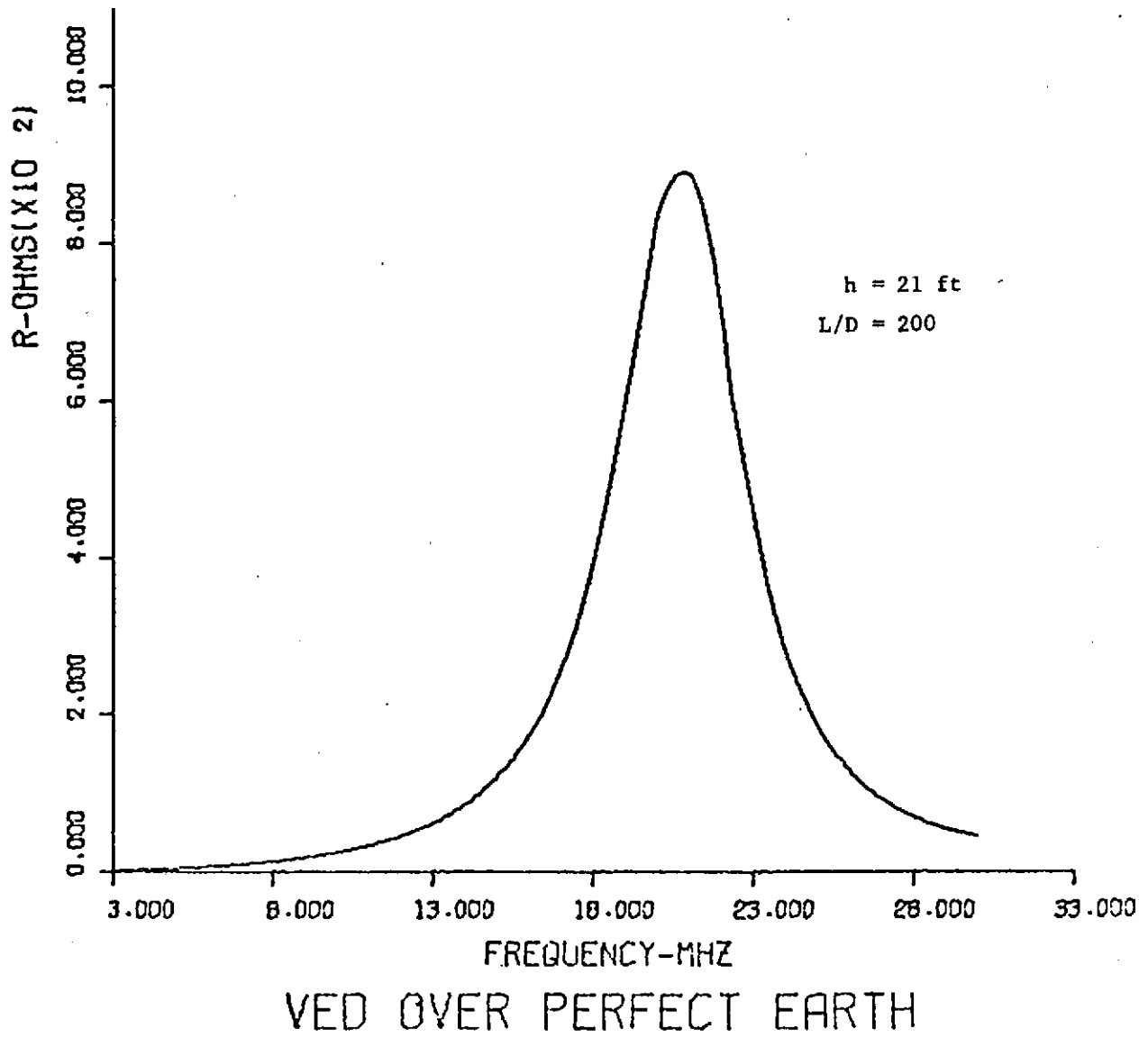


FIGURE 19. RESISTIVE PART OF INPUT IMPEDANCE VERSUS FREQUENCY

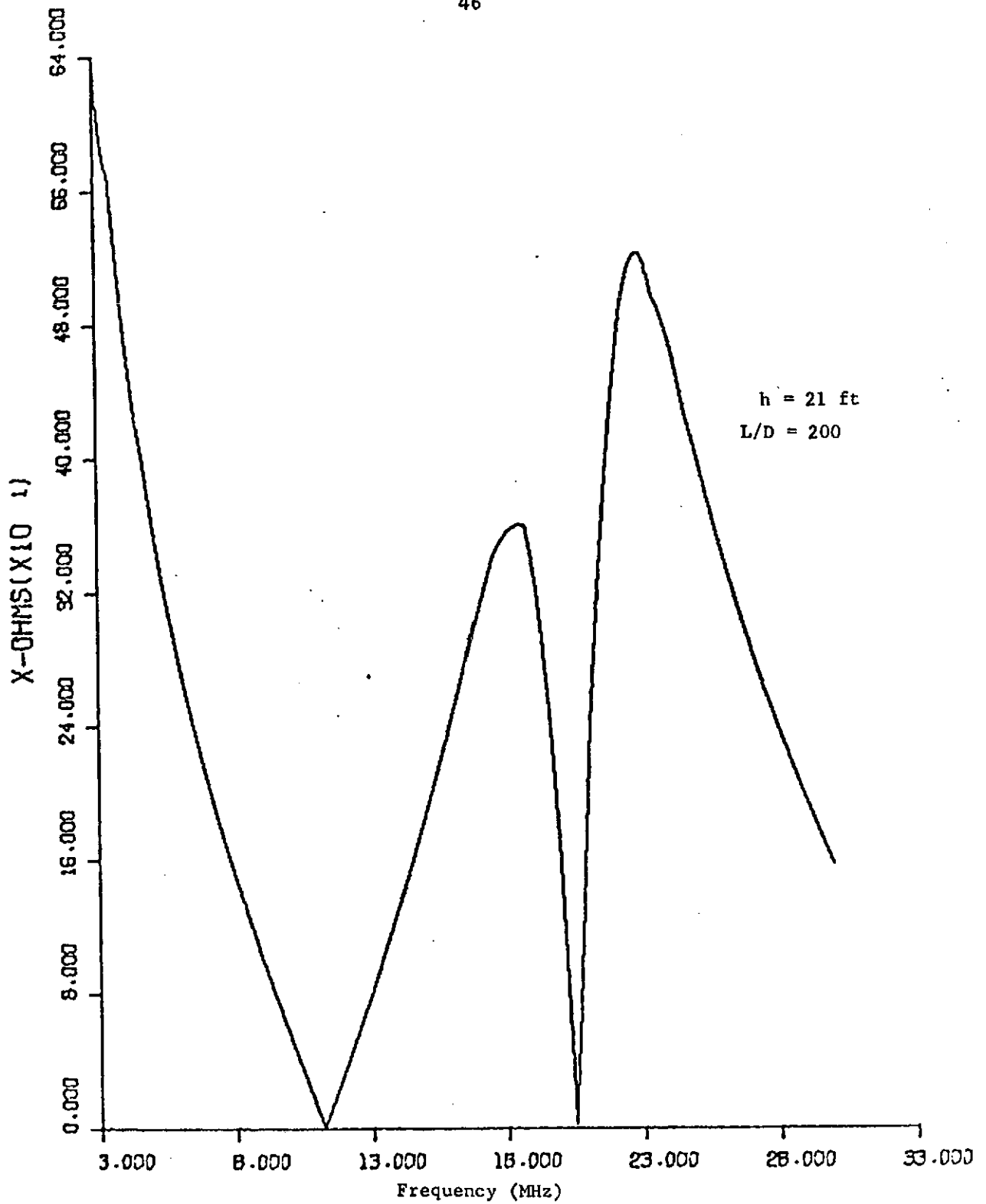


FIGURE 20. REACTIVE PART OF INPUT IMPEDANCE
VERSUS FREQUENCY

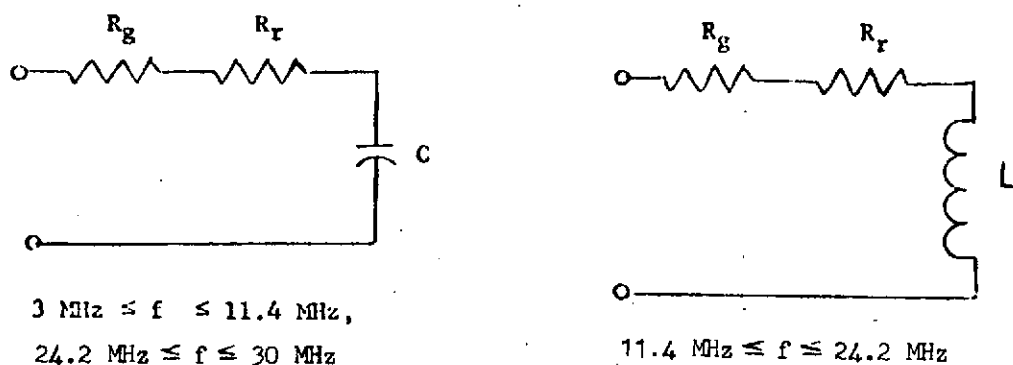


FIGURE 21. EQUIVALENT CIRCUIT OF AN UNLOADED MONOPOLE AS A FUNCTION OF FREQUENCY

Efficiency and Bandwidth of an Unloaded Monopole

A figure of merit for antennas known as the radiation efficiency, η , is defined as the ratio of radiated power to the input power. The radiation efficiency is determined by the following formula

$$\eta = \frac{|I|^2 R_r}{|I|^2 R_{\text{total}}} = \frac{R_r}{R_{\text{total}}} \quad (1)$$

Thus the radiation efficiency, η , reduces to the ratio of radiation resistance to total resistance of the system. The total resistance is the sum of the radiation resistance plus all the resistance arising from dissipative loss such as resistance in conductors and dielectrics, including the resistance of loading coils if used, and the resistance of the grounding system. These dissipative losses are calculated by standard techniques with due regard for skin effect and other high-frequency phenomena.

The radiation resistance of the antenna at the lower HF frequencies around 3 MHz was calculated previously to be less than 2 ohms over a perfectly conducting ground. At these frequencies ground losses are typically 10 to 15 ohms. Calculations of the input impedance of the antenna suggests that the total resistance is approximately 26 ohms over sea water. This would imply that ground losses are on the order of 24 ohms.

These values, are within reason and therefore have been used to obtain estimates for the antenna's efficiency in the HF region. Table 2 gives an estimate of the antenna's efficiency for ten sampled frequencies in the HF region. The estimated efficiencies range from 7% to 3 MHz to well over 50% at frequencies above 9 MHz. Thus, for 5 W delivered to the antenna, only about 1/3 W will be radiated at 3 MHz. These estimates are believed to be conservative; nevertheless, they indicated a need for incorporating design techniques for improving the low frequency performance of the antenna. Notable among the improvements for increasing the efficiency of the antenna at lower frequencies is "top-hat" (capacitive) and inductive loading, and the use of radial ground wires to simulate a more nearly perfectly conducting earth, and hence reduce ground losses. These techniques are discussed in a later section on the final design configuration of the antenna.

TABLE 2. ANTENNA EFFICIENCY AS A FUNCTION OF FREQUENCY*

f MHz	%, η
3.15	7.1
4.15	14.9
5.15	24.3
6.15	35.0
7.15	45.5
9.15	61.1
12.15	79.3
15.15	88.1
19.15	93.6
25.15	90.5

* These values are for an unloaded monopole and do not represent those of the final design.

Unlike the radiation efficiency treated previously, the bandwidth of an antenna does not enjoy a simple and unique definition. Depending upon the operational requirements of the antenna, the bandwidth may be limited by any one of

several factors. For example, changes in pattern shape or directivity, changes in polarization, increases in side-lobe levels, losses in gain, and deterioration in antenna impedance, all affect the bandwidth over a given frequency range. However, in the low frequency limit, changes in gain and impedance have a more pronounced effect on antenna bandwidth; whereas at higher frequencies, changes in pattern shape are more influential. In general, then, the only appropriate definition of the bandwidth of a particular antenna is that band of frequencies within which the antenna meets a given set of performance criterion. The present system design considerations dictate that the standing-wave ratio on the transmission line connecting the RF power amplifier to the antenna be maintained at 2:1 over a bandwidth of 200 kHz. This is necessary to reduce the effect of thermal hotspotting in the amplifier transistors which could cause secondary breakdown. It has been noted, in Figure 18, that the input impedance of the antenna changes with frequency. As a practical matter these changes in impedance with frequency are reflected as changes in the standing-wave ratio on the transmission line connecting the antenna to the amplifier. Thus when the antenna is matched to the transmission line at a particular frequency, usually in the center of the band of frequencies over which the antenna is used, a shift in operating frequency is usually accompanied by a change in the standing-wave ratio.

From Figure 18 one can observe that in a band of frequencies around resonance, the resistance change is fairly small and by itself would not affect the standing-wave ratio to an appreciable degree. On the other hand, the principal factor causing changes in the standing-wave ratio is the change in the reactive component of the antenna impedance when the frequency is varied. If the reactance changes rapidly with frequency, the standing-wave ratio on the transmission line will rise rapidly off resonance. Hence, for a given standing-wave ratio, an antenna that has a relatively slow rate of reactance change will have a wider frequency range or bandwidth. It is possible to determine the lowest theoretically obtainable standing-wave ratio over a required bandwidth by first determining the equivalent Q of the antenna. Or conversely, it will be possible to determine the maximum bandwidth for a permissible value of standing-wave ratio. It is important to note that the bandwidth of the antenna is critically dependent upon the value of Q obtained for the antenna. In general, the higher the Q , the lesser the bandwidth. A method of computing Q when the reactance is not zero at the center frequency is given by the following relationship

$$Q = \left[f(\Delta f)^{-1} \Delta x + \left| \frac{x}{R} \right| \right] \cdot (2R)^{-1} \quad (2)$$

In the above relationship, f is the geometric mean frequency, Δf the frequency interval, Δx the change in the reactance in the frequency interval, and x , R are the reactance and resistance at the geometric mean frequency. Table 3 gives the antenna Q standing-wave ratio and bandwidth for ten frequency increments in the HF band.

The frequency interval, Δf , was chosen to be 200 kHz and the Q of the antenna was computed according to Equation (2). Figure 22 is a plot of the series Q of the antenna as a function of frequency and represents the contribution of the second term in the right-hand side of Equation (2) to the overall Q of the antenna. Note that at low frequencies the Q is high, resulting in a narrow frequency range over which the standing-wave ratio can safely be maintained below 2:1. The results summarized in Table 3 emphasize this point more clearly. Here the results for the

TABLE 3. Q , S.W.R. AND BANDWIDTH OF AN UNLOADED MONOPOLE*

f MHz	Q		S.W.R.		Bandwidth**	
	$\sigma = \infty$	$\sigma = 4$	$\sigma = \infty$	$\sigma = 4$	$\sigma = \infty$	$\sigma = 4$
3-3.2	388.0	62.6	25:1	3.6:1	16.8 kHz	104 kHz
4-4.2	186.0	56.9	8:1	2.5:1	46.0 kHz	151 kHz
5-5.2	94.4	48.4	3.8:1	1.85:1	113.0 kHz	220 kHz
6-6.2	53.3	40.0	1.75:1	1.4:1	240.0 kHz	320 kHz
7-7.2	32.0	32.3	1:1	1:1	465.0 kHz	460 kHz
9-9.2	13.7	20.4	1:1	1:1	1.4 MHz	940 MHz
12-12.2	6.3	12.4	1:1	1:1	4.03 MHz	2.05 MHz
15-15.2	4.2	11.8	1:1	1:1	7.5 MHz	2.7 MHz
19-19.2	2.1	12.5	1:1	1:1	19.2 MHz	3.2 MHz
25-25.2	5.5	2.0	1:1	1:1	9.6 MHz	26.4 MHz

* The values are not those of the final design.

** Required bandwidth for 2:1 S.W.R.

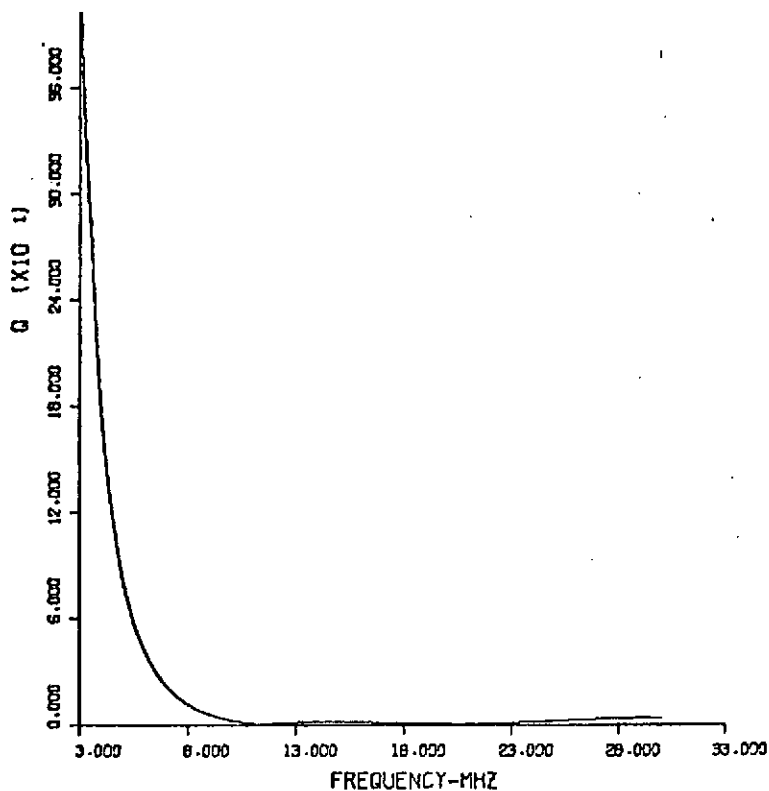


FIGURE 22. ANTENNA Q VERSUS FREQUENCY

perfectly conducting interface along with those for sea water are given for comparison. Columns 2 and 3 represent the theoretically predicted values of the antenna Q. Note that the Q values for the perfectly conducting interface are much larger at the lower frequencies than those corresponding to the antenna over sea water. The prime reason for this lies in the fact that the radiation resistance for the perfectly conducting case is much smaller as previously noted.

The standing-wave ratios given in columns 4 and 5 represent those values that would appear on the transmission line if the antenna were matched at the geometric mean frequency by a network containing two lossless reactive elements. These values are based on a frequency interval of 200 kHz. It is clear from these values that the required value of 2:1 standing-wave ratio over the 200 kHz

frequency interval can safely be maintained only on frequencies above 6 MHz. In order to determine the system bandwidth over which the antenna together with its matching network could maintain the required 2:1 standing-wave ratio, the values for columns 4 and 5 were computed. Again, the bandwidth is less than 200 kHz for frequencies less than about 6 MHz. One can observe from Equation (2) that the bandwidth, being inversely proportional to the Q of the antenna, can be increased by increasing either, or both, the antenna capacitance or resistance. The radiation resistance of the antenna is limited by size of the structure, and adding resistance by any other means reduces the antenna's radiation efficiency. Hence, in order to improve the antenna's low frequency performance, the electrical length of the antenna must be increased. This specifically increases (1) the bandwidth of the antenna and thereby reduces the standing-wave ratio and, (2) increases the radiation efficiency of the antenna by increasing its radiation resistance. It will be shown in a later section that the electrical length of the antenna can be effectively doubled at the low frequency end of the spectrum by simply adding a capacitive top-hat to the existing structure. Unfortunately, these improvements at the low frequency end of the spectrum will also increase the electrical length of the antenna at the higher frequencies where it is least desirable.

For optimum low angle ground-wave coverage, the height of the antenna should not exceed $5/8$ wavelength in the HF region. Thus, the additional height offered by the capacitive hat at the low frequencies is desirable but would prove detrimental as the frequency is increased. Thus, a technique for eliminating the top-hat at the higher frequencies was required.

Vertical Monopole with High Frequency Trap

The capacitive "top-hat" loading discussed previously for improving the low frequency performance also increases the electrical length of the antenna at higher frequencies where it is least desirable. To overcome this difficulty, the properties of a parallel resonant circuit will be used in order to limit the height of the antenna as the frequency is increased. The basic design consists of a monopole antenna designed to operate on several different frequencies. Figure 23 shows a monopole antenna with a parallel LC circuit inserted in series with the antenna at height h_1 . In the common design procedure for "trap" antennas, the lower section

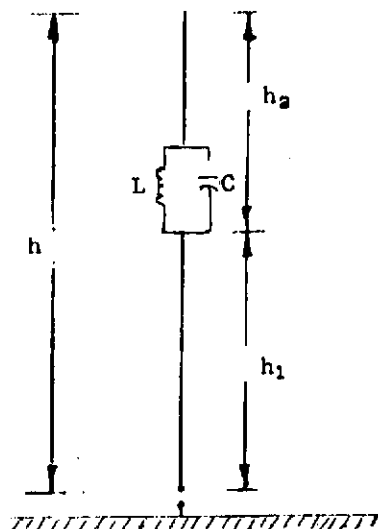


Figure 23. VERTICAL ANTENNA WITH TRAP

h_1 is chosen to be $1/4$ wavelength at the highest frequency of operation. The parallel LC circuit, if disconnected from the antenna, is designed to be resonant at this upper frequency. If the trap is constructed of lossless elements, its impedance at resonance would be infinite and current would not flow in the upper portion of the antenna designated as h_2 in Figure 23. In practice, however, the impedance of the trap will be highly resistive at resonance, and as a consequence, a small amount of current will flow in the upper portion of the antenna. For all practical purposes this current will be negligible if the Q of the components from which the trap is constructed are made comparatively high. As the frequency is decreased, the terminal properties of the trap appear inductive, and the inductive reactance of the trap increases quickly to approximately $7/10$ of the impedance value at resonance. This peak in the inductive reactance occurs at a frequency below the resonant frequency by an amount equal to one-half of the 3-dB bandwidth of the trap. On either side of this frequency, just about any value of inductive reactance is available up to a maximum of $7/10$ the available resistance at resonance. For further decreases in frequency, the inductive reactance drops off to a value near zero at a frequency of approximately 5 bandwidths removed from the resonant frequency. At and

below this frequency, the trap appears as a short circuit allowing current to flow in the upper portion of the antenna as though the two segments h_1 and h_2 were connected together. Hence the overall length of the antenna at the lower frequencies appears as the combined length of the individual sections. The upper length, h_2 , can now be adjusted until the overall length, H , is resonant at the lower frequency. Thus, by inserting a parallel resonant network in series with the antenna, the height of the antenna at the upper frequency can be limited to $1/4$ wavelength.

In practice, the L/C ratio of the trap can be adjusted so that the low frequency performance of the antenna is not degraded. For example, the effect of the L/C ratio may be illustrated by considering one extreme where the capacitor is left out entirely. In this case, resonance can be obtained at the lower frequency only by adjusting the inductance in order to cancel the capacitor reactance that would appear at the antenna terminals without loading. This, of course, assumes that the antenna is being tuned to resonance by the inductance of the trap without the aid of external loading at the base. At the other extreme in which the inductor is left out, resonance can be obtained for the lower section, h_1 , only by adjusting the capacitor. Here it is assumed the length of the antenna, at the higher frequency, is slightly longer than the self-resonant length, and, hence, the input impedance appears inductive. Thus, increasing the L/C ratio tends to improve the low frequency performance at the expense of the performance at the higher frequency. Fortunately, the high-frequency trap incorporated in the final design of the antenna is being used primarily to limit the additional increase in electrical length induced by the capacitive top hat. For this requirement, the L/C ratio of the trap is less demanding.

Capacitive "Top-Hat" Loading of a Short Vertical Monopole

The difficulty in reducing ground losses for the short vertical monopole dictates at the outset that the antenna be made as high as possible in order to increase the radiation resistance of the antenna. At the low HF frequencies around 3 to 4 MHz, the physical heights required for the realization of a suitably high

radiation resistance are normally impracticable. For example, at 3.5 MHz, a quarter-wavelength antenna would extend to slightly over 66 ft. Hence, the design objective for vertical grounded antennas which are necessarily less than a $1/4$ wavelength high is to make the current loop (maximum) come near the top of the antenna, and to maintain the current as large and as uniform as possible throughout the vertical extent of the structure. This in effect requires "top loading" which means replacing the missing height by some form of electrical circuit such that the shortened antenna may be kept in resonance with approximately the same current in its vertical section as when the antenna is extended to a full quarter wavelength without top loading. The distribution of current and charge along the vertical part of the top-loaded antenna is similar to that along the same lower part of the resonant antenna.

One method of top loading consists of a metallic structure in the form of a disk having sufficient surface area to produce a large capacitance with respect to ground. The antenna, thus heavily loaded with capacitance at its ends, has a distribution of current throughout its main section which is nearly uniform. The fields produced by this antenna are nearly identical to those of a current element of the same length. The currents in the loading plates flow radially from the main element and, hence, their fields tend to cancel.

Transmitting Antenna Design

The discussion of the design considerations for a vertical monopole given in the preceding section clearly indicates a need for improved low-frequency performance. In particular, the efficiency and bandwidth of a simple monopole can be improved by increasing the electrical length of the antenna. Capacitive "top-hat" loading can be employed to establish a nearly uniform current distribution over the vertical extent of the structure. Optimum low-angle directivity requires that the antenna's electrical length be constrained to values not exceeding $5/8$ wavelength at any given frequency of operation. While top-hat loading offers considerable advantages at the lower frequencies, it becomes undesirable when the frequency is increased beyond 15 MHz. To cope with this problem, a parallel LC network was inserted in series with the antenna in order to minimize the increase in electrical length at the higher frequencies induced by the capacitive loading. The finalized design of the vertical

antenna is specified along with the matching networks necessary to achieve maximum power transfer between the antenna and a 50 ohm transmission line. Also, the electromechanical band switch is discussed which enables an appropriate matching network to be connected in series with the antenna and transmission line as the transmitting frequency is stepped band-to-band.

Top-Hat Construction

Increasing the effective length of a vertical antenna by capacitive top-loading is usually accomplished by adding a concentrated amount of capacitance at or near the top of the antenna. The capacitance cannot be simply inserted in series with the antenna because this would reduce the total capacitance of the antenna, making it appear electrically shorter rather than longer as desired. Hence, shunt capacitance must be used instead so that the total capacitance between the antenna and ground is increased. The most common method of producing the required shunt capacitance is to use a disk or a "hat" made of sheet metal, mesh, or a wire skeleton. The disk is centered on the top of the antenna and mounted at right angles to the vertical section. This arrangement provides about one picofarad of capacitance for each inch of disk diameter.

The antenna top hat can be considered as a parallel plate over a perfectly conducting ground. In this case the capacitance can be determined by the well-known relation for parallel plate capacitors separated by the height of the antenna. The effective area of the parallel plate is equal to its actual area, plus a fringe area which depends on the antenna's height and the perimeter of the disk. For an antenna height of 21 ft and a disk diameter of 5 ft, the shunt capacitance to ground is approximately 45 picofarads. Figure 24 shows the increase in electrical length that can be obtained for a 5-ft diameter disk mounted on top of the antenna as a function of antenna height. At a height of 21 ft, the disk offers an additional electrical length of about 0.05 wavelength. These values were calculated at 3.15 MHz for antenna heights ranging from 5 to 35 ft. These values are presented numerically in Table 4. As the transmit frequency is increased from 3.15 MHz the effect of the 5-ft diameter top hat, mounted on a 21-ft vertical section, is reflected in the additional increases in electrical length and changes in the antenna's input impedance. Table 5 summarizes these changes as a function of frequency. Note that at the low frequencies the

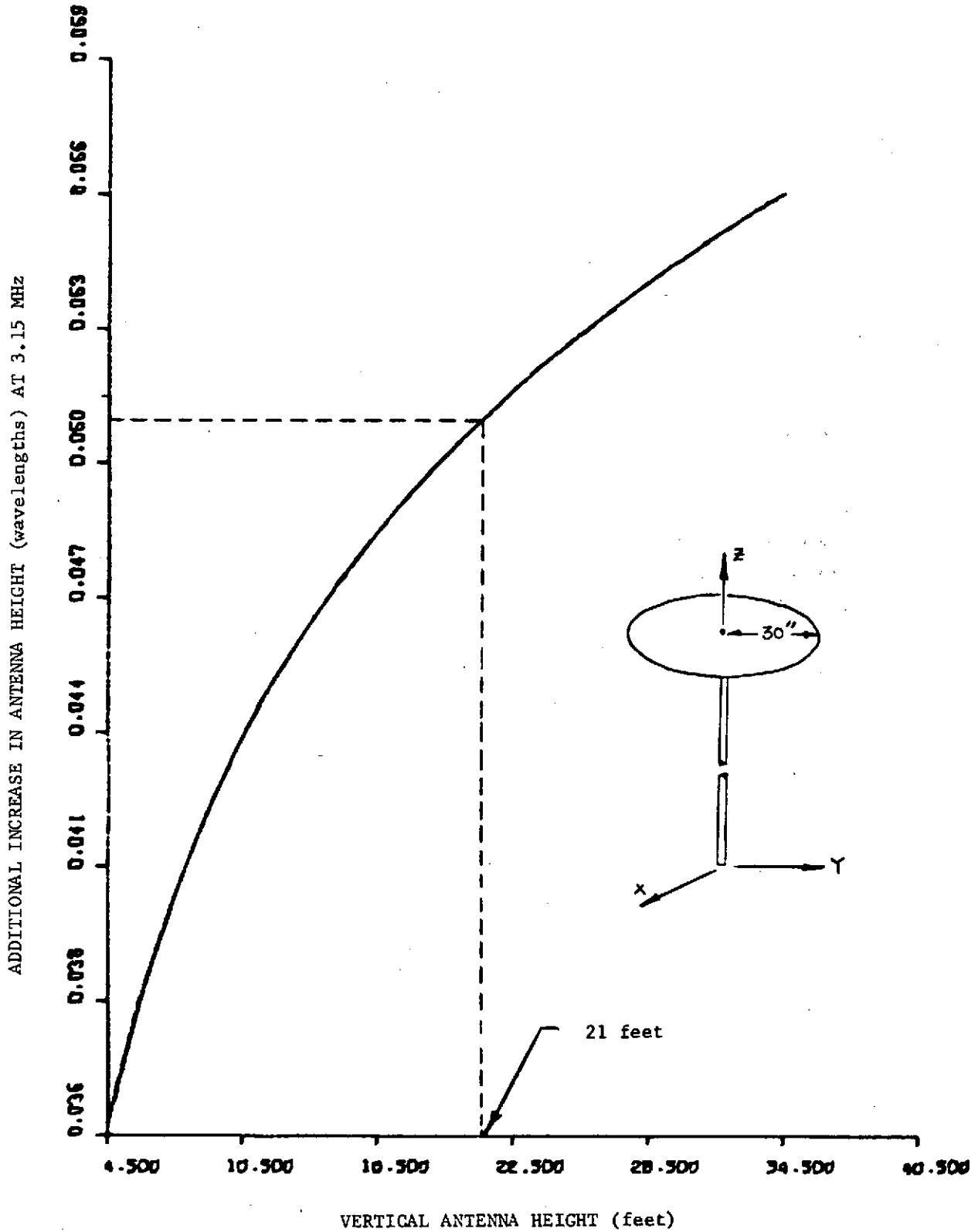


FIGURE 24. ADDITIONAL ANTENNA HEIGHT AT 3.15 MHz FOR A 5 FT DIAMETER TOP HAT

TABLE 4. INCREASE IN ELECTRICAL LENGTH VERSUS ANTENNA HEIGHT

Top Loading				
F = 3.15 MHz				
H-Feet	H/A	R-Feet	L-Wave	L-Degrees
0.50000E+01	0.80000E+01	0.30000E+01	0.43573E-01	0.15686E+02
0.60000E+01	0.96000E+01	0.30000E+01	0.45802E-01	0.16489E+02
0.70000E+01	0.11200E+02	0.30000E+01	0.47686E-01	0.17167E+02
0.80000E+01	0.12800E+02	0.30000E+01	0.49318E-01	0.17755E+02
0.90000E+01	0.14400E+02	0.30000E+01	0.50758E-01	0.18273E+02
0.10000E+02	0.16000E+02	0.30000E+01	0.52046E-01	0.18737E+02
0.11000E+02	0.17600E+02	0.30000E+01	0.53211E-01	0.19156E+02
0.12000E+02	0.19200E+02	0.30000E+01	0.54275E-01	0.19539E+02
0.13000E+02	0.20800E+02	0.30000E+01	0.55254E-01	0.19891E+02
0.14000E+02	0.22400E+02	0.30000E+01	0.56160E-01	0.20217E+02
0.15000E+02	0.24000E+02	0.30000E+01	0.57003E-01	0.20521E+02
0.16000E+02	0.25600E+02	0.30000E+01	0.57792E-01	0.20805E+02
0.17000E+02	0.27200E+02	0.30000E+01	0.58533E-01	0.21072E+02
0.18000E+02	0.28800E+02	0.30000E+01	0.59232E-01	0.21323E+02
0.19000E+02	0.30400E+02	0.30000E+01	0.59893E-01	0.21561E+02
0.20000E+02	0.32000E+02	0.30000E+01	0.60520E-01	0.21787E+02
0.21000E+02	0.33600E+02	0.30000E+01	0.61116E-01	0.22002E+02
0.22000E+02	0.35200E+02	0.30000E+01	0.61685E-01	0.22207E+02
0.23000E+02	0.36800E+02	0.30000E+01	0.62228E-01	0.22402E+02
0.24000E+02	0.38400E+02	0.30000E+01	0.62749E-01	0.22589E+02
0.25000E+02	0.40000E+02	0.30000E+01	0.63248E-01	0.22769E+02
0.26000E+02	0.41600E+02	0.30000E+01	0.63727E-01	0.22942E+02
0.27000E+02	0.43200E+02	0.30000E+01	0.64188E-01	0.23108E+02
0.28000E+02	0.44800E+02	0.30000E+01	0.64633E-01	0.23268E+02
0.29000E+02	0.46400E+02	0.30000E+01	0.65062E-01	0.23422E+02
0.30000E+02	0.48000E+02	0.30000E+01	0.65476E-01	0.23572E+02
0.31000E+02	0.49600E+02	0.30000E+01	0.65877E-01	0.23716E+02
0.32000E+02	0.51200E+02	0.30000E+01	0.66265E-01	0.23856E+02
0.33000E+02	0.52800E+02	0.30000E+01	0.66642E-01	0.23991E+02
0.34000E+02	0.54400E+02	0.30000E+01	0.67006E-01	0.24122E+02
0.35000E+02	0.56000E+02	0.30000E+01	0.67361E-01	0.24250E+02

TABLE 5. INPUT IMPEDANCE OF LOADED MONOPOLE AS A FUNCTION OF FREQUENCY AND GROUND CONDUCTIVITY

f MHz	H in λ		A in Ω	
	Δh	$h + \Delta h$	$\sigma = \infty$	$\sigma = 4$
3.15	0.051	0.118	5.59, -310.	20.7, -733
4.15	0.067	0.156	10.66, -188.4	23.4, -447
5.15	0.083	0.193	18.76, -96.98	29.6, -237
6.15	0.099	0.230	31.83, -17.79	39.4, -63.6
7.15	0.115	0.268	54.1, 60.67	55.7, 113.
9.15	0.148	0.343	180.7, 251.34	128.5, 537.2
12.15	0.194	0.453	857.9, -281.9	1353., -3121
15.15	0.245	0.568	102.1, -307.8	737.7, -1337
19.15	0.310	0.719	457.9, -24.6	632, -1220
25.15	0.402	0.939	503., -182.3	538, -987

antenna's electrical length is approximately doubled, and its radiation resistance is increased from less than 2 ohms for the unloaded monopole to a value slightly over 5 ohms for capacitive loading. This increase in electrical length induced by the top hat improves the antenna's efficiency over sea water to 29% at 3.15 MHz. Table 4 gives the values of the antenna's input impedance for the perfectly conducting earth as well as those for sea water. These impedances can be obtained from Figure 18 by using the values of increased electrical length provided by the top loading. The increased electrical length at the lower frequencies also improves the bandwidth of the antenna. For example, the 2:1 standing-wave ratio bandwidths for an unloaded monopole at 3.15 MHz were 16.8 kHz and 104 kHz, respectively, for the antenna located over perfectly conducting ground and sea water. Doubling the antenna's electrical length at this frequency results in a bandwidth of 124 kHz for the perfectly conducting case, and approximately 196 kHz over sea water. In both cases, this amount to over an 85% increase in the low frequency bandwidth of the antenna due to capacitive loading.

Figure 25 illustrates the mechanical construction of the top hat. The arms form the skeleton structure of a disk and are constructed of 30-in. segments of 1/4-in. diameter aluminum rods. Eight of these rods are clamped at 45 degree intervals to a 9-in. aluminum support disk. This disk is in turn welded to a 10-in. segment of 1-in. diameter aluminum tubing. The entire top hat structure is designed to fit concentrically over an insulating rod that separates the top hat from the upper portion of the antenna. This insulator is used as a physical support for the high frequency LC trap, the electrical specification of which are discussed below.

Specification of High Frequency Trap

Maintaining the electrical length of the antenna less than $5/8$ wavelength assures low-angle coverage. The capacitive top hat increases the electrical length of the antenna at the low HF frequencies, but the antenna exceeds the optimum value of $5/8$ wavelength at the higher frequencies. From Table 5 one can observe that with the top hat at frequencies above 17 MHz the electrical length of the antenna exceeds the optimum value. Figure 18 indicates that in order to reduce the overall height of the antenna to 0.6 wavelength at 19.15 MHz, approximately 209 ohms of inductive reactance must be inserted in series. This can most easily be accomplished by taking advantage of the electrical properties of a parallel LC network.

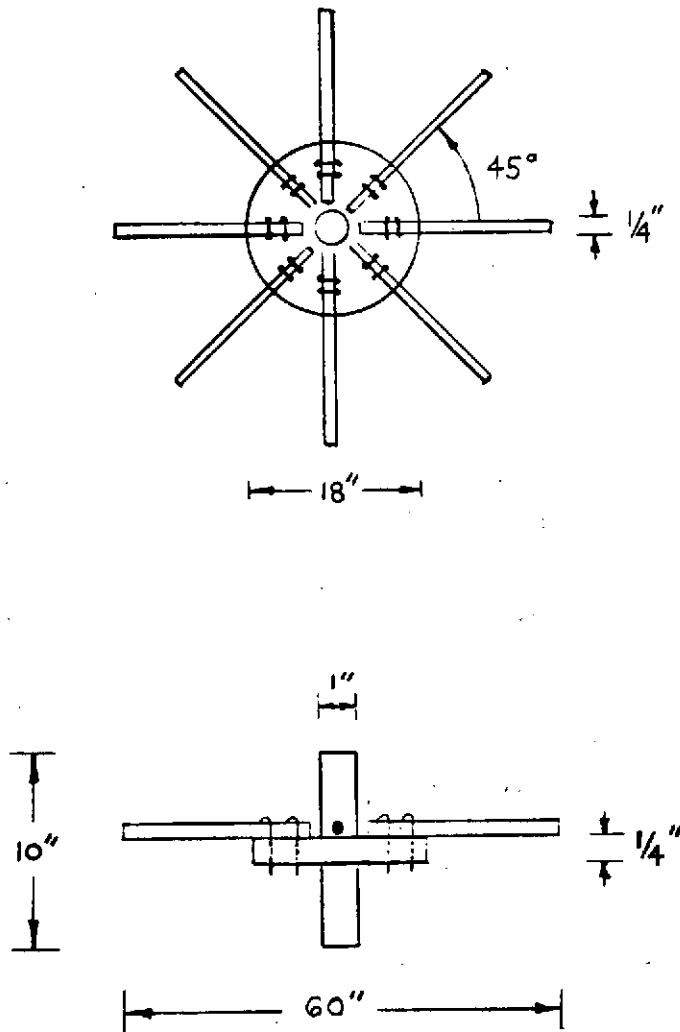
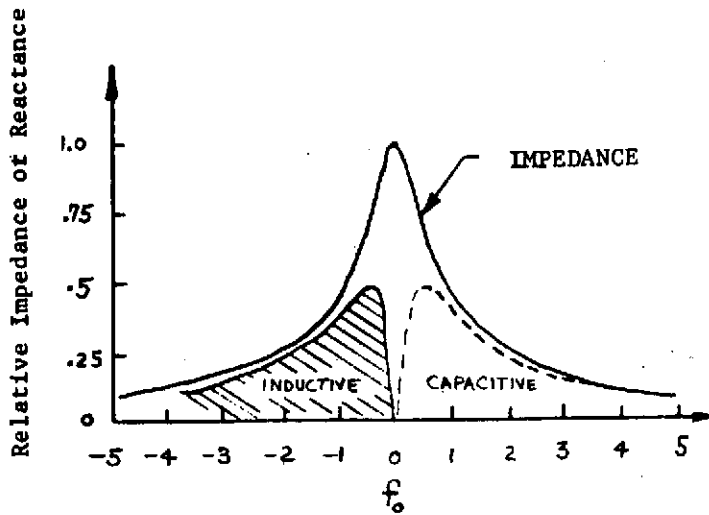


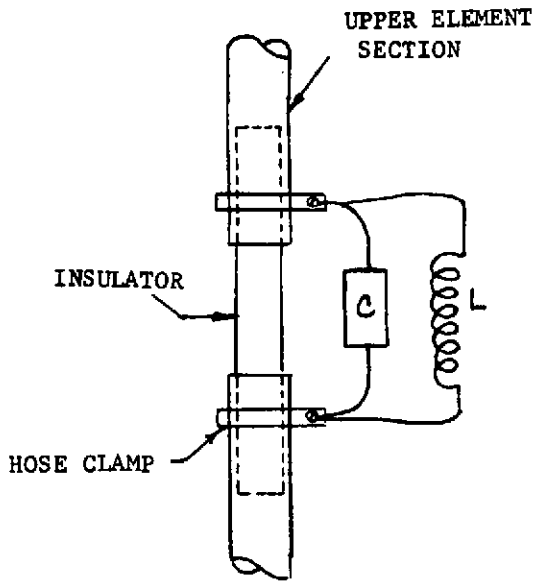
FIGURE 25. MECHANICAL DETAILS OF CAPACITIVE TOP HAT

The total impedance and reactance as a function of frequency of a circuit consisting of an inductor and capacitor in parallel are shown in Figure 26. The values of impedance and reactance are given relative to the shunt impedance at resonance. At resonance this impedance is a pure resistance and equal to the reactance of either the capacitor or the inductor multiplied by the Q . The horizontal scale is given in terms of frequency shift from resonance measured in 3-dB bandwidths. The 3-dB bandwidth is determined by dividing the resonant frequency f_0 by Q . This curve is valid if the Q of the circuit is greater than one. The maximum inductive and capacitive reactances for the LC network occur at frequencies that are, respectively, below and above the resonant frequency f_0 by only one-half the 3-dB bandwidth. These are the frequencies at which the total impedance has dropped to a value of 0.707 of the maximum value. Within this range of frequencies any value of reactance that can be obtained from the circuit is available. Each value of reactance, except the maximum value, is obtainable at a second frequency outside this range. Far from resonance the total reactance is small.

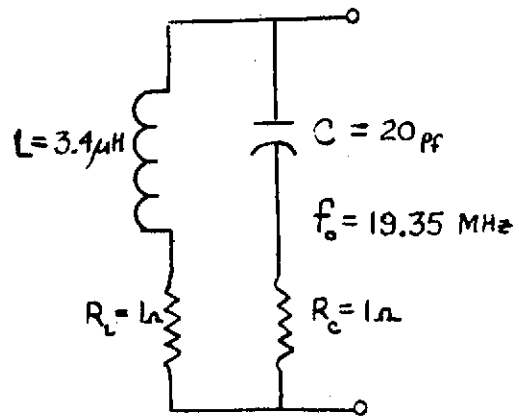
The properties of the parallel circuit can be used advantageously to reduce the electrical length of the antenna to 0.6 wavelengths at 19.15 MHz. The resonant frequency of the trap is set at 19.35 MHz and the 3-dB bandwidth is specified to be 400 kHz. The value of the circuit Q required is 48.25. A capacitance of 20 picofarads and an inductance of 3.4 microhenries are sufficient to achieve resonance at 19.35 MHz. These values result in an L/C ratio of 170 and an impedance at resonance equal to 412 ohms. At 19.15 MHz this impedance will be approximately 206 ohms, a value slightly less than the amount required to reduce the antenna's electrical length to 0.6 wavelengths. As the frequency is increased above 19.35 MHz the parallel circuit appears as a capacitive reactance in series with the antenna. As noted earlier, a capacitor in series with the antenna has an overall effect of reducing the total capacitance of the antenna, and hence making the antenna appear electrically shorter. Figure 26 also contains a sketch of the mechanical construction of the high frequency trap along with its equivalent electrical network. The values of resistance in series with the elements represent loss resistances and are negligible when the component- Q 's are high. With a coil Q of 300, a resistance of about 0.1 ohms at 20 MHz is practical, and at lower frequencies the value should not exceed 5 ohms. Thus, with these values of inductance and capacitance the specification of the high frequency trap is completed.



Frequency Shift from Resonance in 3 dB Bandwidths



MECHANICAL CONSTRUCTION OF TRAP



ELECTRICAL EQUIVALENT CIRCUIT OF HIGH FREQUENCY TRAP

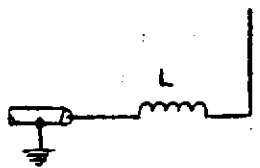
FIGURE 26. ELECTRICAL AND MECHANICAL DETAILS OF HIGH FREQUENCY TRAP CONSTRUCTION

The salient features of the antenna design are summarized as follows. At 3.15 MHz the bandwidth over which a 2:1 standing-wave ratio can be maintained is approximately 200 kHz. This is approximately an 85% increase over that of an equivalent unloaded monopole. The radiation resistance at this frequency is approximately 5.5 ohms for the antenna over a perfectly conducting earth, and the efficiency of the antenna over sea water is approximately 29%. Thus, the overall increase in efficiency employing capacitive loading is about 30%. The antenna extends to a height of 21 ft and is constructed of three telescoping sections of aluminum tubing with the outside diameter of the lower section equal to 1-1/4 in. The vertical section is supported by a 1/2-in. thick circular plate 20 in. in diameter. An insulator is used to electrically separate the antenna from the base. The base plate has provisions for connecting 20 radial ground wires, approximately 0.2 wavelength long, in order to stabilize the input impedance and reduce ground losses. The capacitive top hat is 5 ft in diameter and constructed of 1/4 in. aluminum rods in the form of an eight-spoked wheel which electrically approximates a solid disk. A parallel resonant LC trap has been included to reduce the antenna's electrical length to 0.6 wavelength above 19.15 MHz, thus maintaining nearly optimum low-angle ground-wave coverage.

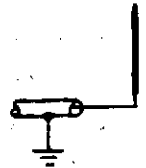
Transmitting Antenna Impedance Matching Networks

Impedance matching networks must be employed in order to transfer maximum power from the 50 ohm coaxial transmission line to the antenna. In general, for maximum power transfer, it is necessary to tune out the reactance of the antenna, and transform its resistance to 50 ohms. Matching performed in this manner is referred to as "conjugate matching" and has numerous applications in RF circuitry.

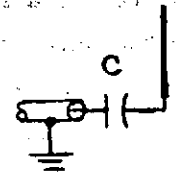
The general philosophy for matching a vertical monopole to a 50 ohm transmission line is represented pictorially in Figure 27 as a function of antenna electrical length. In most practical situations, vertical heights less than about 1/4 wavelength can be matched by simply inserting an inductance of sufficient value, in series with the antenna, to cancel the capacitive reactance. In this case ground losses are sufficiently high that the standing-wave ratio caused by a difference in resistance values is usually less than 2:1 over the required bandwidth. If the monopole is about 1/4 wavelength long the reactance is near zero and the resistance



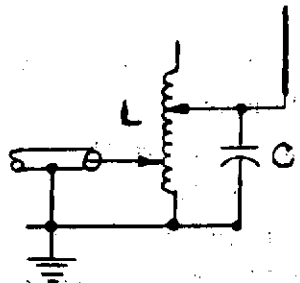
$$h < \frac{\lambda}{4}$$



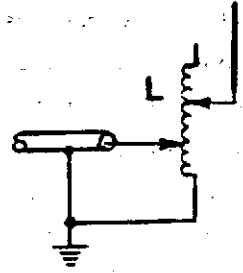
$$h = \frac{\lambda}{4}$$



$$.25\lambda \leq h \leq .3\lambda$$



$$\frac{\lambda}{4} \leq h \leq \frac{\lambda}{2}$$



$$\frac{\lambda}{2} \leq h \leq \frac{5\lambda}{8}$$

FIGURE 27. MATCHING NETWORKS FOR VERTICAL ANTENNA AS A FUNCTION OF ANTENNA HEIGHT

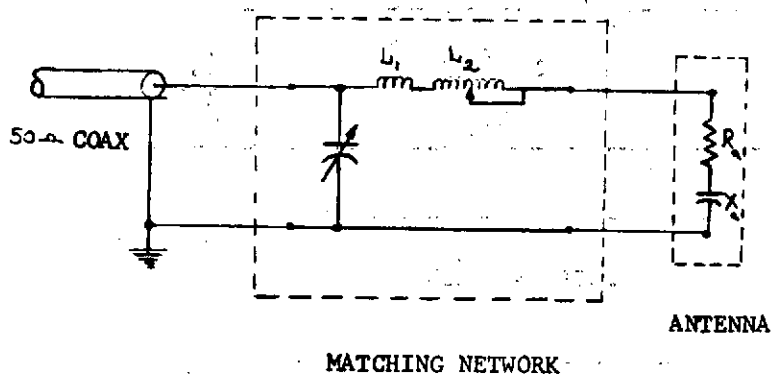
will be a fair match to 50 ohms without any matching network. For antenna lengths between 0.25 and 0.3 wavelengths, the antenna impedance appears inductive and can be resonated by a single series capacitor. For longer lengths it is necessary to transform the antenna's resistance in addition to turning out the reactance in order to achieve a suitable standing-wave ratio. The parallel equivalent circuit for an antenna greater than $1/4$ wavelength, but less than $1/2$ wavelength, appears as an inductor in parallel with a high resistance. The inductive reactance can be cancelled by a parallel capacitor and the high resistance value is normally transformed to 50 ohms by changing the tap positions on the inductor. At heights greater than $1/2$ wavelength, but less than or equal to $5/8$ wavelength the antenna impedance appears capacitive and hence a tapped coil can be used to resonate the antenna as well as transform the resistance.

The general procedures described above can be refined by employing simple L-networks that not only cancel the reactance but transform the impedance such that the 50 ohm transmission line appears to be terminated in its characteristic impedance. Networks specifically designed to conjugately match the power amplifier to the antenna at ten discrete frequencies in the HF region are shown in Figure 28 and 29. Figure 28 gives the inductance and capacitance values necessary to obtain impedance matching at frequencies less than 10 MHz. In a similar manner Figure 29 illustrates the network schematic and element values necessary for impedance matching above 10 MHz. The coils for frequencies less than 10 MHz are wound on Indiana General Q1 toroids whereas the coils used above 10 MHz are wound on Q2 cores. The size of the cores were chosen such that Gauge wire sizes could be used in the low frequency region. At each of the 10 frequencies different values of capacitance and inductance are necessary to obtain an impedance match. This requirement necessitates the use of a switching mechanism in order to insert the proper network between the antenna and transmission line. Since this switching must be accomplished automatically and synchronously with the receiver, an electromechanical switch was necessary.

Electromechanical Bandswitch

Since the antenna is not inherently broadband, the impedance matching networks must be switched between the transmission line and antenna. The dc stepping

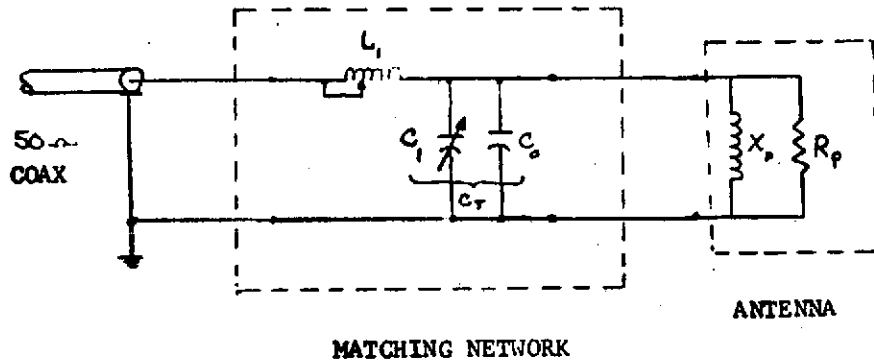
SUMMARY FOR CAPACITIVE INPUT



MATCHING NETWORK

f - MHz	C_1 - pf		L_1 - μ h		L_2 = μ h
	$\sigma = \infty$	$\sigma = 4$	$\sigma = \infty$	$\sigma = 4$	
3.1-3.2	5480.	980.	.45	1.3	32.
4.1-4.2	3150.	875.	.45	.96	19.
5.1-5.2	1950.	735.	.45	.75	11.
6.1-6.2	1350.	600.	.45	.64	7.
7.1-7.2	900.	480.	.48	.56	5.
9.1-9.2	445.	285.	.43	.43	1.6

FIGURE 28. NETWORK ELEMENTS NECESSARY TO CONJUGATELY MATCH TRANSMISSION LINE TO ANTENNA AT FREQUENCIES LESS THAN 10 MHz



f MHz	C_1 - Pf	C_0 - Pf	C_{Total} - Pf	L_1 - μ h
12.15	129	154	283	0.6
15.15	68	38	106	1.5
19.15	40	5.3	46	1.7

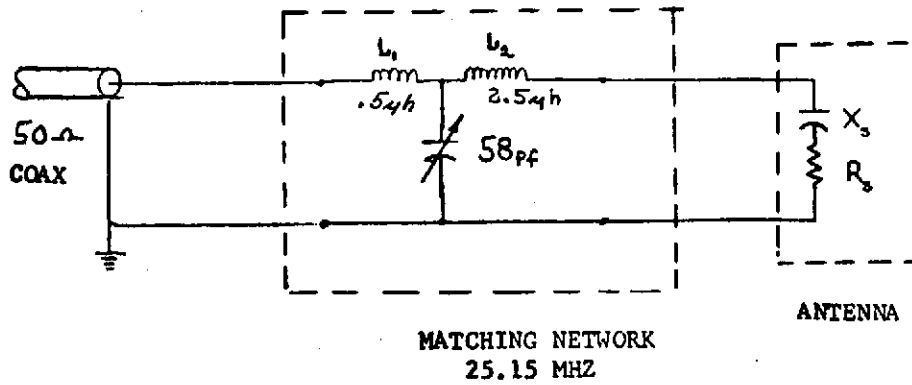


FIGURE 29. NETWORK ELEMENTS FOR CONJUGATELY MATCHING TRANSMISSION LINE TO ANTENNA AT FREQUENCIES ABOVE 10 MHz

switch shown in Figure 30 is used to fulfill this requirement. A command pulse from the transmitter sweep controller-programmer is used to initiate the bandswitching sequence. The interface between the electrical command from the sweep controller module and the rotary stepper is provided by a SN75450 integrated circuit relay driver. The set input to the relay driver is maintained at a logic one by maintaining this pin connection at a positive potential of 5 V through a 22.5 Kohm resistor. The leading edge of the positive going command pulse, after it has undergone a logic transition, is applied to the NAND gate. When both inputs to this gate are at logic one levels, its output undergoes a transition from 0.5 V to 3.5 V driving the transistor into saturation. The collector-to-emitter voltage then drops to a low value allowing current to be drawn by the relay and hence, allowing its contacts to close. The stepping switch motor is then activated by the relay and rotates through 30 degrees for each impulse of current delivered to its coil. The contacts on a two-deck rotary wafer switch are thus advanced to a new position implementing the band change. A ratchet is included on the shaft in order to hold the switch in position when the coil is de-energized. The unit is self-advancing and the shaft rotates from position to position each time the coil is energized.

An essentially identical bandswitching assembly is also used for bandswitching the turned circuits in the receiver pre-selector. This switching is accomplished under the control of the receiver sweep controller-programmer module.

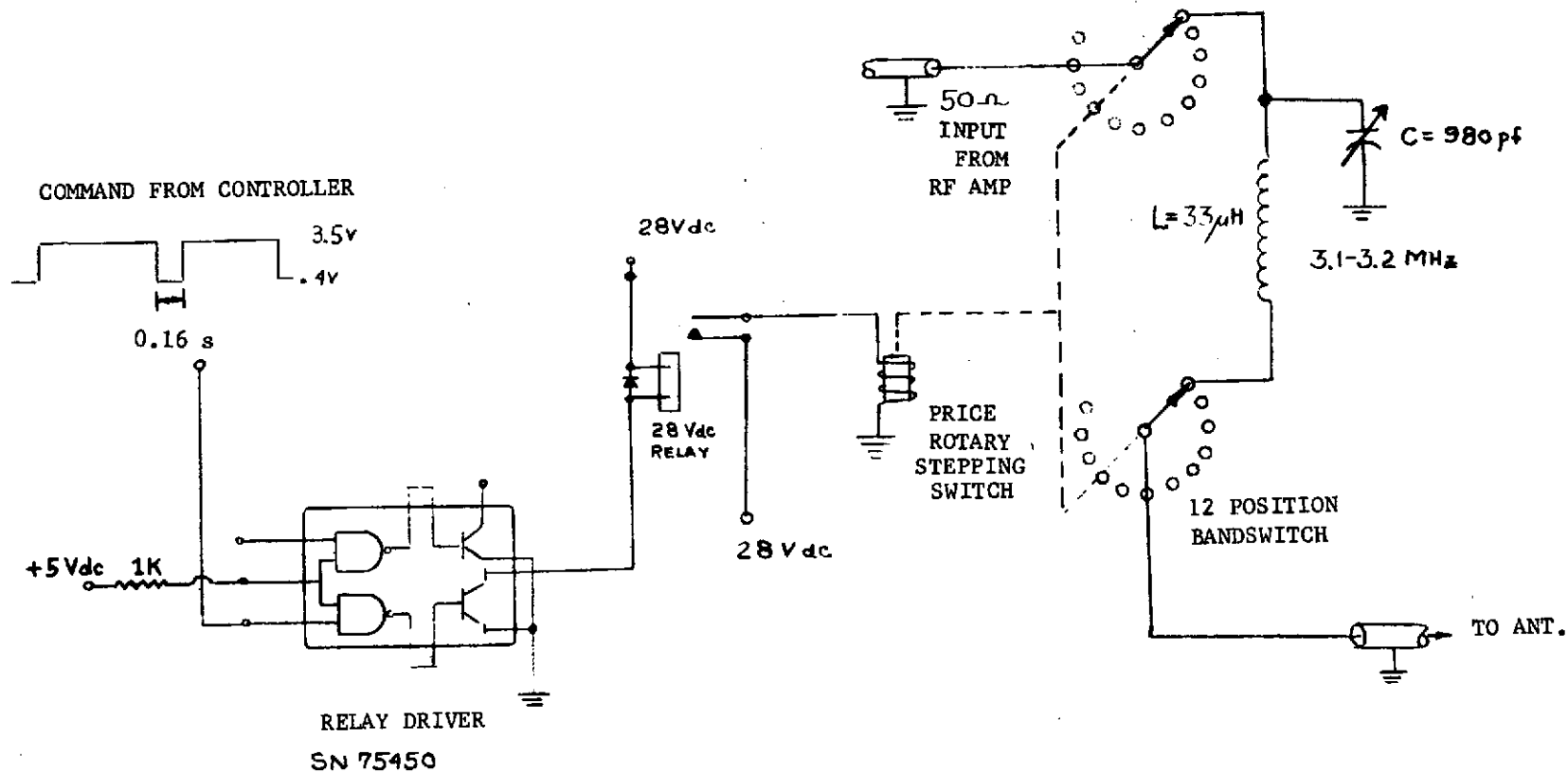


FIGURE 30. BANDSWITCH

ORIGINAL PAGE IS
OF POOR QUALITY

Receiver Pre-Selector

The receiver pre-selector consists of a broadband high-dynamic range FET input stage followed by a tuned amplifier stage using an integrated circuit transistor array. The input stage insures a low noise figure (≈ 5 dB) and has a 140 dB dynamic range, adequate to accommodate the range of signals expected to be encountered in the HF band during the experiment. This stage has a gain of 10 dB and a 3 dB bandwidth of 1-40 MHz.

The tuned stage consists of a common-emitter connected transistor with an additional transistor used as a variable resistor in the emitter of the gain determining transistor. Still another transistor is used as a bias diode for temperature stabilization.

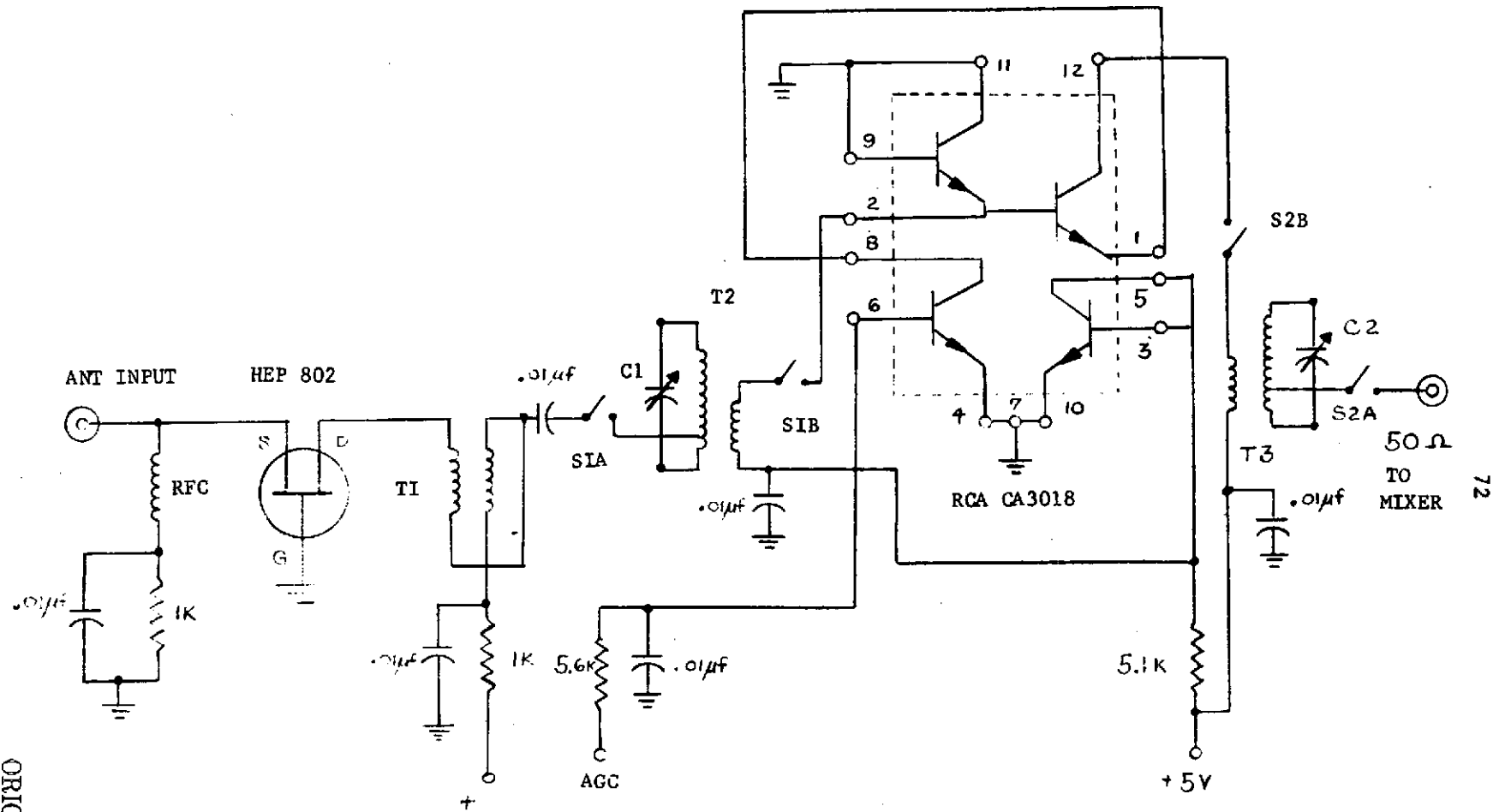
The pre-selector circuit is shown in Figure 31 A, B. Two tuned circuits are used with mismatching to obtain stability. The tuned stage has a gain of 20 dB and a bandwidth of 300 kHz. This is adequate to accommodate the bandwidth of the received signal.

The frequency band is selected by switching tuned circuits via the switches S1 and S2. These are rotary switch decks driven by a stepping motor. The motor is activated by a relay which in turn is driven by an SN75450 driver stage. The input signal for the driver is supplied by the controller and consists of a .16 second pulse with 1.6 seconds allowed for completion of the switching functions. The pre-selector is thus automatically switched from band to band synchronously with the transmitter under the control of a master clock signal from the controller.

The performance parameters of the pre-selector are as follows:

Gain	-	30	dB
Bandwidth	-	300	kHz
Noise Figure	-	5.2	dB
AGC Range	-	45	dB
Dynamic Range	-	140	dB.

ORIGINAL PAGE IS
OF POOR QUALITY



S₁, S₂ Ganged Rotary Electromechanical Bandswitch

C₁, C₂ 24-200 mmf trimmer capacitors

FIGURE 31A. RECEIVER PRESELECTOR CIRCUIT DIAGRAM

FIGURE 31B. TRANSFORMER PARAMETERS FOR RECEIVER PRESELECTOR

<u>Frequency Band</u>	<u>T1</u>	<u>T2</u>	<u>T3</u>
1, 2, 3	Six Twisted Pair Bifilar Turns on F625-9 Ferramic Torroid of H Material	24 Turns on Primary Tapped at 4 Turns. 8 Turns on Secondary Q1 Material	16 Turns on Primary 24 Turns on Secondary Tapped at 4 Turns Q1 Material
4, 5	"	12 Turns on Primary Tapped at 2 Turns. 4 Turns on Secondary Q1 Material	8 Turns on Primary 12 Turns on Secondary Tapped at 2 Turns. Q1 Material
6	"	6 Turns on Primary Tapped at 1 Turn 2 Turns on Secondary Q1 Material	4 Turns on Primary 6 Turns on Secondary Tapped at 1 Turn Q1 Material
7, 8	"	12 Turns on Primary Tapped at 2 Turns 4 Turns on Secondary Q2 Material	8 Turns on Primary 12 Turns on Secondary Tapped at 2 Turns Q2 Material
9, 10	"	6 Turns on Primary Tapped at 1 Turn 2 Turns on Secondary Q2 Material	4 Turns on Primary 6 Turns on Secondary Tapped at 1 Turn Q2 Material

T1, T2 are wound on F 627-8 Ferramic Torroids

Receiver Mixer

The mixer circuit is a broadband double-balanced mixer using an SN76514 integrated circuit as the basic circuit. The output from the pre-selector is provided to the mixer through a 1:4 impedance transformer. This transformer is a broadband transmission line type transformer consisting of a bifilar winding on a ferrite torroid. The torroid used is an Indiana General F624-19 core of O6 material. The bandwidth of the transformer ranges from about 800 kHz to 250 MHz.

The balanced output of the mixer is coupled to the input of a communications receiver through a 4:1 balanced-to-unbalanced broadband impedance transformer. This transformer is also a transmission line type transformer consisting of 10 turns of bifilar winding on another F624-19 O6 torroidal core. The overall bandwidth of the mixer assembly is of the order of 100 MHz, with a response which is essentially flat from 1 MHz to 100 MHz.

The local oscillator driver for the mixer is provided by the programmed output from the synthesizer at a level of .7 volt rms.

The mixer circuit is shown in Figure 32. A conversion gain of 12 dB is obtained over the operating bandwidth with an RF to IF isolation of the order of 30 dB, a local oscillator to IF isolation of 30 dB, and a local oscillator to RF isolation of 60 dB.

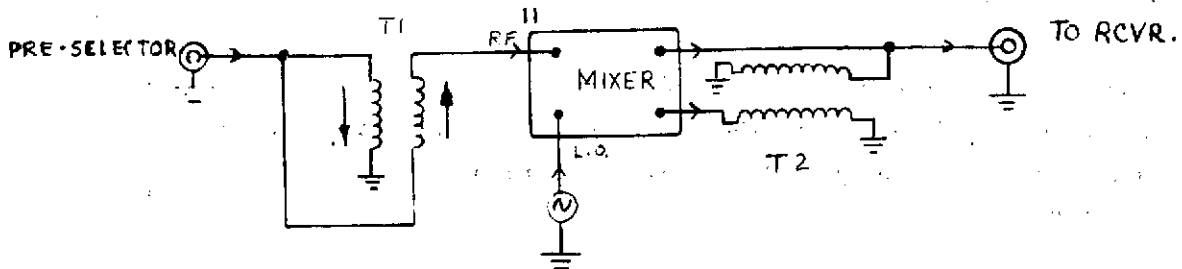
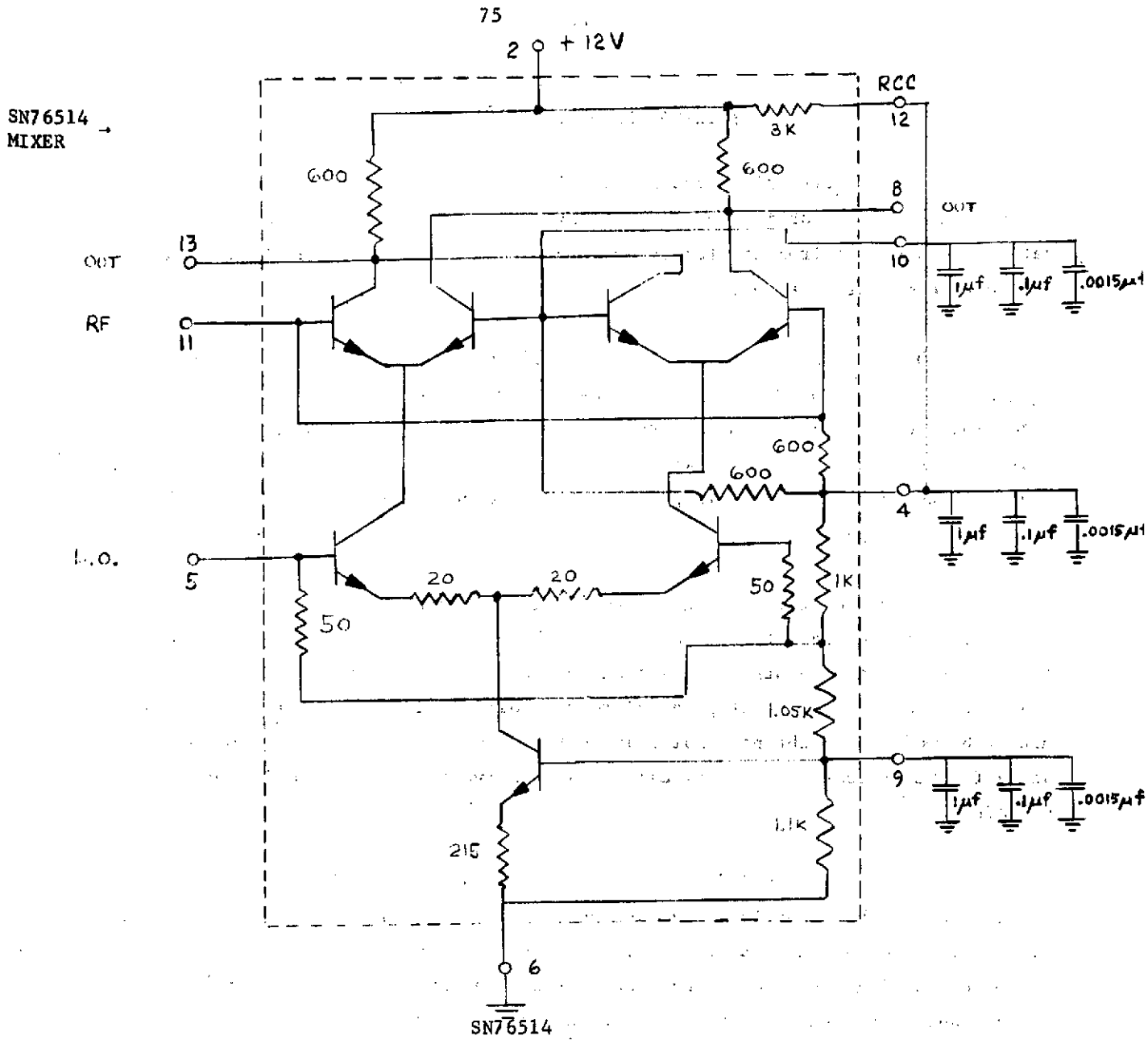


FIGURE 32. MIXER CIRCUIT DIAGRAM

V. THE AIRCRAFT EXPERIMENT

The objective of conducting an aircraft experiment is to validate the basic concept, to establish the required system parameters, and to establish the data processing requirements for recovery of the wave height directional spectrum at the transmitter location.

The specific experimental effort will consist of locating the transmitting equipment either on a ship or at the Coast Guards Chesapeake Light Tower facility with the receiving equipment flown on an aircraft. The specific flight path followed will pass near the transmitter site with the data-taking-interval comprising approximately 10-15 minutes per flight. This provides 2 or 3 essentially redundant sets of data for each flight path.

Several different flight paths will be required in order to determine the sensitivity of the data to the specific flight path and to optimize the recovery of the directional components. In particular, it is desirable that for a particular sea state condition a flight parallel to the mean surface wind direction at the transmitter be made, a flight perpendicular to the mean surface wind direction be made, and a flight at some angle (nominally 45°) relative to the mean surface wind direction be made.

During the actual data-taking-interval (a minimum of five minutes) the aircraft should be flown in-so-far as possible on a constant heading, at a constant altitude, and at a constant velocity. Minor variations ($\leq 10\%$) in the aircraft flight parameters during the data taking should present no problem. Major variations however would require that the aircraft's position and velocity be tracked in order to compensate in the subsequent data reduction.

The specific average altitudes and average velocities at which the flights are made are not critical as long as they are relatively constant during each five minute data taking period. A typical altitude range might be 5,000-10,000 feet at a velocity of 200 mph.

The most desirable data will be obtained when the sea is running quite high at the transmitter location. There are however obvious safety and practical limitations on obtaining this kind of data during these experiments. In-so-far as possible, data runs should be taken under calm conditions (mean surface wind velocities ≤ 10 knots), average conditions (mean surface wind velocities 10-20 knots), and high sea state conditions (mean surface wind velocities > 20 knots).

To insure that the experimental hardware and procedures are functioning as planned, several data taken flights should be made initially and the resulting data processed to assure that valid information is being obtained. Subsequent data taking flights can then make for varying sea state and experimental conditions and detailed analysis of these experimental results carried out.

Prior to any data taking flights, several on-site calibration steps must be performed. Because of the uncertainties of the specific input impedance presented by the transmitting antenna, the matching networks for the transmitter must be fine tuned on each band with the transmitting antenna erected on site (either on the Chesapeake light tower or a boat). Similarly, a field strength measurement should be made to determine the on-site transmitting antenna ground wave gain function.

The HP synthesizers utilized for frequency and time control at the transmitter and receiver derive their basic stability and accuracy from the associated driver units. These drivers must operate for a period of 72 hours in order to stabilize sufficiently to satisfy the required stability conditions. Thus it is planned that the synthesizer drivers will be turned on and allowed to stabilize for 72 hours. The two units will then both be calibrated against a frequency standard and will not be subsequently turned off during the rest of the experiment. This will be accomplished by powering these units from a battery source which is continuously trickle charged by a 110 volt 50-400 Hz primary power source except for those periods during which a driver unit is being transported from the laboratory to the aircraft or to a boat etc. This procedure is necessary to maintain the required coherency between the transmitter and receiver. Only the synthesizer drivers will be operated continuously in this manner. Other experimental hardware components will be turned on only as required.

Prior to each actual data run the sweep controller-programmer must be energized at both the transmitter and receiver and the starting frequencies for the ten frequency bands inserted into the unit's memory. This is done by front panel thumbwheel switches. After these data are inserted, the unit is switched to its sweeping mode and it will then continuously step to a new frequency every 30.4 seconds and repeat the entire cycle every 304 seconds until returned to manual control.

Received Signals For An Aircraft Experiment

The form of the Doppler spectrum obtained from an aircraft experiment will differ considerably from that received by a satellite. The differences are due primarily to two causes. For a satellite, the range from each scattering element of the range ring on the sea surface to the satellite is sufficiently large that the changes of the angular scattering parameters due to the specific location of the scattering area within the total range ring are small. For an aircraft, the aircraft flight path can be such that it intersects the range ring and the resulting angular changes can be large.

A further difference is due to the specific polarization of the aircraft antenna. Since the aircraft antenna will exhibit a specific polarization direction, energy scattered from some sectors of the surface will not be received because it is polarized orthogonal to the aircraft antenna. For a satellite, Faraday rotation in the ionosphere will result in a constant change of the direction of polarization of the scattered field at the satellite. This means that a satellite antenna which is polarized in a particular direction will view a scattered field whose polarization is rotating with time. Over a period of time the average signal will not exhibit polarization effects.

These points can be illustrated by the following Figures. In Figures 33 through 38 the computed received Doppler spectra are illustrated for a satellite whose flight path lies at an angle of 40° to the mean surface wind direction. The surface wind velocity is 20 knots, the satellite velocity is 8 km/s, its altitude is 400 km. The satellite orbit is such that at CPA (closest point of approach), the satellite is located 70 km from the transmitter zenith. Figures 33, 34, and 35

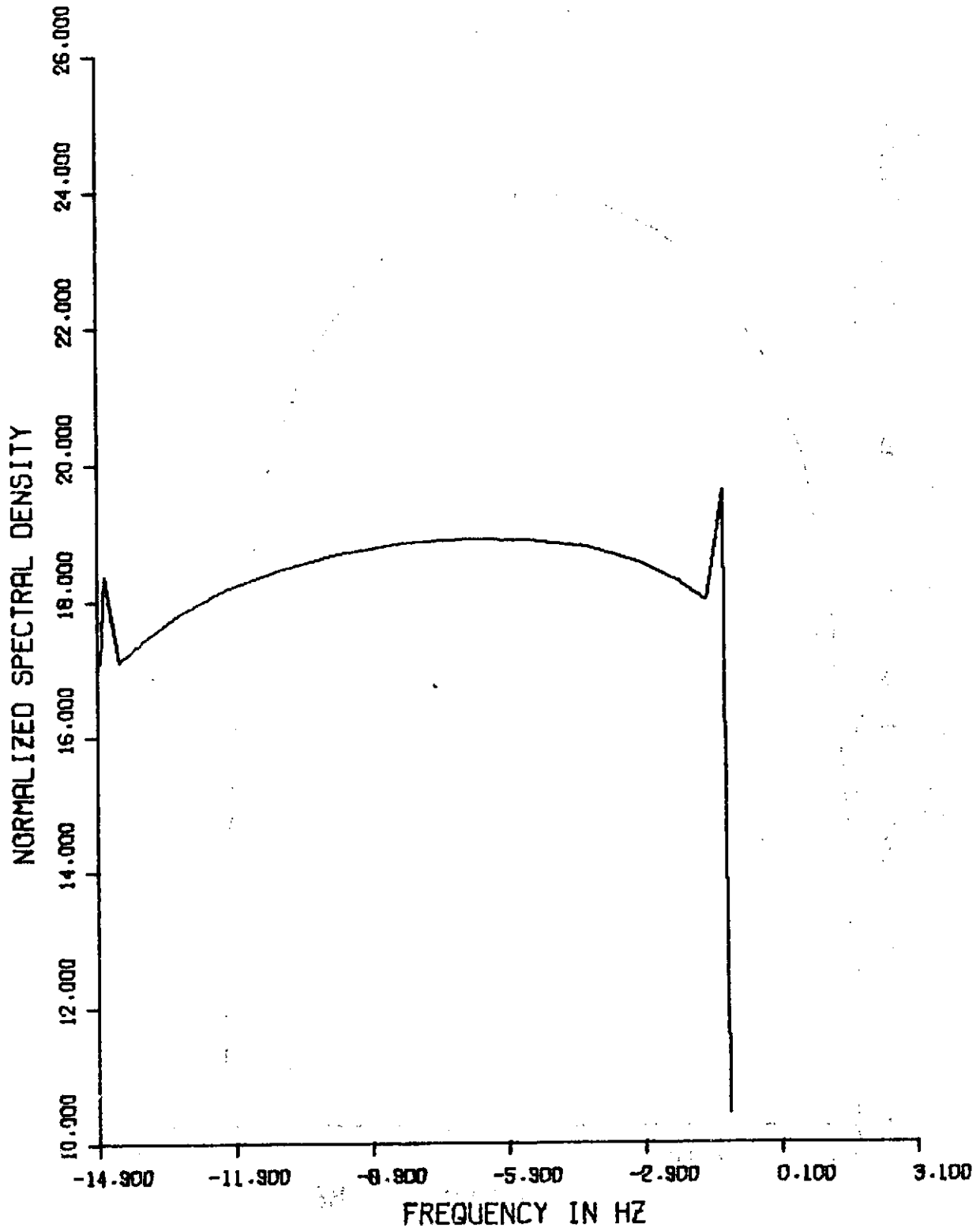


FIGURE 33. SATELLITE RECEIVED SPECTRUM BEFORE CPA FOR ISOTROPIC SURFACE

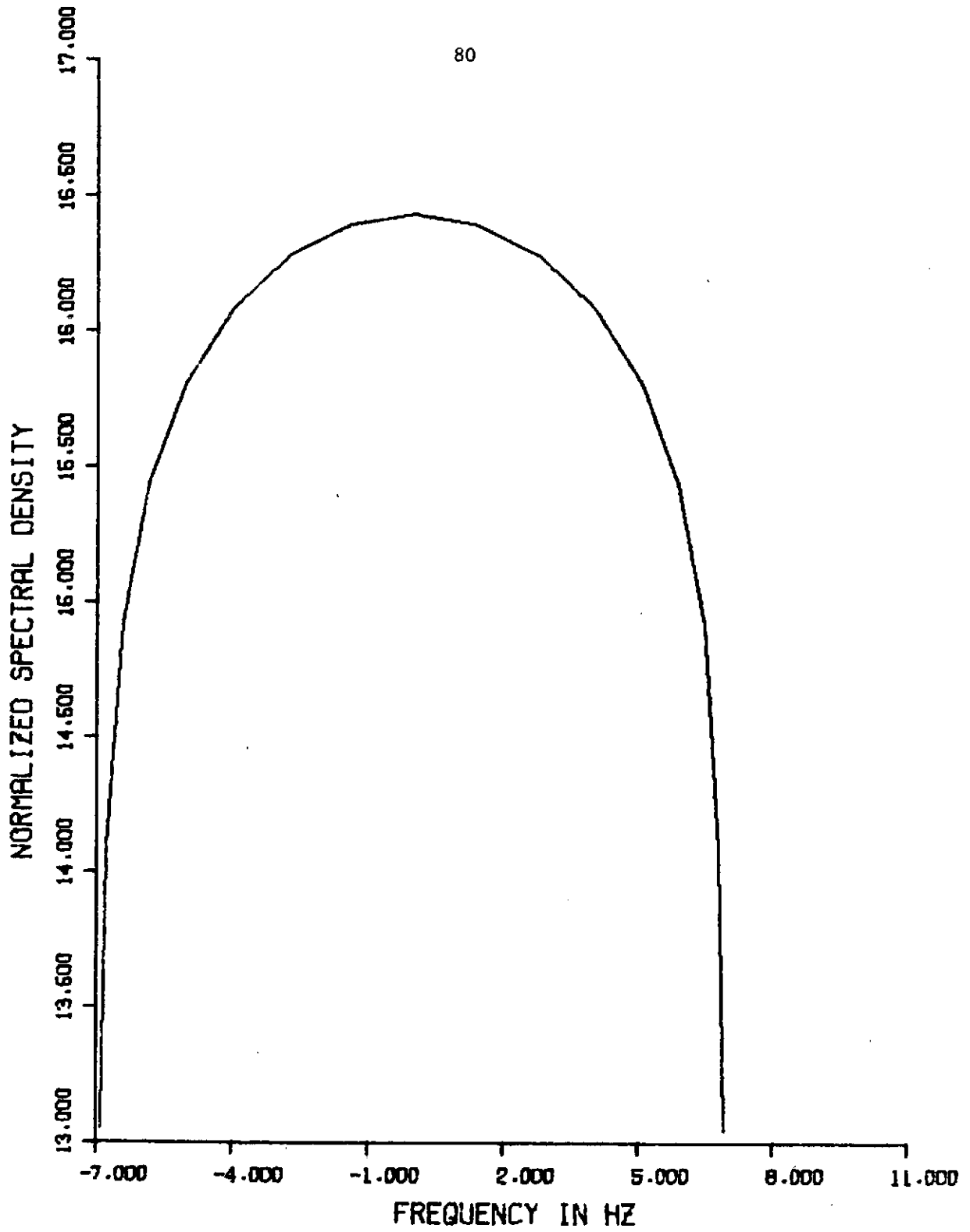


FIGURE 34. SATELLITE RECEIVED SPECTRUM AT CPA IN ISOTROPIC SURFACE

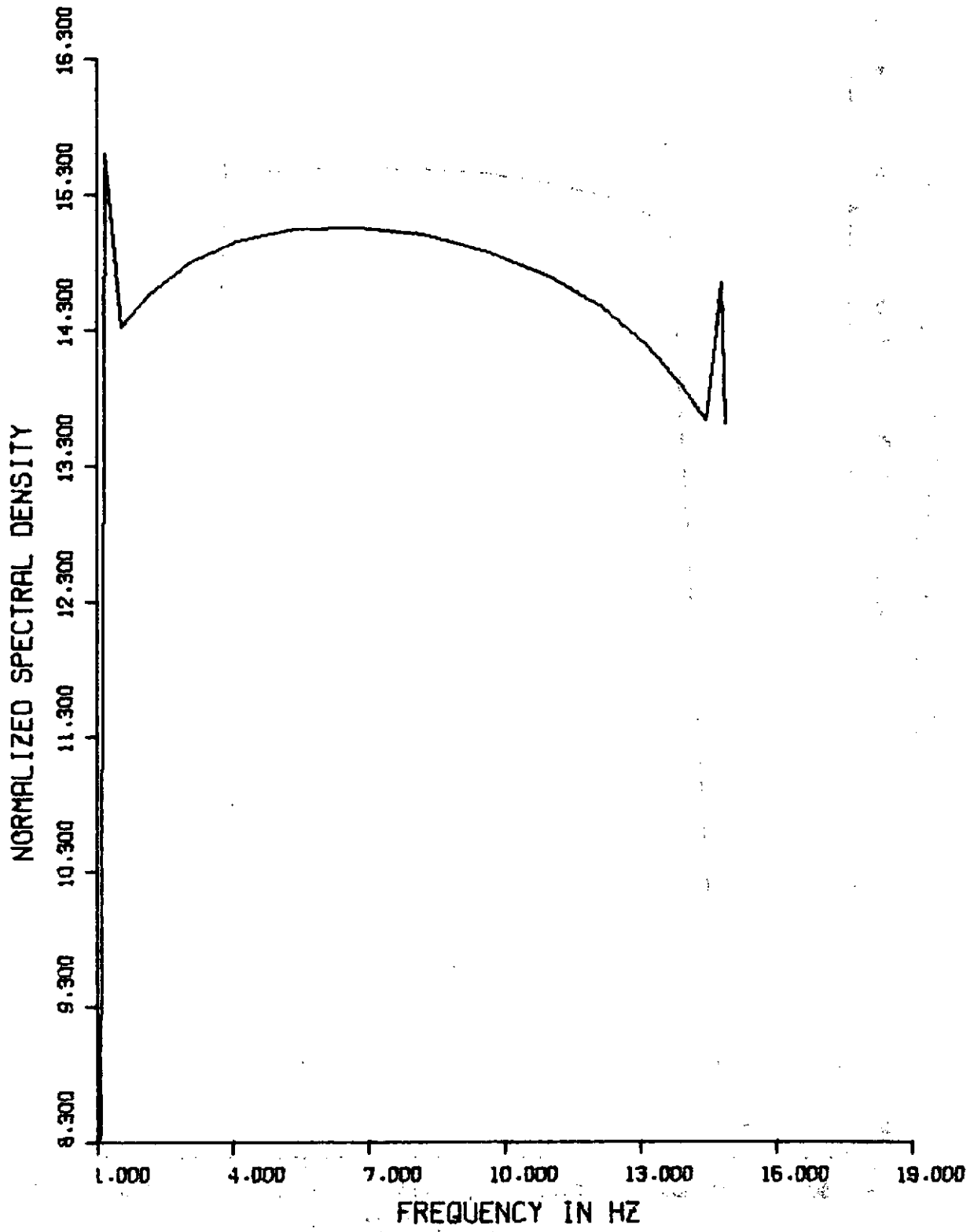
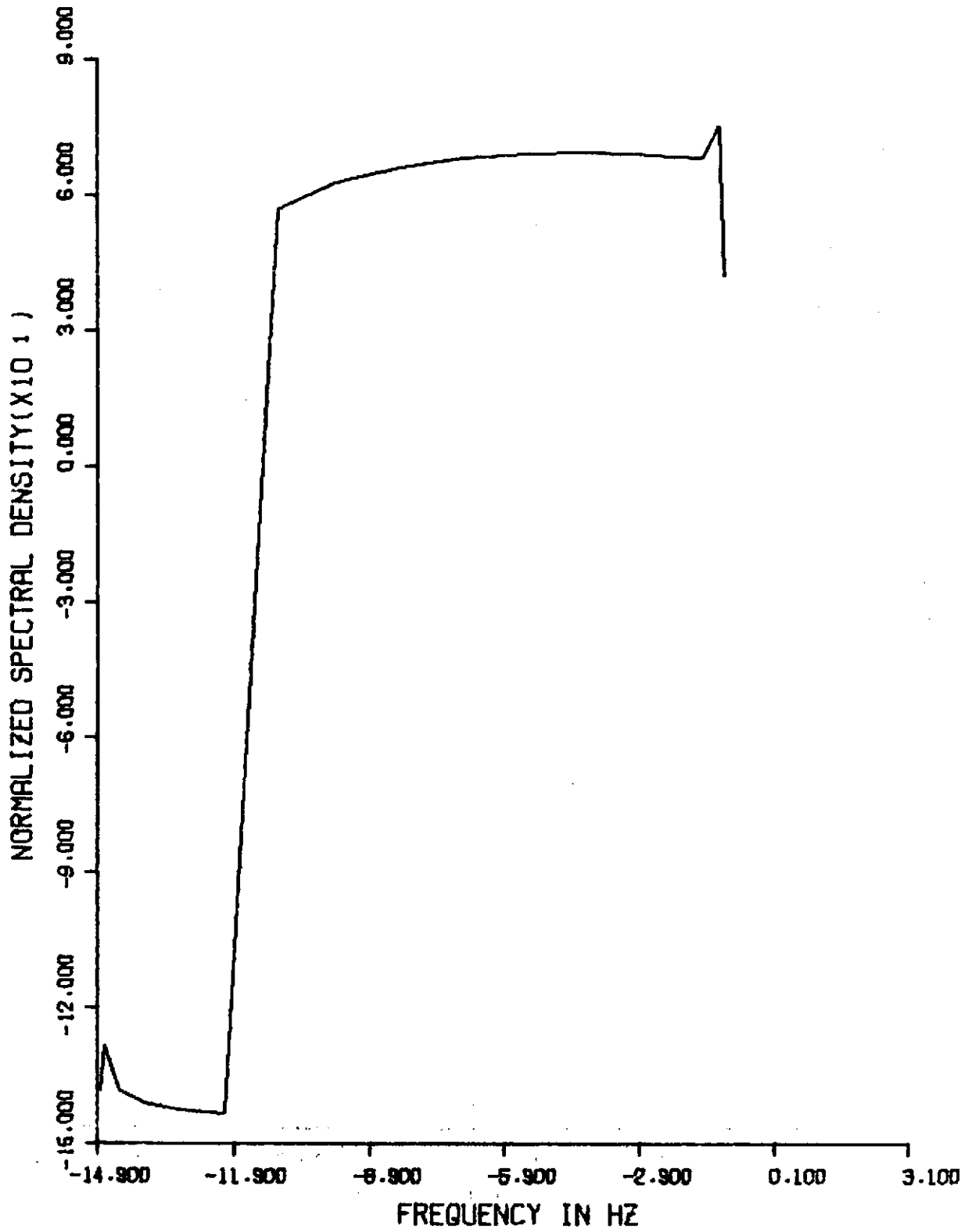


FIGURE 35. SATELLITE RECEIVED SPECTRUM AFTER CPA IN ISOTROPIC SURFACE

FIGURE 36. SATELLITE RECEIVED SPECTRUM BEFORE CPA FOR \cos^2 SURFACE

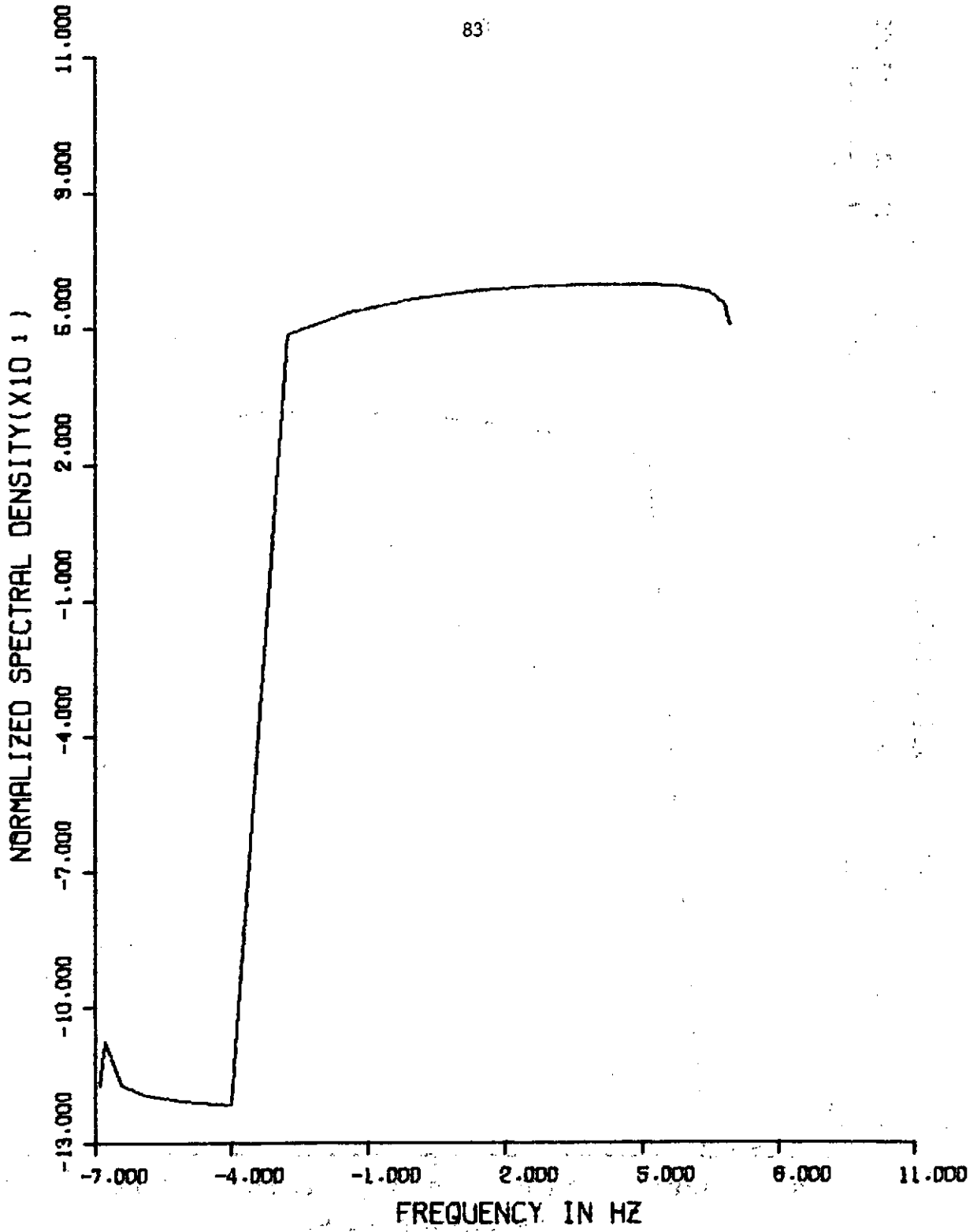


FIGURE 37. SATELLITE RECEIVED SPECTRUM AT CPA IN COS² SURFACE

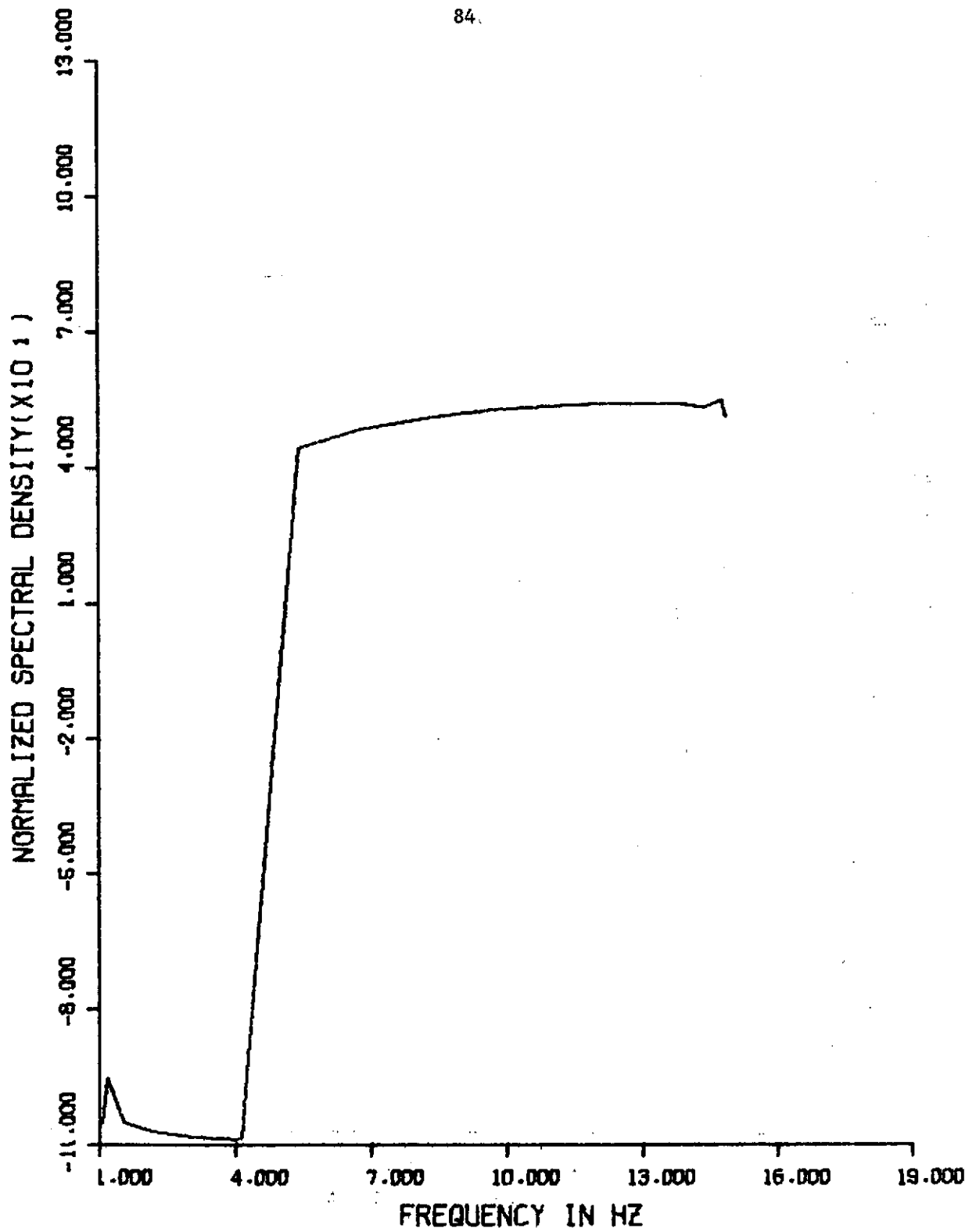


FIGURE 38. SATELLITE RECEIVED SPECTRUM AFTER CPA FOR COS² SURFACE

present the received spectrum for an isotropic surface height spectrum as received at a point before CPA, at CPA, and after CPA respectively. Figures 36, 37, and 38 present the received spectrum for the same satellite locations when the wave height spectrum has a \cos^2 directionality. These curves are smoothly varying and relatively easy to interpret.

For the aircraft case, the received spectra appear quite different. Figure 39 illustrates the received spectrum at CPA for an isotropic surface. For this figure the aircraft was flying at an altitude of 4 km and a velocity of 125 m/s. The distance from the transmitter zenith at CPA was .7 km. The range ring on the surface was located 7.5 km from the transmitter so the aircraft was well within the range ring. It was assumed that the aircraft antenna was polarized parallel to the flight path. The structure of the received spectrum is quite different from the satellite case with variations of the order of 10 dB appearing within the spectrum and a distinct null at zero Doppler. This null is due to a polarization cancellation phenomena and appears for flight patterns lying within the range ring.

To exhibit the effects of a directional surface spectrum for the aircraft case, Figures 40, 41, and 42 illustrate the received spectrum at CPA for flight paths parallel to the mean surface wind direction, 40° from the mean surface wind direction, and perpendicular to the mean surface wind direction when the surface has a \cos^2 directionality. Although the directional effects are exhibited in these spectra, they are not as prominent as for the satellite case and tend to be somewhat obscured by the polarization and angular effects. This does not prevent the recovery of the directional information, however, since the polarization and angular aspect effects can be removed in the data reduction.

Figures 43 through 48 exhibit the received spectra for the aircraft located before and after CPA for flight paths along wind, at 40° and cross wind respectively.

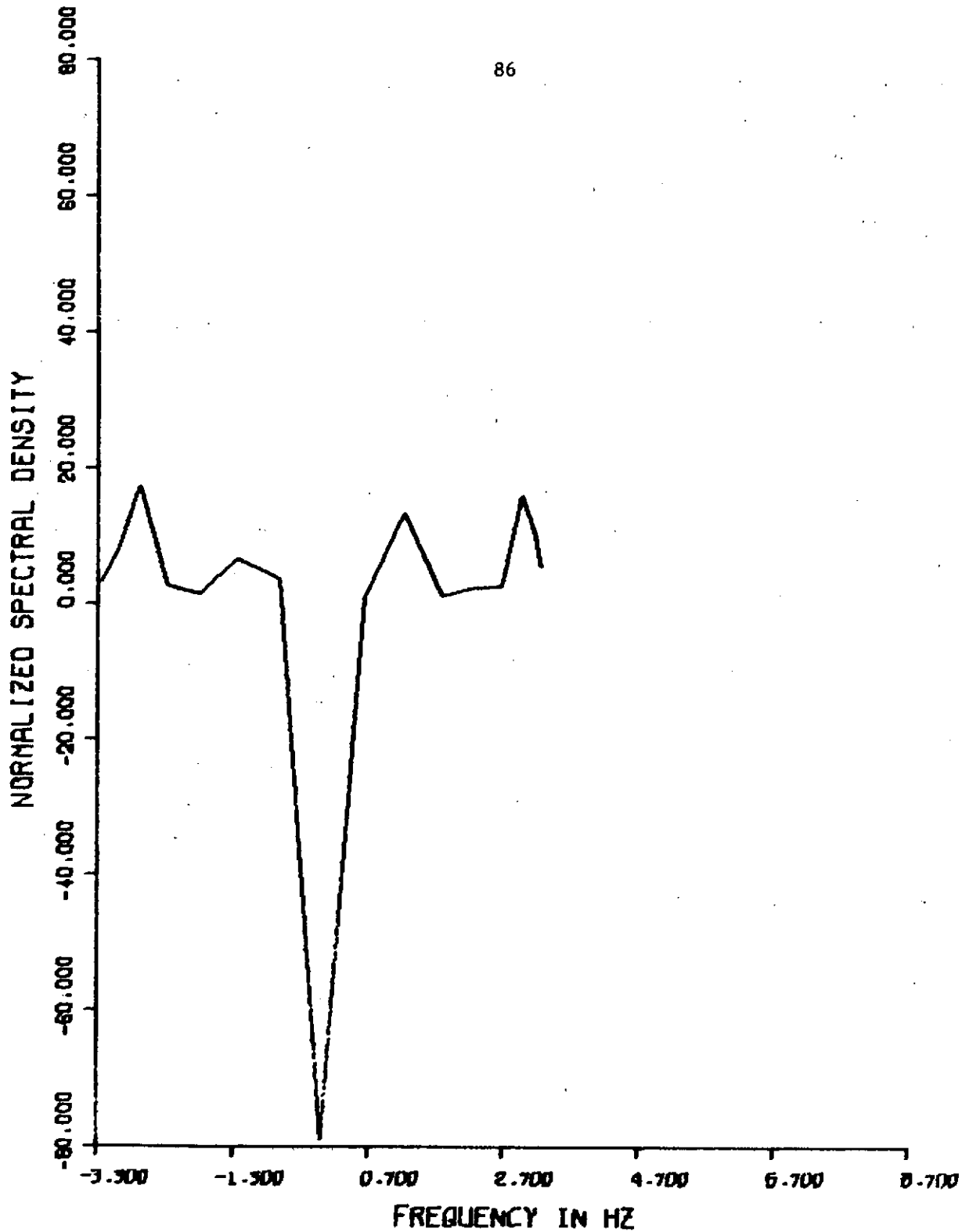


FIGURE 39. AIRCRAFT RECEIVED SPECTRUM AT CPA ISOTROPIC SURFACE

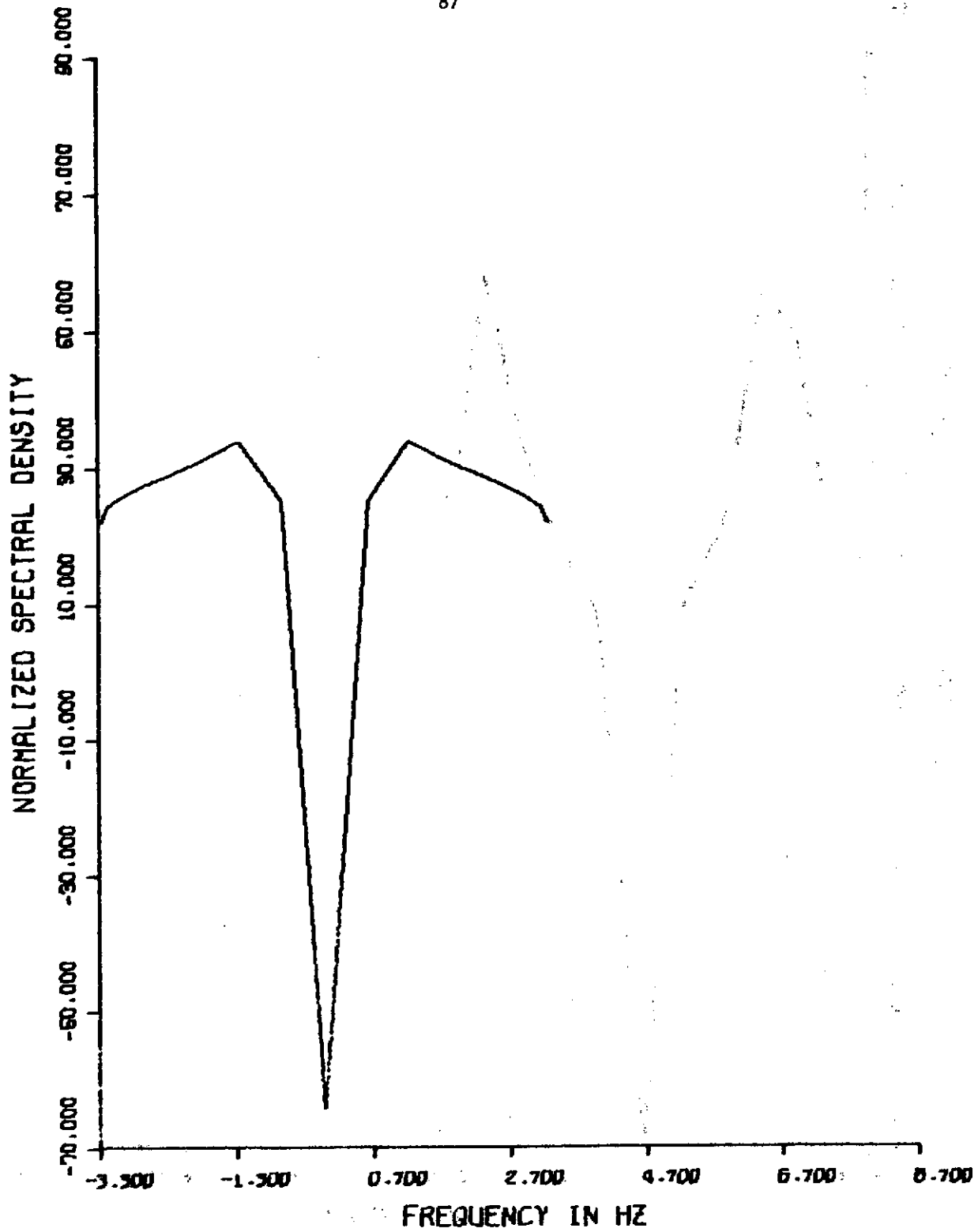


FIGURE 40. AIRCRAFT SPECTRUM AT CPA FOR \cos^2 SURFACE, ALONG WIND FLIGHT PATH

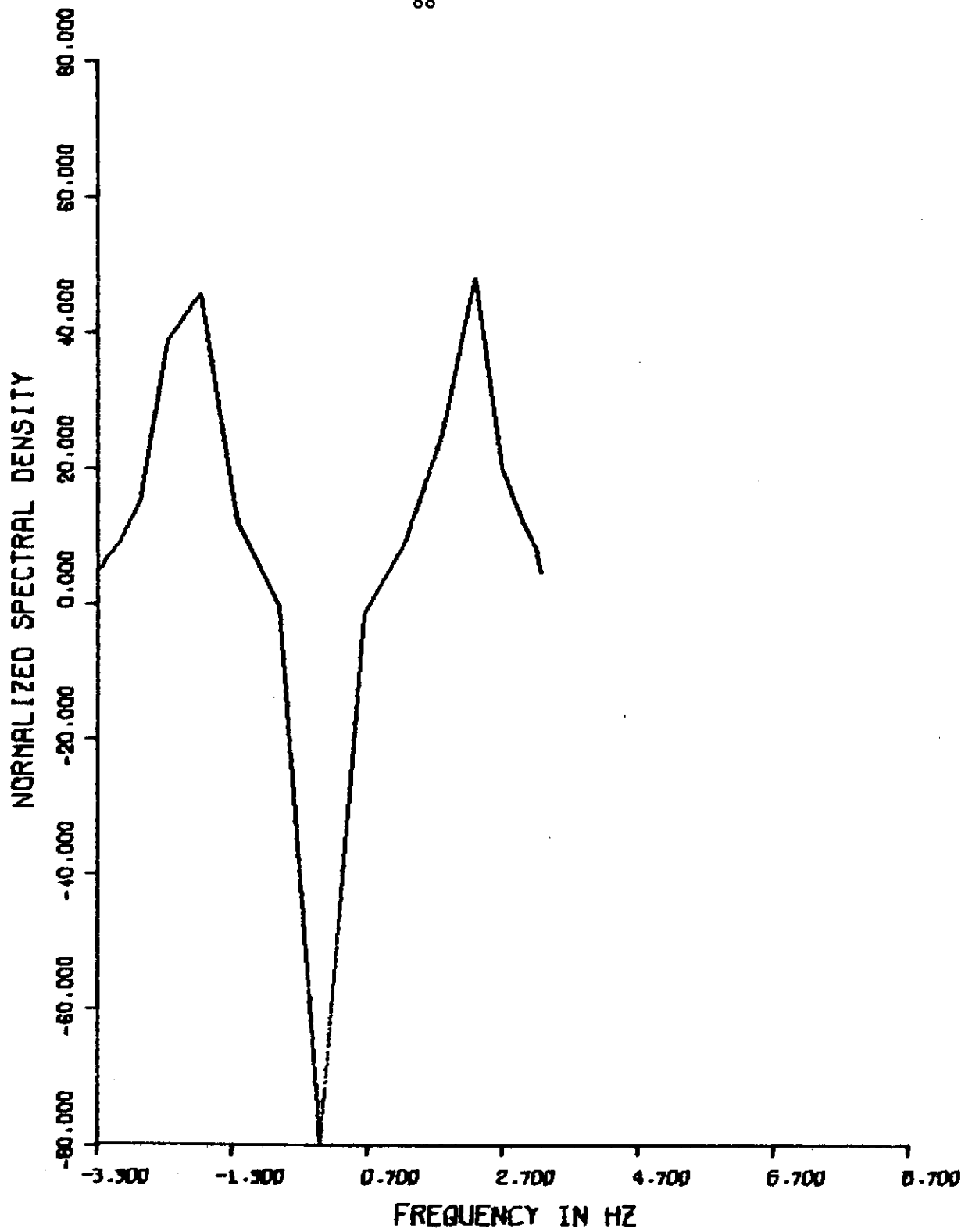


FIGURE 41. AIRCRAFT RECEIVED SPECTRUM AT CPA FOR COS^2 SURFACE-40° FLIGHT PATH

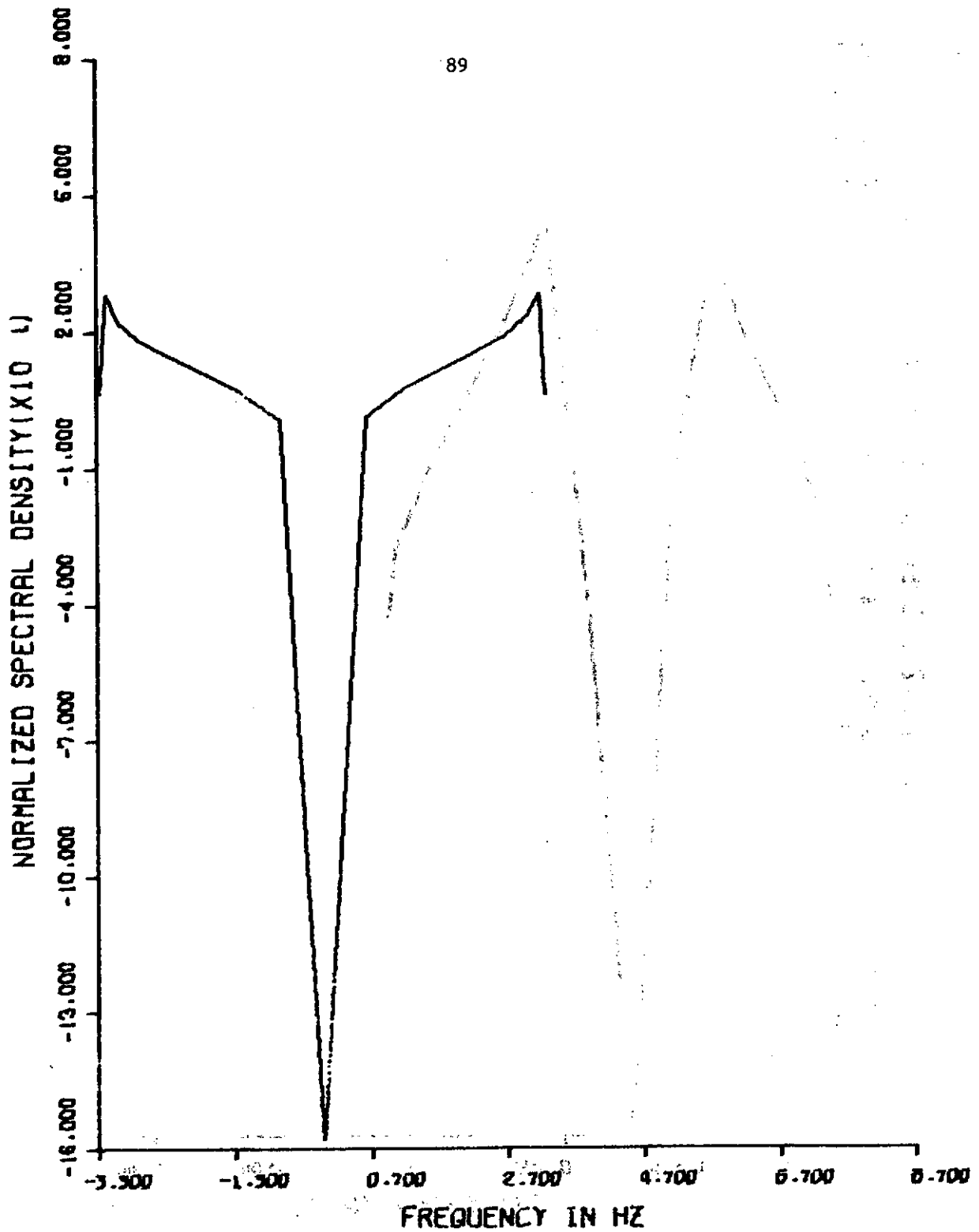


FIGURE 42. AIRCRAFT RECEIVED SPECTRUM AT CPA FOR COS² SURFACE, CROSS WIND FLIGHT PATH

22

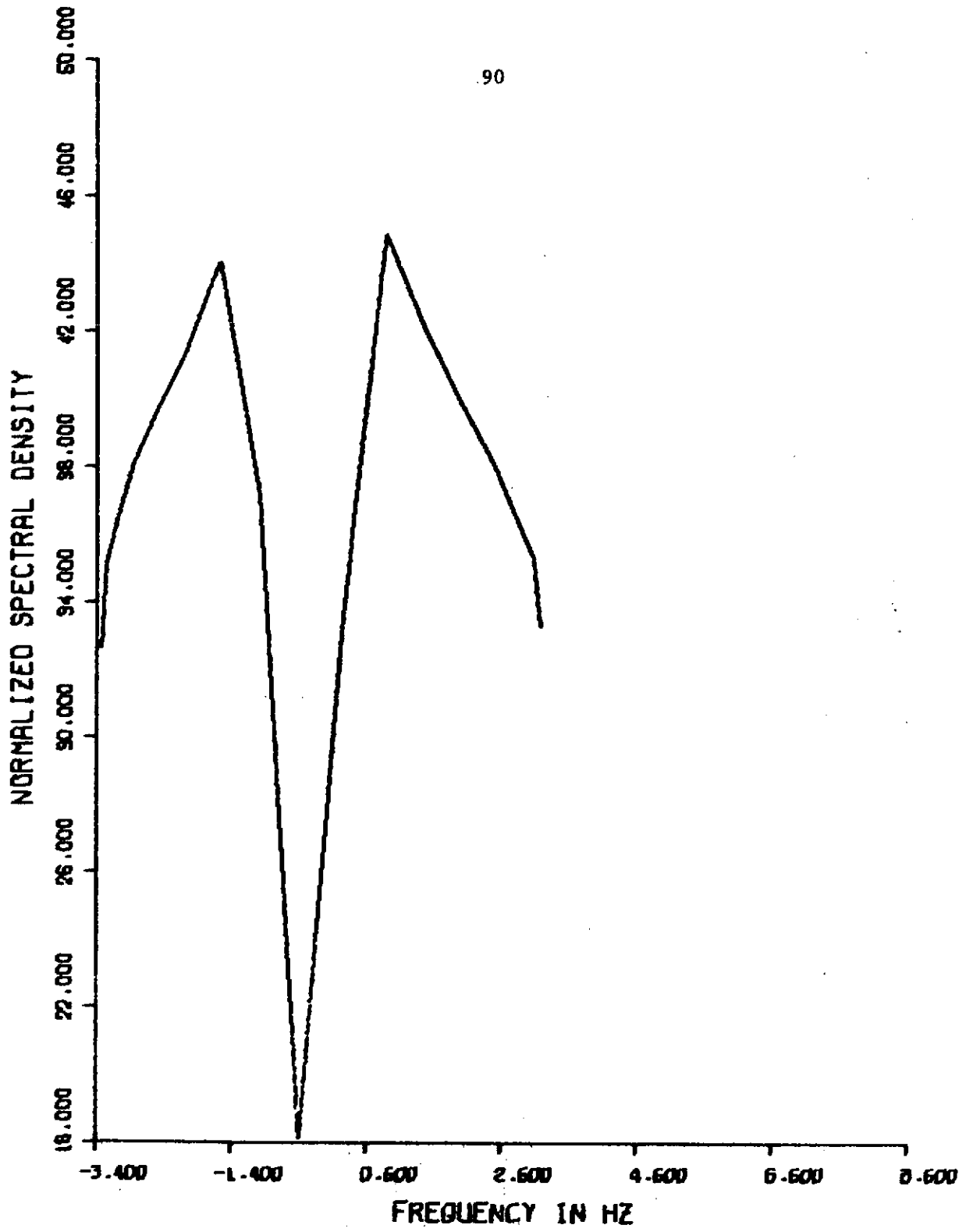


FIGURE 43. AIRCRAFT RECEIVED SPECTRUM BEFORE CPA FOR COS² SURFACE, ALONG WIND FLIGHT PATH

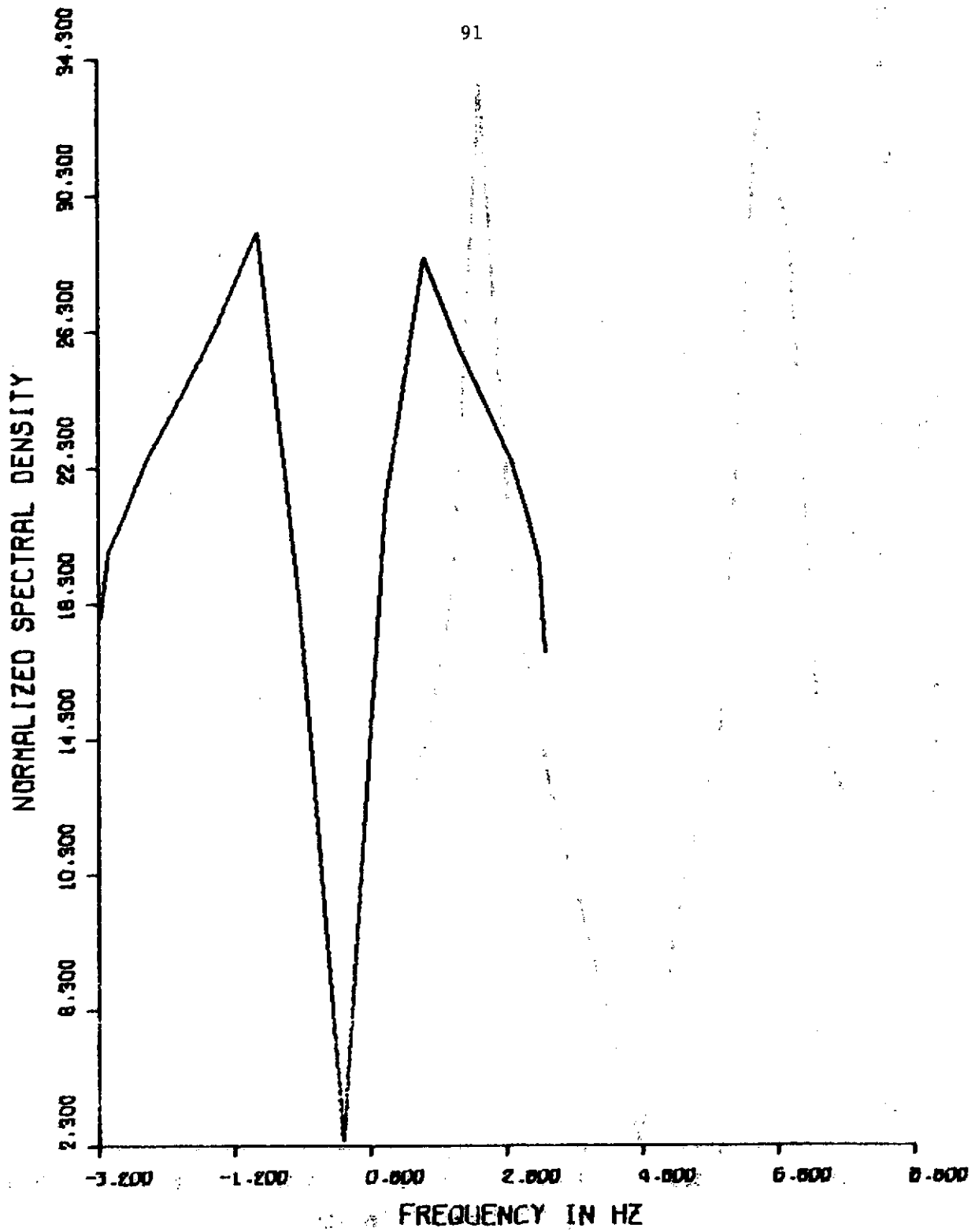


FIGURE 44. AIRCRAFT RECEIVED SPECTRUM AFTER CPA FOR \cos^2 SURFACE, ALONG WIND FLIGHT PATH

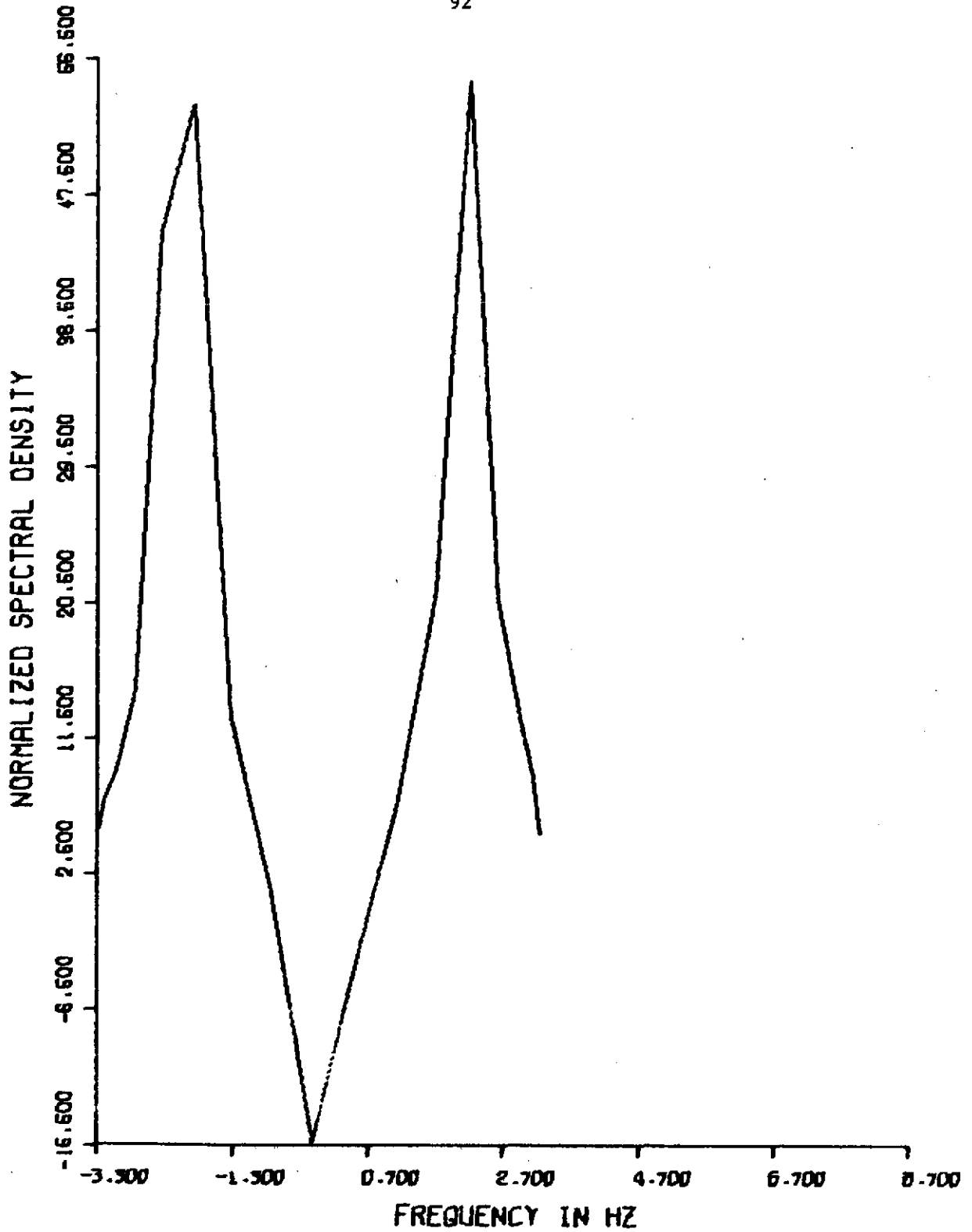


FIGURE 45. AIRCRAFT RECEIVED SPECTRUM BEFORE CPA FOR \cos^2 SURFACE, 40° FLIGHT PATH

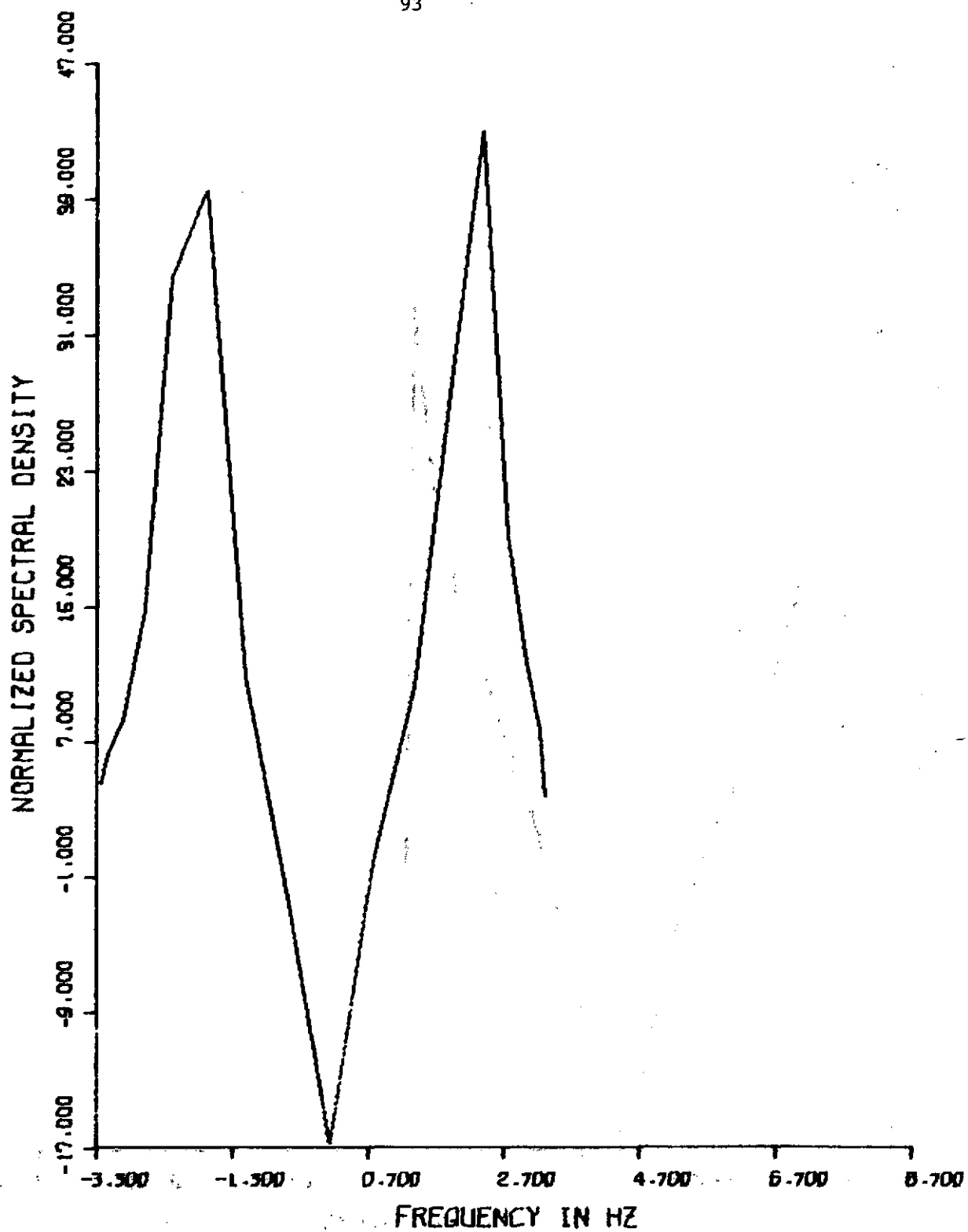


FIGURE 46. AIRCRAFT RECEIVED SPECTRUM AFTER CPA FOR \cos^2 SURFACE, 40° FLIGHT PATH

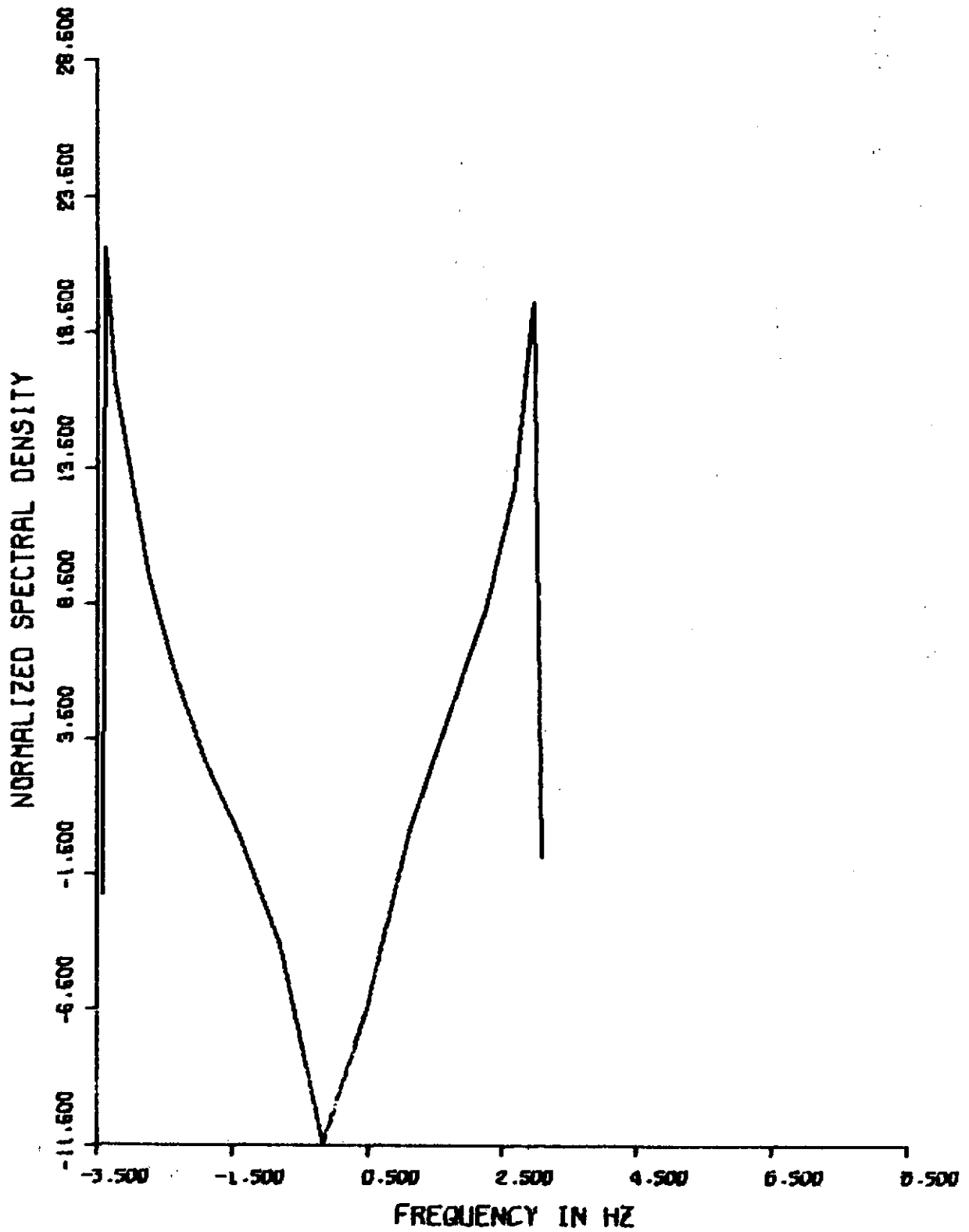


FIGURE 47. AIRCRAFT RECEIVED SPECTRUM BEFORE CPA FOR \cos^2 SURFACE, CROSS WIND FLIGHT PATH

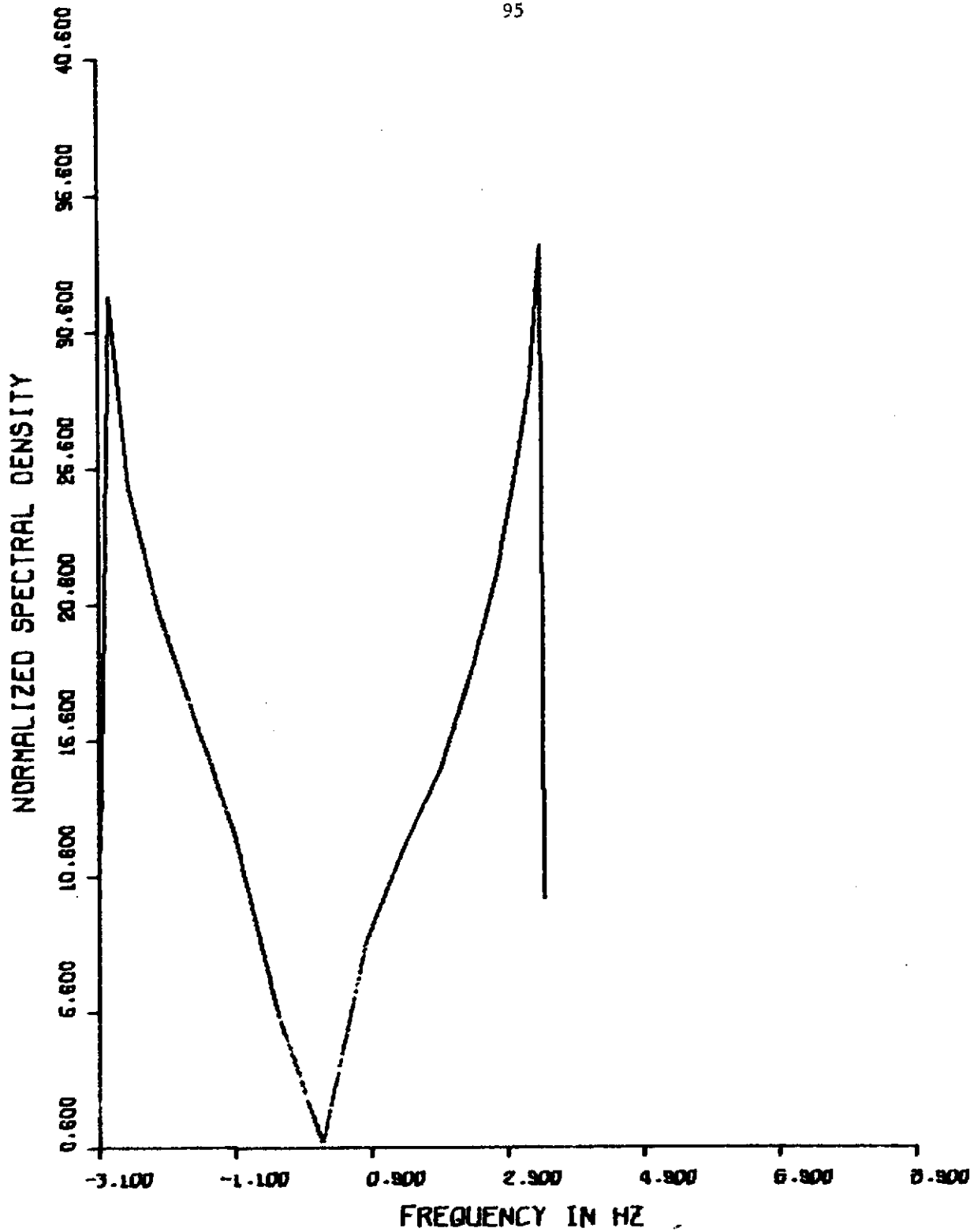


FIGURE 48. AIRCRAFT RECEIVED SPECTRUM AFTER CPA FOR \cos^2 SURFACE, CROSS WIND FLIGHT PATH